

# NHTSA RESEARCH ON IMPROVED RESTRAINTS IN ROLLOVERS

## Allison E. Loudon

National Highway Traffic Safety Administration  
United States

## Doug Weston

Transportation Research Center, Inc.  
United States

Paper Number 11-0213

### ABSTRACT

As part of a comprehensive plan to reduce the risk of death and serious injury in rollover crashes, the National Highway Traffic Safety Administration (NHTSA) has a program to characterize restraint system response in rollovers. A rollover restraint tester (RRT) was developed and utilized to produce a 180 degree roll followed by a simulated roof-to-ground impact. This device was modified to incorporate a reaction surface to analyze how advanced restraints would perform in a more realistic environment. The device was renamed as a rollover reaction surface tester (RRST). The original device (RRT) was discussed in previous ESV papers.<sup>(1,2)</sup> Recognizing the unpredictability of the real world rollover phenomenon, this test device provides a repeatable and consistent dynamic environment for suitable lab evaluation. Technologies that were evaluated for this study included integrated seat systems, pyrotechnic and electric resettable pretensioners, and four-point belt systems. High speed video data were collected and analyzed to examine occupant head excursion throughout the tests and are presented for discussion. The RRST has demonstrated to be repeatable; however, there are some concerns about the real world relevancy of the RRST dynamics in the absence of a lateral component. The RRST does not have a mechanical component for lateral motion that is typical in some real world rollover events.

Results presented in paper 09-0483 demonstrated that excursion characteristics can be affected with the implementation of advanced restraints in tests using the Hybrid III 50<sup>th</sup> and 95<sup>th</sup> percentile male and 5<sup>th</sup> percentile female dummies [Sword, 2009]. This paper presents expanded research with the 50<sup>th</sup> percentile male and 5<sup>th</sup> percentile female dummies using the RRST and compares the results back to the RRT

results. In addition to the RRST testing, a series of full scale dynamic tests was also conducted using a full vehicle in various dynamic rollover scenarios. The advanced restraints were chosen based on the test results of the RRST and availability of the devices. The following tests were conducted and will be discussed in this paper: Federal Motor Vehicle Safety Standard (FMVSS) No. 208 dolly test, curb trip, soil trip, and corkscrew ramp. The goals of the testing were to understand how the improved restraints perform in various conditions and to assess the occupant's kinematics in the various conditions.

### INTRODUCTION

In previous ESV papers,<sup>(1,2)</sup> the rollover restraint tester (RRT) was discussed in detail, as were the advanced restraints. It was a device that provided a repeatable dynamic environment suitable for comparing various restraint configurations. No single device can replicate the dynamics of all rollovers because every rollover crash is very different and unique. This device allowed for consistent repeatability of a specific dynamic environment.

Advanced restraints were tested with the 50<sup>th</sup> and 95<sup>th</sup> percentile male and the 5<sup>th</sup> percentile female dummies. The observations from the previous testing included:

1. Pretensioners and integrated seats reduced lateral and vertical excursions in both pre- and post-impacts.
2. The motorized retractor pretensioners reduced pre-impact lateral excursions
3. The inflatable belts with the pretensioners produced the largest reductions in vertical and outboard lateral excursions.
4. The 4-point belts reduced vertical and inboard lateral excursions.

- The results varied with the dummy size, but general trends held between the restraints.

Based on the observations and repeatability of the RRT, further research was conducted to look at the performance of the improved restraints when used in conjunction with inflatable curtains.

## ROLLOVER REACTION SURFACE TESTER TESTS

### Test Device

The original RRT was modified to include a roof and door structure along with an inflatable curtain and was renamed the rollover reaction surface tester (RRST). The cab structure (the roof and door structure) was taken from a 2006 Honda Ridgeline truck cab, and the inflatable curtain was from a 2007 Chevrolet Silverado 1500. This structure was enhanced by various support beams to ensure multiple testing could be conducted. Although a headliner was not used, a deflection pan was fabricated to ensure a repeatable inflation into the cab structure. Figure 1 shows the curtain inflated in the cab structure. The original characteristics and framework<sup>1,2</sup> of the device remained the same.



Figure 1: Deployed Airbag

Figure 2 is a schematic of the device, and Figure 3 shows the actual test device. The coordinate system is set to the dummy for excursion analysis. The device has four (4) main features consisting of the following:

- 1) A support framework,
- 2) A counter-balanced test platform with rotating axle,
- 3) A free weight drop tower assembly, and
- 4) A shock tower.

### Instrumentation

The RRST was instrumented to help characterize the dynamics of the testing. An angular rate sensor (ARS-1500, DTS, Inc.) was used to monitor the roll rate. Two (2) 50,000 lb. load cells were mounted to the roll table at the point of impact to record the impact force. A string potentiometer was utilized to measure the shock absorber deflection. A 2,000 g rated accelerometer, mounted to the platform directly underneath the center line of the seat was used to collect the acceleration at impact.

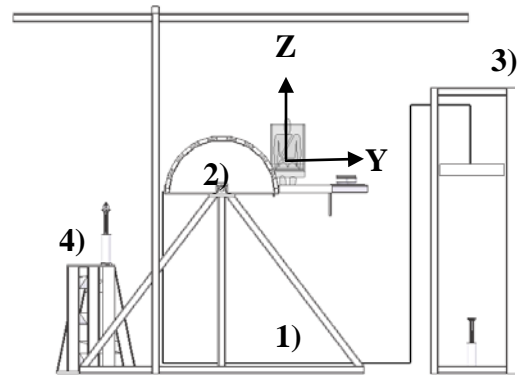


Figure 2: Rollover Restraint Tester (RRT)



Figure 3: Rollover Reaction Surface Tester (RRST)

The Hybrid III dummies used for testing contained head, neck, chest, and pelvis instrumentation. Seat belt load cells were used for both the lap and shoulder portions of the belts. The event was filmed with high speed digital (1000 frames per second) cameras that were used to obtain excursion measurements using TEMA film analysis software.

The inflatable curtain and pretensioners (if applicable) were deployed when the device platform reached 45 degrees of rotation (based

on previous testing<sup>2</sup>). The RRST had a roll rate velocity on average of 310±5 degs/sec (compared to the RRT device with an average of 320±10 degs/sec). **Test Matrix**

The test matrix for the restraint evaluation is included in Table 1. It includes the configuration description, code, and the test series for the 50<sup>th</sup> percentile male and 5<sup>th</sup> percentile female adult dummies. Each configuration was repeated three times with each dummy. Configuration C was the baseline treatment for test comparison. It was a standard 3-pt. non-integrated seat belt without pretensioning. The seat belts chosen for this series of testing were the available, better performing devices based on the RRT testing.

**Table 1:**  
**Test Matrix for 50th & 5th Hybrid III Dummies**

<i>Configuration Description</i>	<i>Code<sup>2</sup></i>	<i>50<sup>th</sup></i>	<i>5<sup>th</sup></i>
Integrated Seat	A	X	X
* 3-pt. Non-Integrated (3PN)	C	X	X
(3PN) Retractor w/Buckle Pretensioner	G	X	X
(3PN) Motorized Retractor w/Buckle Pretensioner	I	X	X
4-pt system w/Pretensioner	M	X	X

*\*Baseline Configuration for comparison*

#### **Evaluated Restraint Technology**

A variety of seat belt configurations were selected for testing. They ranged from current consumer-available technologies to prototype devices. The details of the restraints were discussed in the previous ESV paper [Sword, 2009]. The restraints used for this research testing are described below.

- **Configuration C:** 3-point non-integrated seat belt without pretensioners.
- **Configuration G:** 3-point non-integrated seat belt with pretensioners in both the retractor and buckle.
- **Configuration I:** 3-point non-integrated seat belt with a motorized retractor and a buckle pretensioner.
- **Configuration A:** 3-point integrated seat belt without pretensioners.

- **Configuration M:** 4-point non-integrated seat belt with pretensioners in both the retractor and buckle.

The inflatable belts (Configuration K) were not tested in this series due to unavailability.

## **RESULTS**

### **Dummy Kinematics**

As discussed before in the previously mentioned ESV papers, dummy kinematics were influenced by a combination of platform rotational and gravitational forces. At the onset of the test, the dummy was seated in an upright position. Gravity was the primary initial force acting on the dummy during the slow starting action of the rotating platform. As the platform began to rotate, the dummy's course was changed, and gravitational forces tended to move the dummy inboard (negative Y-direction).

The angular velocity of the platform increased with the centripetal or normal acceleration, creating the appearance of an outward or centrifugal force on the dummy. This outward force pushed the dummy outboard and up (toward the roof of the vehicle) (positive Y-direction, positive Z) during the pre-impact roll event. The dummy tended to start moving in the positive Y-direction at about 90 degrees of platform rotation. Gravitational forces continued to play a role for Z-direction motion (out of the seat toward the roof) past 90 degrees of rotation, until impact.

After impact, the dummy immediately changed from an outboard and up (i.e. off the seat) motion to a dramatic inboard and amplified up motion. The centripetal accelerations were eliminated when the table stopped, leaving momentum and gravity to act on the dummy.

### **Dummy Head Excursion**

Video data of the dummy's head were collected for excursion analysis. X-direction (fore and aft) data have been omitted. The kinematics of the RRST do not have an X-direction motion component, and the analysis for the RRST shows less significance X-direction motion compared to the Y and Z directions. The presented data will focus only on Y and Z-direction motions.

Figures 4 and 5 plot the average Y-direction and Z-direction head excursion for the tested configurations for both the 50th percentile male and 5th percentile female dummies. The figures contain both the non-reaction (RRT) and reaction surface (RRST) tests. The non-reaction (RRT) tests data was discussed in previous ESV papers<sup>1,2</sup>.

The blue bars represent the 5th percentile female dummy, and the red bars represent the 50th percentile male dummy. The solid colored bars represent the non-reaction tests, and the hatched bars represent the reaction surface for the lateral excursions plot (Figure 4). The lighter shades of the red and blue bars represent the non-reaction surface, and the darker shades represent the reaction surface testing on the vertical excursion plots (Figure 5). The hatched versus non-hatched bars represent the pre- and post- impact results.

### **Y-Direction Excursion**

Compared to the non-reaction surface testing, the lateral outboard excursions were reduced for the reaction surface testing for both sized occupants for all of the configurations. This was primarily because of the curtain deploying into the occupant compartment along with the dummy contacting the door which did not allow the occupant to move outboard. The inboard movement was reduced for Configuration C for both occupants and increased for Configuration M. (Note: The Configuration M seat in the original testing had a more defined seat bolster than that used originally in the non-reaction surface testing, causing slightly different occupant kinematics.) Overall, the lateral inboard and outboard excursions for the reaction surface testing were all less than 120 mm, while some exceeded 200 mm in the non-reaction surface testing.

For the reaction surface testing, Configuration I produced the least inboard excursion for both dummies, followed by Configuration A. For the

5th percentile female, Configurations C and G produced very similar inboard excursions, while it was somewhat higher for Configuration M. For the 50th percentile male, Configurations C and M resulted in similar inboard excursions, while it was reduced in Configuration G.

### **Z-Direction Excursion**

The Z-direction or vertical excursions for the reaction surface testing are plotted in Figure 5. The reaction surface reduced these excursions for all configurations for both sized occupants, compared to the tests without the reaction surface. The air curtain allowed for minimal movement outboard, which slowed the occupant kinematics and kept the occupant in the seat as the platform rotated. This allowed for the seat belt to maintain better engagement with the occupant, thus allowing less vertical movement.

For the reaction surface testing, Configuration I produced the least vertical excursion for the 5th percentile female and only slightly more than Configuration G for the 50th percentile male. Configuration I had a motorized retractor and a buckle pretensioner and also allowed the lowest lateral excursions. For the 5th percentile female, Configurations G and M also produced lower excursions than the baseline configuration (C), while Configuration A results were similar to baseline. For the 50th percentile male, Configurations A and M allowed for similar excursions as baseline. The pre-impact vertical excursions were all under 60 mm, and total vertical excursions were all less than 150 mm.

### **Summary of RRST Testing**

Testing with the reaction surfaces (roof, door, and air curtain) produced less lateral outboard and vertical excursion than the non-reaction surface testing, for both dummies and all of the belt configurations. This was not necessarily the case for inboard lateral motion. Configuration I generally had the lowest, or nearly the lowest, excursions for both dummies.

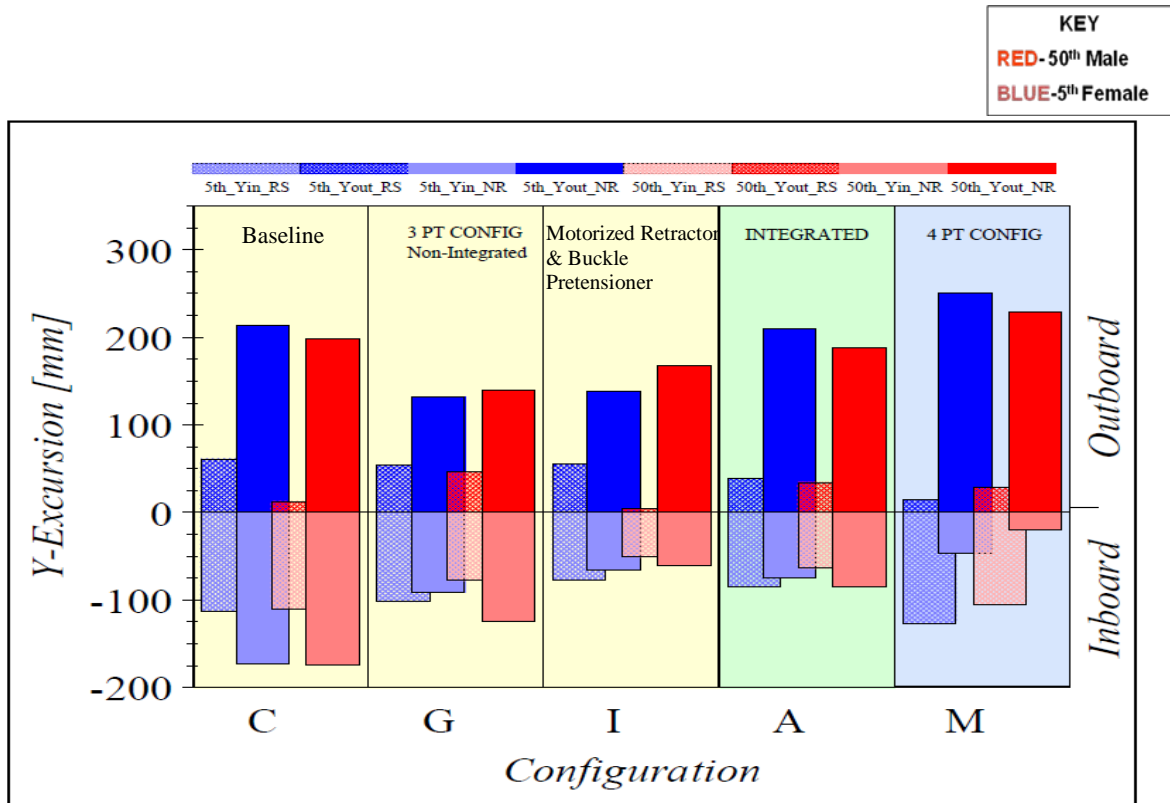


Figure 4: Reaction vs Non-Reaction Lateral Excursions

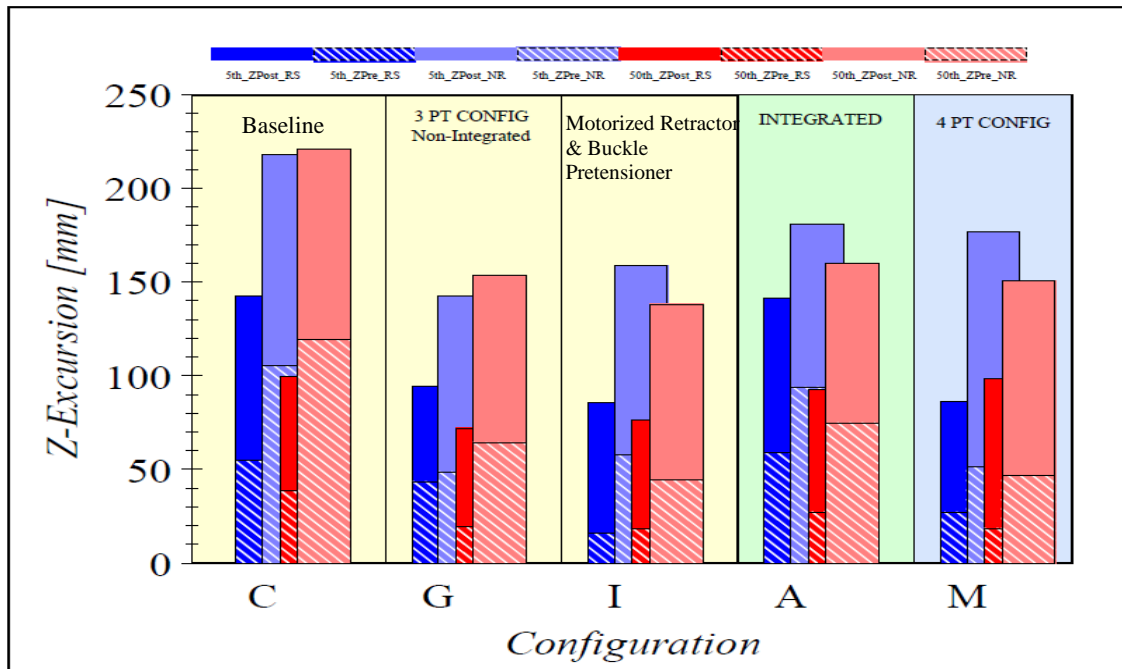


Figure 5: Reaction vs Non-Reaction Vertical Excursions

## FULL-SCALE DYNAMIC ROLLOVER TESTS

A series of full-scale dynamic rollover tests were conducted with a modified 2007 Ford Expedition. Various restraint configurations were chosen based on their performance in the RRT/RRST tests. The full-scale tests were conducted in order to help identify the dynamics and occupant kinematics in various rollover scenarios; assess what dynamics and occupant kinematics should be considered when evaluating restraint performance; and compare the performance of the restraints to that in the RRT/RRST tests.

### Setup/Test Matrix

A 2007 Ford Expedition was modified by replacing the 2<sup>nd</sup> row bench seat of the vehicle with a front seat. Replicating the front seat/belt configuration in the 2<sup>nd</sup> row was done to allow a more direct comparison between the front and 2<sup>nd</sup> row test results. The factory installed restraints were removed and replaced with the different configurations listed in Table 2.

The following test scenarios were tested using the Hybrid III 50th percentile male dummies.

- FMVSS No. 208 Dolly
- Soil Trip
- Curb Trip
- Corkscrew Ramp

Table 2 shows the test matrix and what restraints were used for all occupants. The front-to-rear comparisons were set-up on the trailing side of the vehicle, which differed depending on the test mode. For each test, the trailing edge dummies were seated similarly using a FARO Arm (FARO Technologies, Inc.). Figure 6 shows the two dummies placed in the vehicle.

Except for the FMVSS No. 208 dolly tests, two tests were conducted in each of the test modes. For the first test of each mode, the trailing side front and rear occupants and the leading side front occupant were restrained using the baseline configuration (C). For the second test of each mode, the trailing side front and rear occupants were restrained using Configuration I, and the leading side front passenger was restrained using Configuration G. These same configurations, and others, were also tested in the four FMVSS No. 208 dolly tests, but not necessarily in the

same order. See Table 2 for details. This paper focuses on the results from the trailing side occupants.



Figure 6: Trailing Front and Rear Occupants

### Instrumentation

The Hybrid III dummies used for testing contained head, neck, chest, and pelvis instrumentation. The vehicle was instrumented with accelerometers in the engine, rear deck, roof rail, center of gravity, multiple seat locations, and all A-D Pillar locations. Roll rate sensors were located at the center of gravity and rear deck locations. Seat belt load cells were used for both the lap and shoulder portions of the belts.

The event was filmed with high speed digital cameras that were used to obtain excursion measurements. The inflatable curtain and pretensioners (if applicable) were deployed manually at a pre-determined time, depending on the test mode. The motorized retractors (Configuration I) were activated prior to the launch of the vehicle.

### Test Modes

FMVSS No. 208 Dolly: The vehicle was mounted on the dolly platform, which was rotated 23 degrees from horizontal, with the left side of the vehicle being the trailing side (Figure 7). The dolly was propelled at 30 mph and then abruptly decelerated, allowing the vehicle to fly off the dolly and freely roll about its longitudinal axis into the desired area.



Figure 7: Dolly Cart with Vehicle

**Table 2 TEST MATRIX**

Test Type	Config C	Config I	Config G	Config A	Air Curtain/Fire Time
FMVSS 208 Dolly #1	1, 2				NO/
FMVSS 208 Dolly #2	3	1, 2			NO
FMVSS 208 Dolly #3			3	1, 2	NO
FMVSS 208 Dolly #4		1, 2	3		YES/100 ms
Corkscrew Ramp	1, 2, 3				YES/300ms
Corkscrew Ramp		1, 2	3		YES/300 ms
Soil Trip	1, 2, 3				YES/100 ms
Soil Trip		1, 2	3		YES/100 ms
Curb Trip	1, 2, 3				YES/100 ms
Curb Trip		1, 2	3		YES/100 ms

**KEY: 1 – Front Occupant, Trailing Side 2 – Rear Occupant, Trailing Side 3 – Front Occupant, Leading Side**  
**\*\*Firing times were based on discussions with Ford safety engineers.**

Corkscrew Ramp Trip: The vehicle was propelled at 30 mph and released prior to the ramp, allowing it to freely roll up a corkscrew ramp (height of 6' and maximum twist angle of about 50°). The right side of the vehicle was the trailing side (Figure 8).



**Figure 8: Corkscrew Ramp**

Soil Trip: The vehicle was pulled laterally at 30 mph and then released prior to the soil so that it could rotate freely into the soil. The soil consisted of #9 crushed limestone aggregate in a 300 square foot area (see Figure 9). The left side of the vehicle was the trailing side.



**Figure 9: Soil Pit and Aggregate.**

Curb Trip: The vehicle was pulled laterally at 20 mph into a curb structure (Figure 10) and then released. The wheels interacted with stops that decelerated the vehicle, allowing the vehicle to freely roll about its longitudinal axis. The left side of the vehicle was the trailing side.



**Figure 10: Curb Trip**

## RESULTS

A comparison of Configuration I and Configuration C is included for each test mode. The overall occupant kinematics is discussed along with vehicle kinematics. Each section contains a summary table identifying lateral and vertical excursions, roll angle and restraint status for the front and rear trailing occupants. The lateral excursions recorded are peak inboard and peak outboard measurements. The vertical excursions recorded, are initial movement up (usually around 180°) and secondary movement up (usually at the end of the event). Plots of peak excursion and neck compression values are located in Appendix A. The tests were conducted at TRC, Inc. and are located in the NHTSA database.<sup>(3)</sup>

### FMVSS No. 208 Dolly Test Results

In a typical dolly test, the vehicle comes off the platform with some rotational velocity. Then the leading side tires (right side for these tests) interact with the ground, tripping the vehicle and

causing it to rotate one or more quarter turns (Figure 11).



**Figure 11: FMVSS No. 208 Dolly Test**

Four FMVSS No. 208 dolly tests were conducted using several different restraint configurations (see Table 2). In two of the four tests, the vehicles completed eight quarter turns (tests 1 and 2), while the vehicle in test 3 completed only one quarter turn, and the vehicle in test 4 did not roll. As shown in Figure 12, the roll velocities were not repeatable. Even for the two vehicles that completed eight quarter turns (red and green curves), the angular velocities were different, particularly after the vehicles impacted the pavement (at about 0.4 sec.).

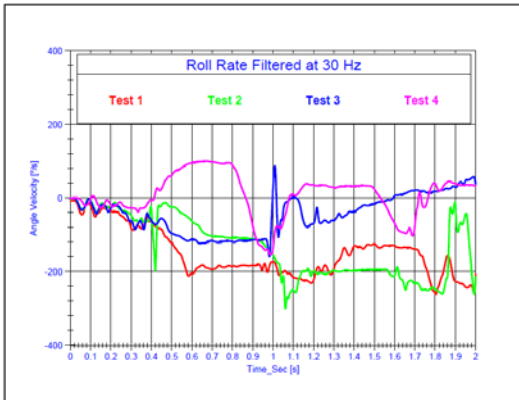


**Figure 12: FMVSS No. 208 Dolly Roll Velocities.**

The roll velocities were slower than in the RRT/RRST tests, but the initial vehicle roll (up to 180 degrees) provided occupant kinematics responses similar to those in the RRT/RRST testing. The occupants showed little longitudinal movement in the dolly tests.

Table 3 provides the summary of the data for all four of the dolly tests conducted, although this paper focuses on tests 1 and 2.

**Table 3  
FMVSS No. 208 Dolly Summary**

NHTSA #	Dolly			
	Test 1	Test 2	Test 3	Test 4
6957	6956	6955	6954	6954
Belt Configuration	C	I	A	I
Speed (mph)	30	30	30	30
Roll	720°	720°	120°	No Roll
Time to 180°	1.2 sec	1.47 sec	120° at 1.5s	N/A
<b>Restraints</b>				
Front Trailing Occupant	slid off .42 sec 17°	slid off .59 sec 15°	slid off .44 sec 43°	slid off 1.79 sec N/A
Rear Trailing Occupant	Stayed ON	Stayed ON	slid off .39 sec 34°	slid off .32 sec N/A
<b>Video Analysis</b>				
Front Trailing Excursion Lateral In/Out (mm)	389	242	Loet Camera view	479 115
Front Trailing Excursion Vertical Up1/Up2 (mm)	30	130		29 115
Rear Trailing Excursion Lateral In/Out (mm)	341	199	160 178	378 102
Rear Trailing Excursion Vertical Up1/Up2 (mm)	30	62	38 80	29 123

In test 1, the trailing side front occupant’s belt slipped off the shoulder soon after the vehicle was separated from the dolly (17°). The rear occupant’s belt remained on during the entire rollover event. The vehicle completed 2 full rolls (720°).

In test 2, the trailing side front and rear occupant kinematics were similar to test 1 occupant kinematics. The test vehicle also completed 2 full rolls (720°). The trailing side front occupant slid out of the shoulder belt early in the event (15°). The rear occupant on the trailing side remained in the shoulder belt and slid out slightly in the second roll.

The excursions were measured from the head of the dummies using video analysis. The high speed camera data for the trailing side front occupant was lost in test 2, so this analysis could not be done for that dummy. For the rear seat occupant, lateral inboard and outboard movements were less in test 2 (Configuration I) than in test 1 (Configuration C). See Appendix A, Plot 2.

Appendix A, Plot 4, shows the neck compression results of the comparable tests. The blue bars represent Configuration C and the orange bars represent Configuration I. The black lines in the bars represent the peak neck compression when the vehicle was at 180 degrees.

In tests 1 and 2, curtain airbags were not present. Both trailing side front occupants exceeded the injury assessment reference value (IARV) for upper neck compression (4000N). In test 1, the peak neck response of 4037 N occurred during

the first roll (188°) slightly after the vehicle was at 180°, whereas in test 2, the neck compression was 505 N in the initial roll.. Neck compression exceeded the IARV of 4000 N in the second roll with a value of 6605 N.

The trailing side rear occupant in test 1 had a neck compression of 890 N. In test 2, the trailing side rear occupant neck compression exceeded 80% of the IARV with a value of 3623 N, but it only reached 396 N during the first 180°.

The high neck responses in both the trailing side front and the rear occupant locations can be attributed to a combination of pillar and roof crush and the dummies slipping out of the shoulder belts. Other injury criteria including Head Injury Criterion (HIC) and the Neck Injury Criterion ( $N_{ij}$ ) were low for all occupants. See Figure 13 and Appendix A, Plot 4, for additional details.

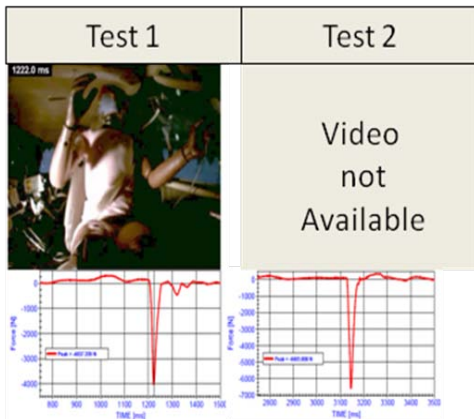


**Figure 13: Front Trailing Occupant Neck Compression Response**

There was extensive roof and A-pillar lateral and vertical crush on the trailing side front rows in both tests, as shown in Figure 14. Refer to the report for actual crush measurements<sup>3</sup>. Video motion analysis of test 1 indicated a vertical head excursion for the front occupant of 130 mm. The video of the front occupant in test 2 was lost during the test therefore no excursion measurements could be obtained.



**Figure 14: Dolly Test Vehicles**

The trailing side rear occupants were subjected to lower vertical excursions, as shown in Table 3. Roof crush was less behind the B-pillar on both sides of the vehicles.

### Corkscrew Ramp Results

These tests were conducted such that the trailing side was the right side of the vehicle. The vehicles were released at the base of the ramp at 30 mph. As the vehicles rolled up the ramp, the right front corner rose rapidly, and the vehicles rolled counter clockwise (Figure 15).



**Figure 15: Corkscrew Ramp**

The kinematics of the vehicles in the two corkscrew ramp tests were similar through the first 90°. In test 1, the vehicle rolled 180° and landed on its roof. In test 2, the vehicle rotated about 114°, but came back to about 90°, ending up on its left side.

The roll velocities of the two tests are shown in Figure 16, and they are somewhat similar, peaking at about 120 degs/sec. This was a slower roll rate than in the other test modes. Table 4 provides the corkscrew ramp summaries for both tests. The curtains and other pyrotechnics were fired manually 300 ms into the event.

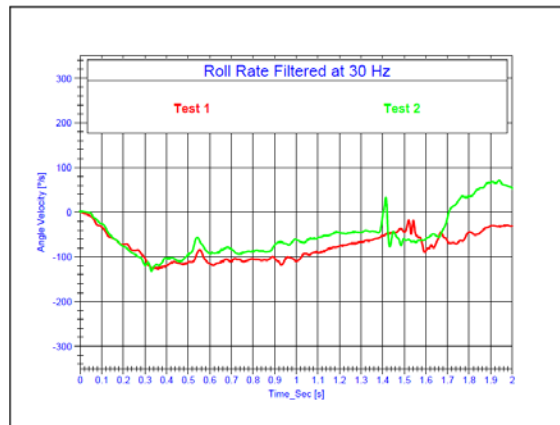


**Figure 16: Corkscrew Ramp Roll Velocities**

**Table 4:  
Corkscrew Ramp Summary**

	Corkscrew			
	Test 1		Test 2	
NHTSA #	6961		6962	
Belt Configuration	C		I	
Speed (mph)	29.9		30.1	
Roll	180°		114°	
Time to 180°	2.59 sec		1.71 sec	
<b>Restraints</b>				
Front Trailing Occupant	slid off 1.01 sec 72°		slid off sec 1.45 100°	
Rear Trailing Occupant	Stayed ON		Stayed ON	
<b>Video Analysis</b>				
Front Trailing Excursion Lateral In/Out (mm)	480	159	157	138
Front Trailing Excursion Vertical Up1/Up2 (mm)	24	0	0	0
Rear Trailing Excursion Lateral In/Out (mm)	141	116	154	208
Rear Trailing Excursion Vertical Up1/Up2 (mm)	47	47	0	0

In test 1, the trailing side front occupant's belt slipped off the shoulder early in the event (72°). The rear occupant's belt remained on the entire rollover event. In test 2, the front occupant's kinematics were similar to those in test 1, with the occupant slipping out of the restraint after completing ¼ roll (about 100°). The trailing side rear occupant's shoulder belt remained on throughout the event.

This test mode resulted in forward longitudinal movement as the vehicle rolled up the ramp, and there was more belt spool out in Configuration C (no pretensioning) than in Configuration I. This was more dominant with the trailing side front occupant than for the rear occupant. Figure 17 shows the trailing side front occupant and the corresponding vehicle position at several times during the event.

The longitudinal excursions were not measured for the front occupants. This forward motion was not observed in the other test modes or the RRT/RRST testing.

The trailing side front occupant had less lateral inboard and outboard excursion with Configuration I than with Configuration C, while the opposite occurred for the rear occupant. Vertical excursions were less for both the trailing side front and rear occupants with Configuration I than with Configuration C. Note that these results can at least partially be explained by the

difference in the amount of rollover between the two tests.

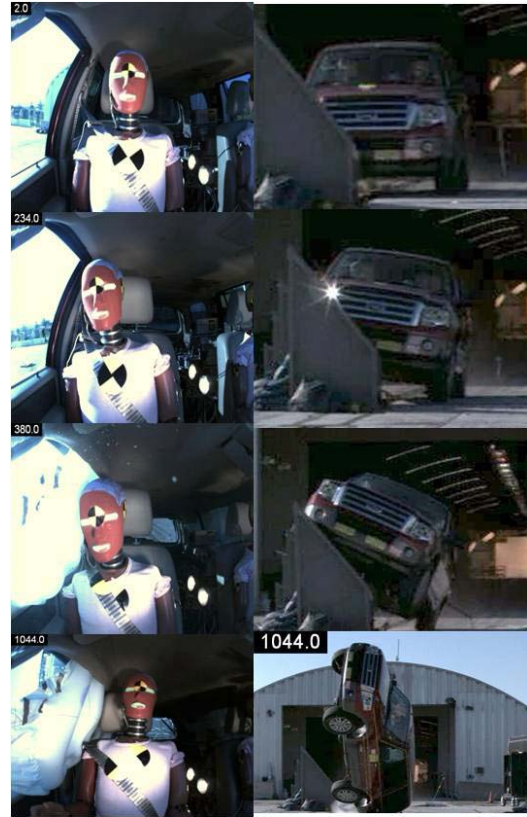


**Figure 17: Trailing Side Front Occupant and Vehicle Positions**

Roof crush was focused on the leading side A-pillar in test 1. Test 2 had minimal roof crush damage.

### Soil Trip Results

The vehicles were pulled laterally into a crushed limestone aggregate soil pit, which represented soft soil. As the vehicles were released, the tires dug into the stone, decelerating the vehicles and causing them to roll laterally (Figure 18).



**Figure 18: Soil Trip**

In the first test, the vehicle rolled 720° (two complete rolls), and in the second test, it rolled 630° (1 ¾ rolls). The vehicle's maximum roll rate velocity was about 300 deg/sec for test 1 and

about 340 deg/sec for test 2 (Figure 19). These roll rates were the most comparable to the RRT (about 320 deg/sec).

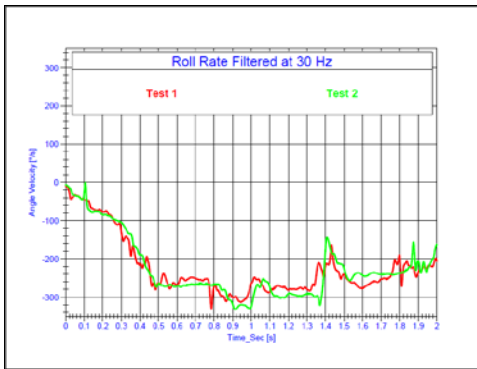


**Figure 19: Soil Trip Roll Velocities**

A summary of the soil trip tests is provided in Table 5. In both tests, the front occupant kinematics were similar during the initial 180°, but as the vehicles continued to roll, the occupant in test 1, Configuration C, began slipping out of the shoulder belt resulting in higher excursions. Then as the vehicles began into the second roll, occupant kinematic differences appeared. The front occupant slipped out of the restraint for both configurations. The rear occupant’s shoulder belt stayed on during test 2, Configuration I, resulting in lower vertical excursions.

In test 1, the trailing side front occupant’s belt slipped off the shoulder late in the first roll of the event (vehicle at 294°). The dummy’s peak upper neck compression was recorded as 2853 N, which is 71% of the IARV. In association with high neck compression, the roof and A-pillar were crushing into the vehicle (Figure 20). In the comparative test with Configuration I, the neck response was 791 N. The dummy remained in its shoulder belt during the first roll and did not contact the roof. See Appendix A, Plot 4 for additional information.

In test 1, the rear occupant’s belt came off the shoulder early in the event (5°), thus allowing for more vertical and lateral movement. In test 2, the shoulder belt remained on the rear occupant throughout camera coverage (494°).

**Table 5:  
Soil Trip Summary**

	Soil Trip			
	Test 1	Test 2		
NHTSA #	6960	6959		
Belt Configuration	C	I		
Speed (mph)	30.3	30.5		
Roll	720°	630°		
Time to 180°	.94 sec	.95 sec		
<b>Restraints</b>				
Front Trailing Occupant	slid off 1.76 sec 294°	slid off 1.93 sec 433°		
Rear Trailing Occupant	slid off .20 sec 5°	Stayed ON		
<b>Video Analysis</b>				
Front Trailing Excursion Lateral In/Out (mm)	116	143	98	100
Front Trailing Excursion Vertical Up1/Up2 (mm)	71	107	45	72
Rear Trailing Excursion Lateral In/Out (mm)	86	204	124	113
Rear Trailing Excursion Vertical Up1/Up2 (mm)	72	109	26	26

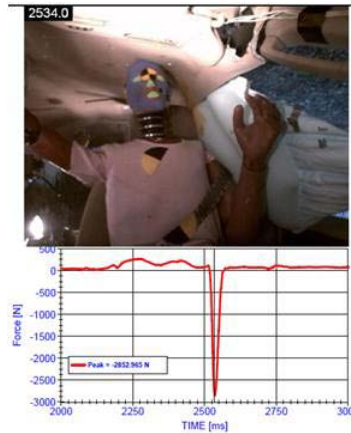


**Figure 20: Trailing Side Front Occupant-Peak Neck Compression**

Compared to Configuration C, the test with Configuration I showed reduced vertical and lateral outboard excursions for the trailing side front and rear occupants. The lateral inboard excursions were also slightly reduced for the trailing side front occupant with Configuration I. This is shown in Appendix A, Plots 1-3.

The two vehicles obtained similar damage to the roof and the A through D-pillars. In test 1, the front occupant slipped out of the belt and contacted the roof, and this was not seen in test 2 or with the rear occupant. Figure 21 shows the roof crush damage from the two tests.



**Figure 21: Soil Trip Vehicles**

### Curb Trip Results

The vehicles were pulled laterally into a deformable curb, which used flat plates mounted onto honeycomb to interact with the wheels and decelerate the vehicles, forcing a trip over event (Figures 10 and 22).



**Figure 22: Curb Trip Test**

This test mode had a very abrupt impact, which causes the trailing side occupants to move forcefully inboard, allowing them to slip out of the shoulder belts. This happened with both belt configurations, although the vertical excursions were less for both the front and rear occupants with Configuration I than with Configuration C (Table 6).

**Table 6:  
Curb Trip Summary**

	Curb Trip			
	Test 1		Test 2	
NHTSA #	6958		6963	
Belt Configuration	C		I	
Speed (mph)	20.7		20.6	
Roll	180°		270°	
Time to 180°	1.37 sec		1.03 sec	
<b>Restraints</b>				
Front Trailing Occupant	slid off .11 sec 15°		slid off .13 sec 19°	
	slid off .25 sec 44°		slid off .11 sec 15°	
Rear Trailing Occupant	slid off .25 sec 44°		slid off .11 sec 15°	
<b>Video Analysis</b>				
Front Trailing Excursion Lateral In/Out (mm)	615	0	427	63
Front Trailing Excursion Vertical Up1/Up2 (mm)	126	155	79	82
Rear Trailing Excursion Lateral In/Out (mm)	473	0	230	0
Rear Trailing Excursion Vertical Up1/Up2 (mm)	84	103	53	53

In test 1, the vehicle completed 1/2 roll (180 degrees). The trailing side front and rear occupants slid out of their shoulder belts early in the event (15° and 44°, respectively). In test 2, similar kinematics were observed, with the front occupant slipping out at about 19° and the rear occupant at about 15°.

Configuration I reduced the inboard lateral and vertical excursions for both trailing side occupants, compared to Configuration C. This is shown in Appendix A, Plots 1-3. The outboard lateral excursions were very low in all cases. The trailing side front occupant had the greatest vertical excursion measurement in any of the full-scale rollover tests during the first 180 degrees of roll (126 mm).

The roll velocities in the two tests were very similar, about 269-276 deg/sec (Figure 23). The vehicle in test 1 rolled about 180°, and the vehicle in test 2 rolled about 270°.

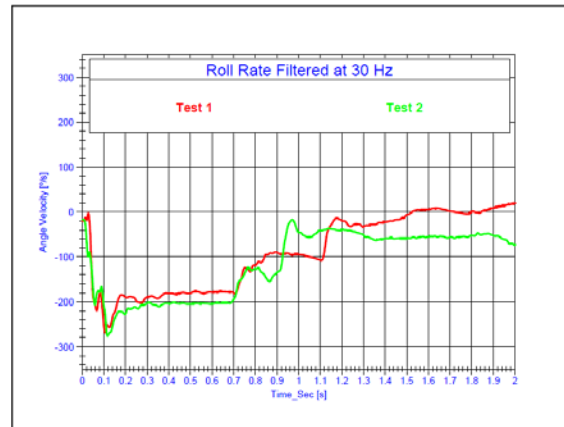


**Figure 23: Curb Trip Roll Velocities**

In test 1, the maximum roof crush was on the trailing side A-pillar. In test 2, the leading A-pillar area struck the back side of the curb approximately 170° into the event (Figure 24) causing more damage.



**Figure 24: Post Test Curb Trip Vehicles**

## **FULL-SCALE DYNAMIC ROLLOVER TEST SUMMARY**

### **Improved Restraints**

Front and rear occupant kinematics were similar to one another during the first 180 degrees of the event for the majority of the test modes. As each of the events continued beyond 180 degrees of rotation, the occupant interaction became more erratic and different kinematics were observed.

The belt slid off the trailing side front occupants' shoulders before the vehicles came to rest in all test modes. The belt slid off of the trailing side rear occupants' shoulders in both curb trip tests and in the soil trip test with Configuration C.

### **Occupant Excursions**

In general, excursions with Configuration I (motorized retractors and buckle pretensioners) were reduced when compared to Configuration C (non-pretensioning). This was a consistent trend that was also seen in RRT/RRST tests.

### **Injury Criteria**

Injury measures were generally low. No clear injury trend was observed for Configuration C vs. I. Upper neck compression exceeded 70 percent of IARV in three tests (excluding dolly test #4). Two of the high neck compressions occurred in Configuration C test modes, and one occurred in a Configuration I test mode. This could be attributed to a combination of roof/pillar crush and restraint performance.

### **Test Mode Repeatability**

The four full-scale FMVSS No. 208 dolly rollover tests were not repeatable. The roll rates varied, as did the roll angles.

The roll rates were similar in the corkscrew ramp tests, although the roll angle was not repeated. The ramp test mode added longitudinal movement that produced differences in the restraint performance.

The soil trip test was the most repeatable. The roll rates were similar, and the vehicles rolled 1¾ and 2 complete turns.

The curb trip tests had similar roll rates, and both vehicles rolled at least 180 degrees of rotation, although one vehicle rotated 270 degrees.

## **OBSERVATIONS**

Different test methods resulted in various roll speeds and various vehicle kinematics. The motorized retractors and buckle pretensioners generally reduced occupant excursions, as compared to the standard 3-point belts with no pretensioning for both RRST and full-scale dynamic rollovers. The shoulder belts slipped off the shoulders of both front and rear occupants in the full-scale tests, but more frequently for the front occupants. Since the higher excursions tended to result when this slippage occurred, restraint designs that reduce or eliminate this slippage may provide for improved performance. Additional research would be needed to confirm this.

## **ACKNOWLEDGEMENTS**

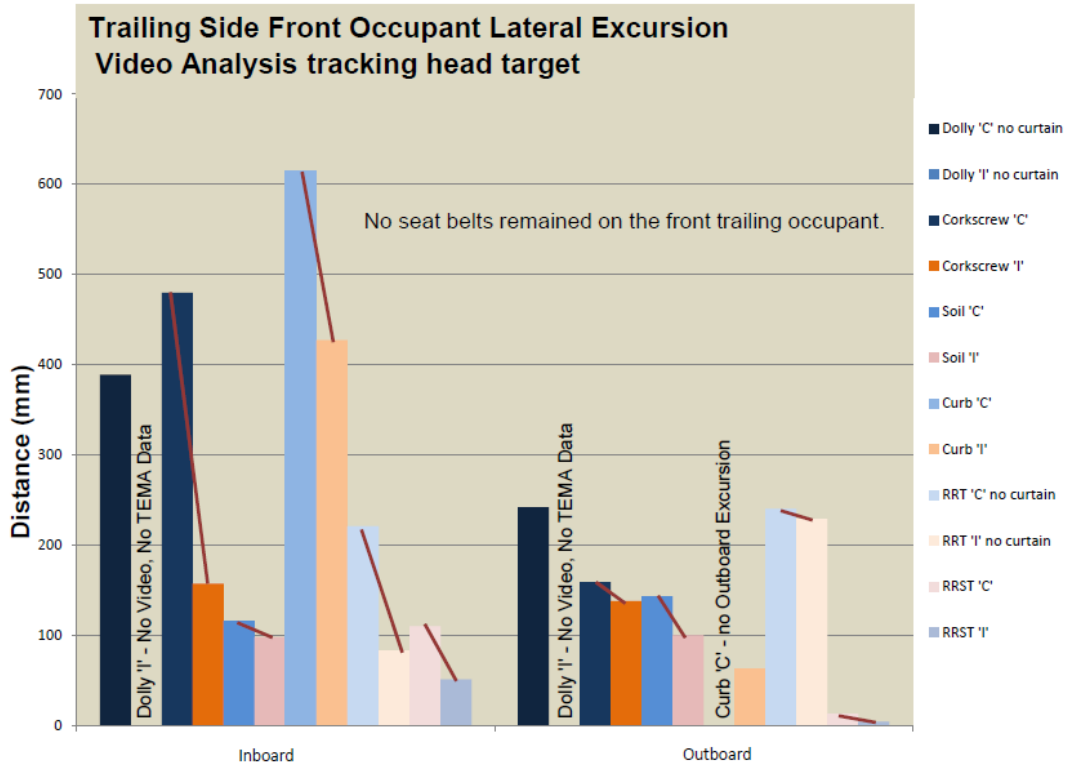
The authors would like to acknowledge the Transportation Research Center, Inc., Autoliv Test Center, Inc., Honda of America R&D, and Ford Motor Company for providing details about test procedures, test setup, and sensor development.

## **REFERENCES**

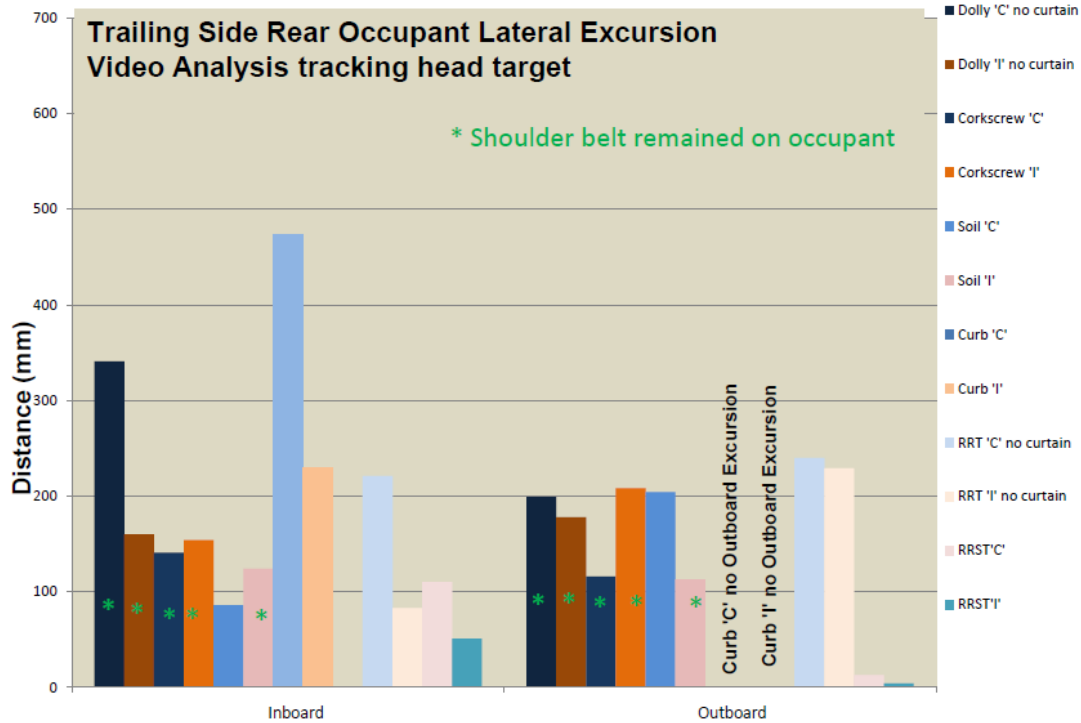
1. Sword, Michael L., and Sullivan, Lisa, K. "NHTSA Research on Improved Restraints in Rollovers" 20<sup>th</sup> International ESV Conference Proceedings, 07-0279, 2007, Lyon France.
2. Sword, Michael L., and Loudon, Allison E. "NHTSA Research on Improved Restraints in Rollovers" 21<sup>st</sup> International ESV Conference Proceedings, 09-0483, 2009, Stuttgart, Germany.
3. <http://www.nhtsa.gov/Research/Databases+and+Software>

## Appendix A

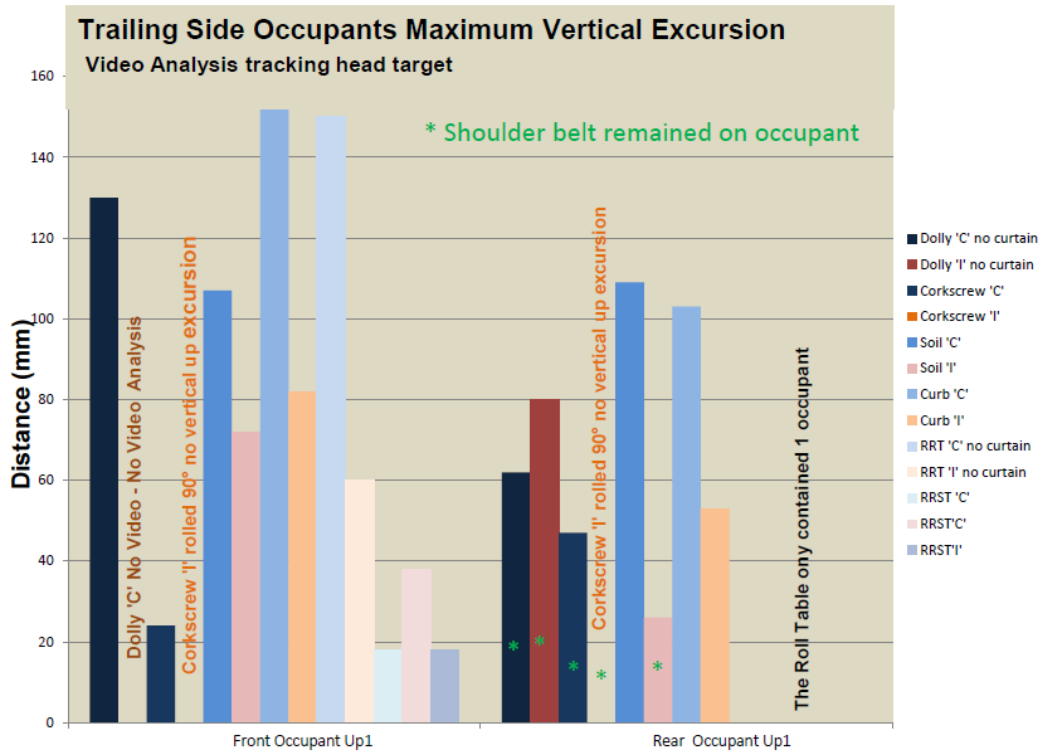
**PLOT 1: Trailing Side Front Occupant Lateral Excursion**



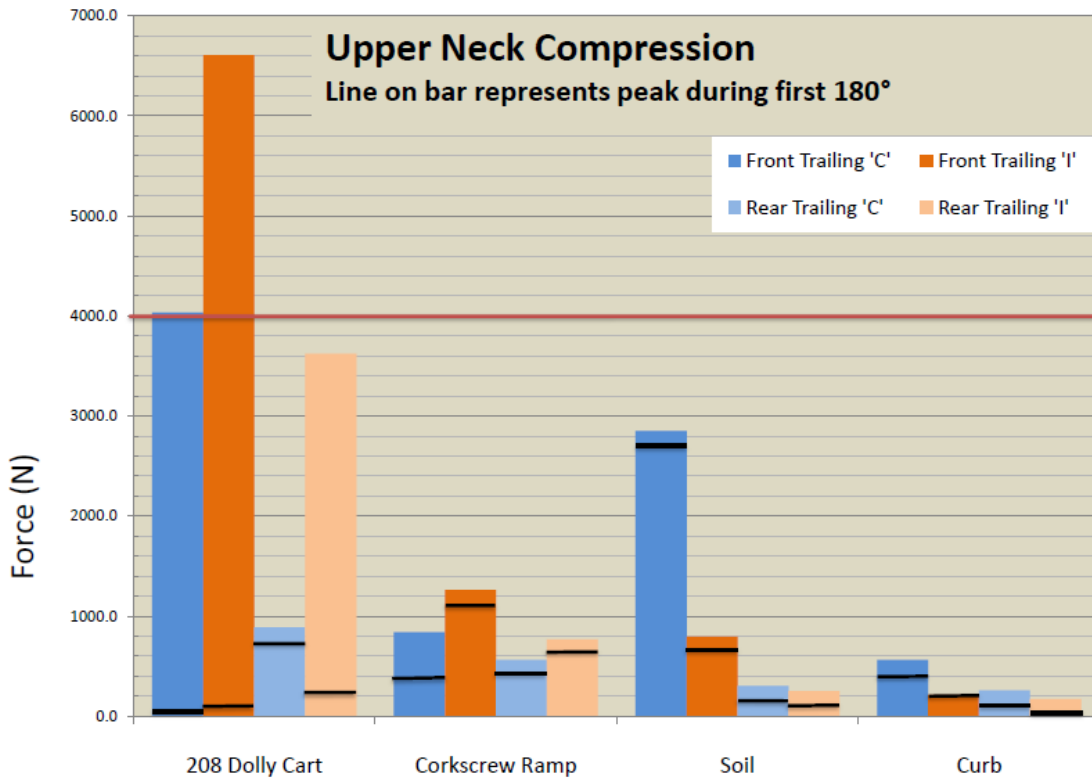
**PLOT 2: Trailing Side Rear Occupant Lateral Excursion**



**PLOT 3: Trailing Side Front and Rear Occupant Vertical Excursion**



**PLOT 4: Trailing Side Front and Rear Occupant Upper Neck Compression Configuration C vs I**



# CRASH-TEST RESULTS TO ANALYSE THE IMPACT OF NON-PROFESSIONAL REPAIR ON THE PERFORMANCE OF SIDE STRUCTURE OF A CAR

**Uwe, Schmortte**  
KTI GmbH & Co. KG  
Germany  
Paper Number 11-0310

## ABSTRACT

Non-professional repairs can have a negative influence on the deformation behaviour of a vehicle involved in a crash. The introduction by OEM's of new materials and production techniques in cars makes it increasingly important that the repair of such cars is carried out with appropriate techniques and quality. These are the aims described in a project named "Fair Repair", to which this paper is linked. This research project deals with the influence of non-professional repairs, on the behaviour of a car's structure in an additional crash. KTI, with the support of the OEM (VW) tested the side structure of a VW Passat, MY 2005. With a side impact at 50 km/h (Euro NCAP standard) it was shown that a non-professional repair of a vehicle previously damaged in the same side impact scenario results in negative influences on the crashworthiness and protection afforded by the structure. The repair of the damage caused by the first crash was carried out using incorrect repair methods and equipment, e.g. welding machines. It is evident that the safety of such a vehicle after the non-professional repair is not to the same high level as that of the original build, or to the standard of a professionally repaired vehicle.

## INTRODUCTION

Increasingly, over the last 10 years we have seen new generations of materials introduced by the OEM's. Aluminium, Magnesium, Plastics and Fibre Reinforced Composites in combination with newly developed high strength and ultra-high strength steels have been introduced to save weight and secure a stronger body shell at the same time. A modern Body-in-White is normally made up of a number of modern steels (Figure 1).

The new materials mean that body shops must continuously ensure that they are conversant with the requirements for new tools, procedures and information about the repair processes. New welding machines need to be used, training is required and OEM information has to be accessed to make sure that the correct repair methods will be applied. Without this knowledge it is likely that an inadequate repair will be the result, potentially placing the car and its occupants at much higher risk in a later crash.

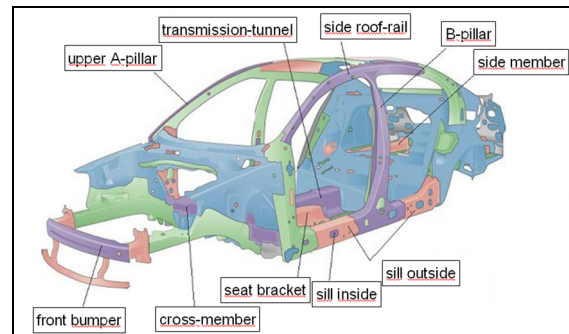


**Figure 1. Distribution of steel in a VW Passat B6 (Source - VW)**

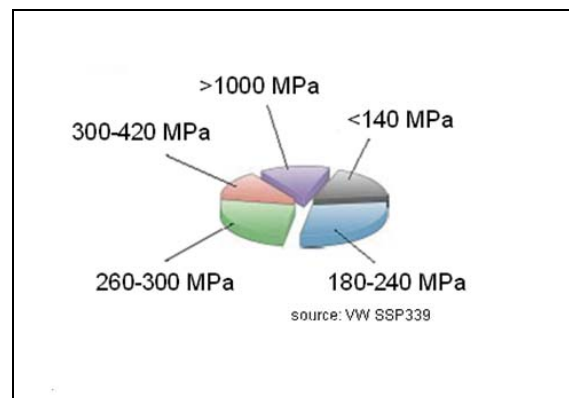


**Figure 2. steel grades in a VW Passat B6 (Source - VW)**

In parallel to the introduction of new materials, single component parts of earlier vehicles have been replaced by highly integrated, multi-material components on more recently designed cars. The production of a modern Body-in-White is characterised by complex manufacturing processes and bonding techniques.

Taken together, the technical progress made by the OEM's has resulted in corresponding new challenges for the repair shops. Repair shops must ensure they have well trained staff and are equipped with appropriate tools to cope with the techniques needed for professional repairs on today's cars when they are damaged in an accident. If such techniques and knowledge are not available, a non-professional repair may lead to a significant reduction in the safety and quality of these cars.

Unprofessional repairs may result from of all or any of the following:

- Incorrect method and/or sequence of repair
- Poor assembly of correct/incorrect spare parts, components and sub-systems
- Fitment of low-quality spare parts, components and sub-systems
- Incorrect assembly and connection of electrical/electronic systems and sub-systems
- Absence of correct, special or custom tools
- Repair of damaged parts when actual replacement is necessary

### PRELIMINARY CONSIDERATION

The following scenario, including two high-speed crash tests was carried out, and then analysed:

1. The car was damaged by a side impact similar to an intrusion by the front of another car into the passenger side of the test vehicle, according to the side-impact tests of Euro NCAP.
2. A repair was carried out as if done in a car body shop or garage with no information about the correct way to repair this particular car and without the correct tools or welding machines. The repair conforms to a typical standard carried out about 10 years (two car generations) ago. This would be considered as a non-professional repair by today's standards.
3. After the repair, this vehicle was involved in a follow-up crash simulation in the same configuration i.e. a side impact on the repaired passenger side, at the same speed.

In this project KTI wanted to examine and describe the effects of non-professional repairs on modern, state-of-the-art cars in order to highlight/picture reasons why using OEM information is necessary. The focus of the tests is on the side of a car because a small intrusion distance in the deformed area results in a higher risk for the occupants than in frontal or rear-end impacts at similar speed.

The baseline was a crash test according to Euro NCAP - Side Impact- according to EU issue 96/27/EG and ECE-R95 that guaranteed reproducible results. The exemplary vehicle, a VW Passat model B6 variant was chosen for the tests as its structure represented state of the art car bodies with several high-strength and ultra high-strength steels with one of the highest torsional stiffness values of about 30,000 Nm/° in its segment of mid-size cars.

As depicted in Figures 2 and 3 (the first crash test setup), the car was positioned relative to the carriage with its deformable barrier. The test was carried out at a speed of 50 km/h (+/- 1 km/h). A Dummy, ES-1, 50% male, 72 kg (+/- 1.2 kg) was positioned on the front passenger side seat and weight dummies of 76 kg on the back seat. The restraint systems were active. After the crash, the damaged car was repaired with recognized methods of car repair, but without specific information for this model i.e. non-professional repair. Subsequently the Passat underwent a second crash test in the same configuration. Finally, differences in deformation behaviour between the two crashes were analysed to determine the implications for passenger safety.

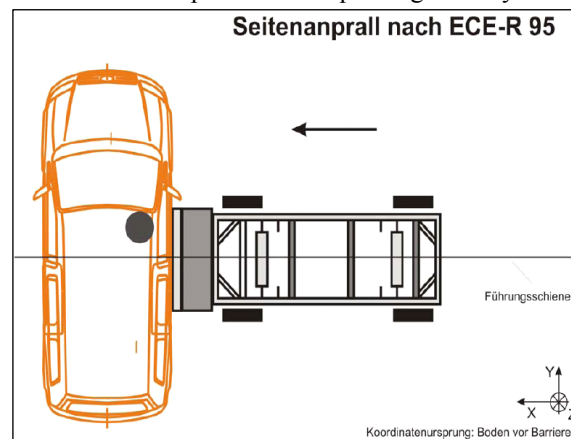


Figure 2. Test setup



Figure 3. Positioning the mobile barrier

## CRASH TEST 1

After the side impact the car was severely damaged on the passenger side, as intended. The sill and the floor/undercarriage behind it were particularly distorted. Additionally, the doors and the B-pillar were considerably damaged (Figure 5). There was no damage to the screen pillar or windscreen glass. The pyrotechnic protection/restraint systems (Front and rear passenger side airbags, front passenger belt pre-tensioner and passenger side curtain airbag) were correctly deployed. Overall the car body structure deformed and behaved as expected. As well as the visual analysis, electronic measurement of the car body was carried out. This showed the maximum intrusion to be 161 mm.



Figure 4. Head-on view



Figure 5. Damage to passenger side

## NON-PROFESSIONAL REPAIR

The damaged car was repaired with an older spot welding machine with fixed pressure and 6.4 kA maximum current.

It is recommended that an Inverter type welding machine is used with 10 kA maximum current and a variable pressure (maximum 10 bar) to join the high strength steel safely. The deformed inner sill, made from ultra high strength steel, was re-shaped and partially replaced on a bench then re-fitted using a MAG welding process. Figures 6 to 9 show the non professional repair being carried out.

The "Professional" repair would include complete renewal of the B-Pillar and other deformed structures with components made from high strength steel. A partial repair of such steels is not acceptable, as the structure and therefore the strength of the material will be severely degraded while welding and reforming.



Figure 6. MAG-welding the inner sill



Figure 7. Adapting the lower end of the B-pillar



**Figure 8. Positioning the outer panel**



**Figure 9. The completed repair**

## CRASH TEST 2

After completing the repair the car was crashed again under the same conditions as the first test in order to make a fair assessment on equal terms. It was immediately evident that there was a substantial difference, with far more comprehensive deformation of the car body after the second impact. The B-pillar had noticeably higher intrusion into the passenger compartment in comparison with the first crash, especially at the lower part at the connection with the sill (Figures 10 and 11). Note: Later measurement of the car body confirmed there was 60 mm more intrusion after the second test, compared to the first crash.

Other differences were noticeable at the cant rail/roof and the transmission tunnel which both displayed severe deformation not seen in the first crash. It seems that the load paths were quite different in the second crash. It was also notable that the top right corner of the windscreen was damaged in the second crash, further indication of changed load paths. These comparisons made it evident that a change of load paths and therefore of the energy dissipation was due to the unprofessional repair. The pyrotechnic protection/restraint systems (Front and rear

passenger side airbags and the front passenger belt pre-tensioner) were correctly deployed but the passenger side curtain airbag failed to operate.



**Figure 10. Damage after second crash**



**Figure 11. Higher intrusion to passenger compartment**

## RESULTS

To make clear the differences between the two tests, we compared photographs, sequences of high-speed crash-movies and electronic measurement of the car body.

With the help of the time analysis in the high-speed crash-movies we can for instance compare the time of highest intrusion (Figures 12 and 13). The analysis clearly shows higher intrusion at the same moment in time in the second crash test.



Figure 12. Crash 1



Figure 13. Crash 2

The higher deformation of the B-pillar has an important influence on the intrusion of the doors, which moved further into the seat area of the passenger compartment, increasing the bio-mechanical stress on the occupant, the co-driver in this case (Figures 14 and 15).



Figure 14. Side structure after first crash



Figure 15. Side structure after second crash



Figure 16. B-pillar and sill after first crash



**Figure 17. B-pillar and sill after second crash**

After removing the doors and the sill trim panel the deeper intrusion can be clearly seen on the side frame (Figures 16 and 17). The movement of the sill has reduced the normal distance between the B-pillar/door and the co-driver's seat dramatically (Figures 18 and 19). Additionally, although the front passenger's side airbag deployed, it was restricted by the close proximity of the seat to the pillar. Consequently a controlled deployment of the bag was not possible because the space between B-pillar and seat was too small, too early in the deformation process.



**Figure 18. Passenger seat after first crash**



**Figure 19. Compressed seat after second crash**

After removing all the seats and necessary trim the deformation of the transmission tunnel after the second test was clear to see. The cross-member which supported the front seat had pushed into the transmission tunnel, distorting it severely. In comparison, there were no measurable changes at the transmission tunnel during the first attempt. (Figures 20 and 21).



**Figure 20. Front seat anchor cross member/transmission tunnel after first crash**



**Figure 21. Front seat anchor cross member/transmission tunnel after second crash**

The deformation differences between Crash 1 and Crash 2 can also be represented by measurements taken after both crashes (Figure 22 and Table 1). At each measuring point the range of movement and deformation depth was measured. The table shows differences in movement up/down (Height), forwards/rearwards (Length) and Intrusion (Width). As an example, at point 1 which is nearly 100 mm above the sill on the B-pillar, the electronic measurement shows an important difference in Intrusion of 60 mm. The difference in deformation has enormous effects on the bordering body-parts which in turn have broader repair consequences, above all affecting passenger safety.

**Table 1. Differences in body movement**

	Measurements of the lower parts of the car body												Measurements of the upper part of the car body																					
Point Number	13	14	16	17	18	1	2	3	4	5	6	7	8	9	10	11	12	1	2	3	4	5	6	7	8	9	10	11	12					
Length (mm)	5	6	4	1	5	0	23	1	25	39	17	1	2	0	0	2	20	1	0	1	1	1	35	0	1	1	9	9						
Width/Intrusion (mm)	4	9	49	17	39	60	61	7	27	1	6	3	21	75	50	9	9	4	9	49	17	39	60	61	7	27	1	6	3	21	75	50	9	9
Height (mm)	0	0	24	5	25	2	0	0	2	20	1	0	1	1	35	0	1	0	0	24	5	25	2	0	0	2	20	1	0	1	1	35	0	1

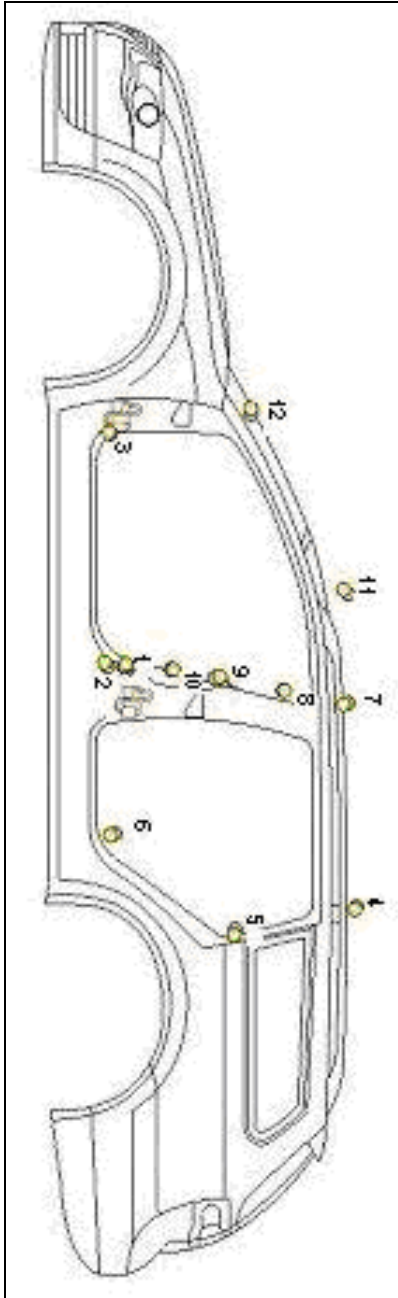


**Figure 22. Measurement points**

OEM information was not used during the repair after the first crash. Figures 23 and 24 show the disruption at the joining points after the second crash. These are positions where the inappropriate spot welding machine was used. The disconnection between inner sill and floor panel shows that the spot welds have not withstood the impact and were destroyed. The spot welds need to have a minimum diameter of 4.9 mm at a sheet thickness of 1.5 mm. The optimum would have been 6.7 mm diameter. It is clear that the spot welds were inadequate.



**Figure 23. Disconnection of the sill after second crash**



**Figure 24. Disconnection of the inner sill after second crash**

The connection of the B-pillar with the inner sill was joined with MAG welding. The structure of the high-strength steel parts was changed by the welding process and re-shaping. The welded seam was totally broken after the second crash, being unable to withstand the stress and the distortion (Figures 25 and 26).



**Figure 25. Disconnection between lower B-pillar**



**Figure 26. Disconnection between lower B-and inner sill after first crash**

pillar and inner sill after second crash

## SUMMARY

From the results obtained by this project it is clear that only a repair carried out according to the OEM's information could be described as Expert and Professional. The information would describe the recommended methods and joining procedures, including possible partial repairs in order to guarantee that a repair would have no adverse effect on the protection afforded to passengers in the event of a later collision.

## REFERENCES

- [1] Bürkle, Heiko et al.: Relevanz der Kompatibilität im realen Unfallgeschehen heute in Verkehrsunfall und Fahrzeugtechnik, 7-8, 2006, S. 193
- [2] Kramer, Florian: Passive Sicherheit von Kraftfahrzeugen, Vieweg Fachbuch 2. Auflage, S. 37 ff
- [3] Watson, Brock et al.: Study of vehicle dynamics and occupant response in side impact crash tests, ESV 2009 Stuttgart
- [4] Bröckerhoff, Markus: Karosserie-Strukturverbesserungen für den seitlichen Pfahlaufprall, Dissertation an der RWTH Aachen, 2006, S. 14
- [5] Der Passat '97 - Die Vorstellung - Konstruktion und Funktion, Selbststudienprogramm 191, Volkswagen AG
- [6] Der Passat Modelljahr 2001, Selbststudienprogramm 251, Volkswagen AG
- [7] Der Passat 2006, Selbststudienprogramm 339, Volkswagen AG, S. 10 und 11
- [8] Der neue Passat, Sonderausgabe ATZ/MTZ, April 2005, S. 45
- [9] <http://www.euroncap.com>, Stand November 2009
- [10] Rusch, Hans-Jürgen: Reparaturschweißen, Vogel Fachbuchverlag, Würzburg 2005, S. 34

## DEPLOYMENT CHARACTERISTICS OF SEAT MOUNTED SIDE IMPACT AIRBAGS

**Karen M. Balavich**

**Nathan R. Soderborg**

**Robert C. Lange**

**Harry Pearce**

Exponent

United States

Paper Number 11-0358

### ABSTRACT

There are over 230 current model year vehicles in the U.S. market that offer seat mounted side airbag systems. Compared to the considerable amount of crush space present in frontal crashes, the relatively limited amount of crush space available in side crashes creates a challenge for side airbag deployment performance. In the case of seat mounted side airbag technology, when the side impact sensor senses an impact that warrants deployment, it sends a deploy signal to the airbag module located in the outboard seat bolster. The airbag must then deploy from the seat and continue to move into position between the occupant and the interior door surface before the gap closes due to the intruding object. The deployment timing and positioning of the airbag is critical in providing enhanced occupant protection.

In this study, 88 front seat mounted side airbag systems from 1999-2010 model year vehicles were analyzed. The side airbag systems included airbags that deploy through seat bolster seams and systems that deploy through discrete seat deployment doors. Of the 88 production seat side airbag systems tested, 38 were equipped with side airbags that provide only thoracic coverage, 27 provided a combination of head and thoracic coverage, and 23 provided thoracic and pelvic coverage. Seventy-eight of the systems were unique; ten of the systems were repeat deployments.

The front seats equipped with side airbag systems were mounted on a generic fixture with the outboard seat bolster packaging the airbag placed approximately 100 mm from a Plexiglas reaction surface. The Plexiglas was backed with a grid of 2 inch squares to utilize in film analysis of the deployment. High speed cameras were placed to capture front, profile, and rear views of the airbag deployment.

The deployment time intervals associated with initial break out (airbag first becomes visible), two inch

extension forward, six inch extension forward and full extension position were recorded. The average deployment time calculated for break out, two inch extension, 6 inch extension, and full extension deployment intervals for the total set of seats was calculated as 3.3 ms, 5.0 ms, 7.3 ms, and 14.9 ms, respectively. The standard deviation characterizing the variation within each deployment interval was calculated as 1.17, 1.17, 1.83, and 5.73 ms, respectively. Further comparisons of average time and variation in timing between types of side airbags (thorax, head/thorax, and pelvis/thorax), deployment mechanisms (through seam vs. discrete door), repeat deployments, and across model years were also made. Discussion regarding the factors that influence the variation in deployment timing among the airbag types, deployment mechanisms, and model year groupings is included.

### INTRODUCTION

Side airbags entered the market in 1995 appearing on limited Mercedes Benz and Volvo models. Today there are over 230 current model year (2011) vehicles that offer seat mounted side airbags systems. This is approximately 85% of the new passenger vehicle models available in the U.S. market place. With recent change to Federal Motor Vehicle Safety Standard, FMVSS 214, side airbags will eventually become standard equipment on most passenger vehicles by 2014[1].

Passenger vehicles provide side impact protection through vehicle structural design and energy absorbing materials. Seat mounted side impact airbags are an energy absorbing component of a system providing occupant injury control. The side airbag not only interfaces with the seat where it is packaged but also with the side interior door and pillar trim.

The distance between the point of contact on the side of a vehicle and the occupant seated in the front seat in a typical side impact is limited to a few inches.

This small distance places great demands on side airbag performance for sensing deployment decision, breakout, and inflation to full capacity.

Seat mounted side airbags are packaged relatively close to the occupant. They are concealed within the outer bolster of the seat back. The modules are built into the seat and deploy through a seam in the seat trim or through a separate cover often referred to as an exposed deployment door (Figure 1). To achieve desired performance from the side airbag, the deployment timing to break out of the seat and continue to move into position between the occupant and intruding surface requires optimization. The side airbag module generally consists of an inflator, air bag or “cushion,” and cover. The module inflates when it receives a signal from the sensor, commanding deployment in certain types of side impact accidents. There are three basic types of side airbags, those that provide thoracic coverage, combination head/thoracic coverage, and combination pelvic/thoracic coverage.



(a) Built in seat – deploys through seat seam

(b) Separate module – deploys through a deployment door

**Figure 1. Seam deployment vs. deployment door.**

Prior to the FMVSS 214 requirement that was released in September 2007 (with phase in beginning in 2010) side airbag systems were not necessary to satisfy regulatory requirements for side impact occupant protection. Manufacturers developed their vehicles to their internal requirements guided by government regulated side impact full vehicle crash tests.

In 2000, a voluntary agreement was released to guide the performance of side airbags systems when evaluated to occupant out of position testing. Vehicle systems developed after the 2000 calendar year were designed to comply with the Technical Working Group’s Recommended Procedures for Evaluating Occupant Injury Risk from Deploying Side Airbags (referred to as the TWG procedures) [2].

In 2003, the Insurance Institute for Highway Safety (IIHS) released a new consumers rating tool, the IIHS Moveable Deformable Barrier Side Impact test (referred to as IIHS MDB) [3]. The IIHS procedure applied new requirements on side impact performance which influenced side airbag design and performance. Due to changes in the public domain, working group and regulatory requirements over time, side airbag designs have also evolved and changed. As side airbags systems evolved to meet the new requirements, the rate at which they deploy from the seat, the size, shape and volume of the airbags, and the internal pressure characteristics of each airbag changed over time.

### VEHICLE SYSTEMS ANALYZED

A vehicle set consisting of vehicles equipped with seat mounted side airbags was identified. The set was composed of the following vehicle brands: Acura, Audi, Buick, Cadillac, Chevrolet, Chrysler, Dodge, Ford, Honda, Hyundai, Infiniti, Jaguar, Kia, Lexus, Lincoln, Mazda, Mercedes-Benz, Mercury, Mini, Mitsubishi, Nissan, Pontiac, Saab, Saturn, Scion, Subaru, Suzuki, Toyota, Volvo, and Volkswagen. Vehicle models in model years 1999-2010 for which seat mounted side airbags were available as either standard or optional equipment were identified. Determinations of availability of seat mounted side airbags were made by consulting the IIHS online “Vehicles Equipped with Side Airbags” database as well as other automotive websites and resources (4, 5, 6).

### TEST PROTOCOL

Static ambient side airbag deployment testing was used for the purposes of evaluating the side airbags deployment.

Autoliv America’s Auburn Hills Technical Center, an accredited test facility in airbag deployment with extensive experience in seat mounted side airbag deployments, was chosen as the test facility.

For each test, the production seat system was mounted to a test platform through the seat track attachment points. Vehicle specific seat attitude as positioned in its unique vehicle environment was unavailable therefore a simulated position was used. Mounting blocks were constructed to allow for level attachment of the seat to the test platform. The seat track angle was adjusted to  $0^\circ \pm 3^\circ$  from horizontal. When the inclinometer was placed on the seat cushion in the middle of the seat it read approximately  $15^\circ \pm 5^\circ$  for the majority of the

samples. The seat was placed in the full rear seat track position. Seats that adjusted up/down were placed in the full down position. The seat back angle was measured on the back outboard side of the seatback and was adjusted to  $20^\circ \pm 2^\circ$  which correlated to a  $5^\circ \pm 2^\circ$  measurement at the headrest posts on most samples.

Each seat was orientated such that the outboard bolster containing the side airbags was positioned next to a Plexiglas reaction surface. The distance between the side bolster and the Plexiglas surface was approximately 100 mm at the airbag location.

The Plexiglas was backed with a grid of 2 inch squares to utilize in film analysis of the deployment.

For deployment a DC current of 3.5 A +/- 0.5 A was applied to the side airbag module through squib wires for 3 ms. The module electrical resistance (terminal-to-terminal) was verified pre-test. The fire command current was measured and recorded for each test.

Three camera views were used to capture the deployment (Figure 2). The film speed was 2000 fps, which allowed capture of 0.5 ms intervals during deployment. Photographs were taken before and after deployment.

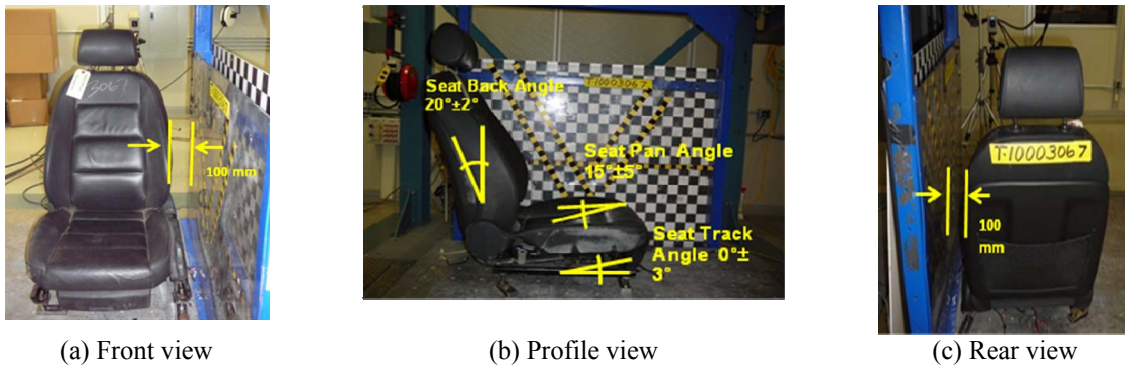


Figure 2. Test set up.

### DEPLOYMENT ANALYSIS

There were four stages of deployment at which deployment timing comparisons were made: initial break out, two inches extension forward of the seat bolster, six inches of extension forward of the seat bolster, and full extension.

Initial break out was the first instant the seam splits or deployment door opens and bag material can be seen. The second measurement point was defined as the instant at which the bag reaches two inches forward extension. The third measurement point was defined as the instant at which the bag reached six inches forward extension. The final measurement point was defined as full extension of the bag. Full extension requires some amount of judgment and was determined by viewing the deployment frame by frame until it appeared maximum shape was maintained, i.e. if advancing to the next frame the bag appeared to be deflating or reducing in size the previous frame captured the full shape.

Using a frame by frame software viewer, deployment of the airbag was analyzed. The front view was used to determine the initial time at which the bag was visible through the seat seam or deployment door. The profile view was used to track the extension of the bag two and six inches forward of the seat bolster referencing the distance off the checkered grid and the time was noted. Full extension timing was determined using all three views. It was defined at the time the bag appeared to be completely extended forward, up, and down and advancing one more frame the bag appeared to be reducing in size.

When analyzing repeat deployment timing for a single design, the deployment views from each test were viewed side by side to compare the deployment shapes at the various intervals. The extension times recorded reflected the instant at which the two samples appeared to have had the same shape for each extension interval.

Since side airbag system deployment varies for each vehicle sample, it is difficult to set a standard location on each seat to measure the extension. As a

guideline, the point at which the seat bolster first expanded forward was used (Figure 3).

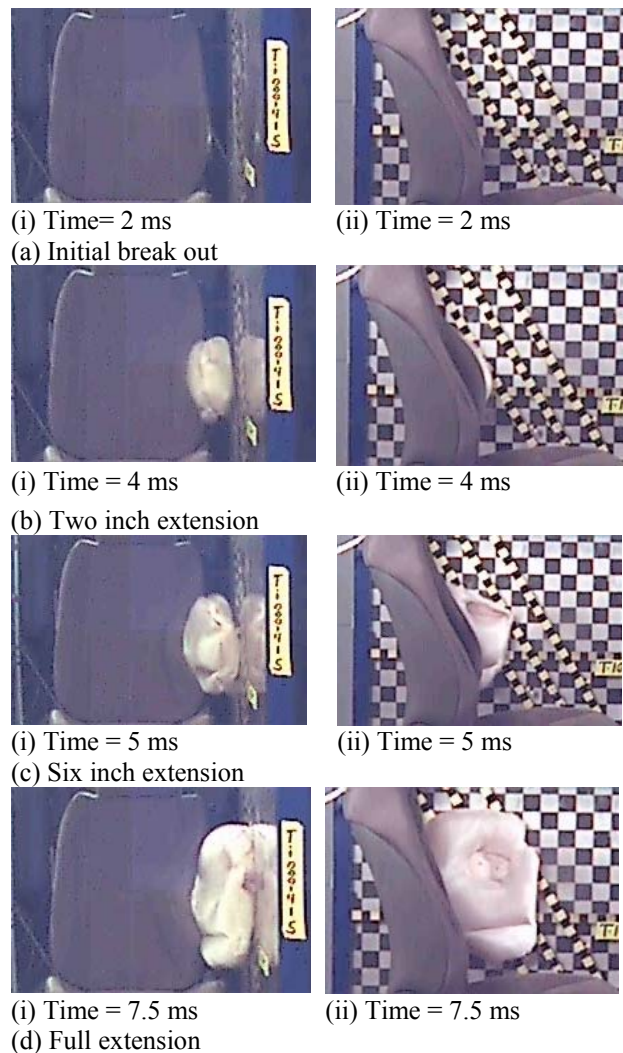


Figure 3. Example of deployment analysis.

## DEPLOYMENT TIMING RESULTS

### Total Samples

There were 88 vehicle seat side airbag systems evaluated: 38 thorax bags, 27 head/thorax bags, and 23 pelvis/thorax bags. Out of the 38 thorax bag systems, one system was only evaluated for break out time due to error in setup. The average break out time for the total set was 3.3 ms. The average extension times were 5.0 ms, 7.3 ms, and 14.9 ms for two inch, 6 inch, and full extension, respectively.

The corresponding standard deviations were 1.2, 1.2, 1.8, and 5.7 ms respectively. Part of the variation in average deployment timing across the total set can be contributed to the three types of side airbags. Thorax bags are smaller in size and volume than head/thorax and pelvis/thorax bags. Head/thorax bags generally are larger than both thorax and pelvis/thorax airbags. The volume of the airbag increases as the airbags unfold during extension and positioning. Breakout and two inch extension exhibit the least amount of variation presumably because the size and volume of the bag at those increments has less influence during initial deployment.

Comparing breakout times for side airbag type, the average breakout times were 2.83 ms, 3.48 ms, and 3.93 ms for thorax, head/thorax and pelvis/thorax, respectively. Referring to Figure 4, the mean breakout times were plotted along with their 95% confidence intervals (CI). The analysis does not reveal a significant difference between head/thorax and pelvis/thorax average breakout times, but thorax bags appear to breakout and become visible quicker on average than pelvis/thorax and head/thorax bags. However, this is not true in general for individual comparisons; there are some cases for which thorax breakout times exceeded the majority of pelvis/thorax and head/thorax times. The samples of thorax bags included significantly more deployment door systems than head/thorax and pelvis/thorax bags.

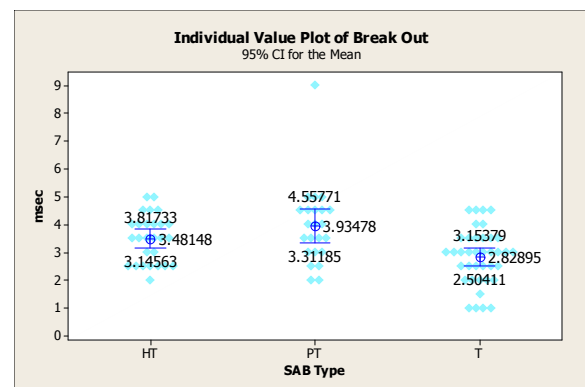
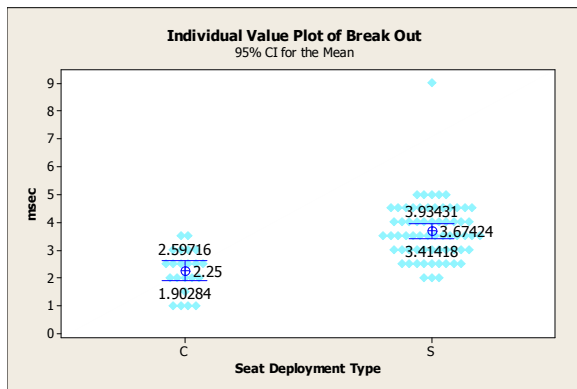


Figure 4. Breakout times for head/thorax (HT), pelvis/thorax (PT), and thorax (T) air bags.

## Deployment Mechanism

This section analyzes the deployment timing of the side airbags broken down into deployment mechanism types: deployment doors (C), and seam deploy (S). The average breakout times were calculated to be 2.25 ms and 3.67 ms for deployment doors and seam deploy, respectively. The 95% confidence interval suggests average breakout times are significantly different (Figure 5).



**Figure 5. Breakout times by deployment type: door (C) and seam deploy (S).**

As the bags extend forward, the average two inch extension times were calculated to be 4.83 ms for deployment door types and 5.08 ms for seam deploy. The 95% confidence intervals for the two deployment types overlap each other completely, so there is no indication that average two inch extension times for the two types were significantly different (Figure 6). Although the breakout times (defined as when the bag is visible) were different on average, at the time of two inch extension deployment characteristics for seam deployed side airbags and door deployed side airbags are extremely similar on average with the 95% confidence interval for seam deploy falling within the confidence level for deployment doors. This suggests that the motion of the bag forward is not, in general, influenced by the deployment mechanism type: deployment door vs. seam deploy. The average extension times at 6 inches and full extension were 6.64 and 12.26 ms, respectively, for deployment door modules and 7.51 and 15.74 ms for seam deploy modules. As bags begin to extend forward, their size and volume begin to influence the rate at which they deploy. A side airbag system that

may have very similar bag size and volume can vary in fold pattern resulting in extension time differences. The fold may be unique to balance in position timing performance with other requirements such as occupant out of position performance (Technical Working Group's Recommended Procedure for Developing Side Airbags) [2]. Slower extension does not mean an airbag system is inadequate. The performance of the complete system needs to be considered as other features of the system may compensate for extension timing. The study discussed in this paper did not analyze complete vehicle systems which would include but not be limited to vehicle specific door trim panels, intrusion rates and occupant position.

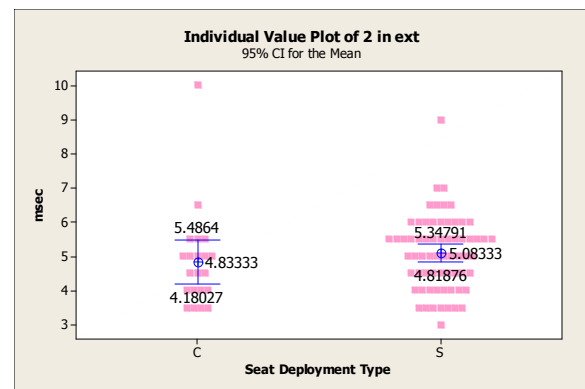


**Figure 6. Two inch extension times by deployment type: door (C) and seam (S).**

## Thorax Systems

There were a total of 38 thorax bag samples: 22 seam deploy and 16 deployment door designs. All 38 were used in analyzing breakout time. Only 37 of the 38 were used in extension time analysis due to error in sample set up which reduced the door deploy samples to 15.

The average breakout time for thorax bags was 2.22 ms for deployment door modules and 3.27 msec for seam deploy modules. Calculating and plotting the confidence intervals indicates that the breakout times are different (Figure 7).

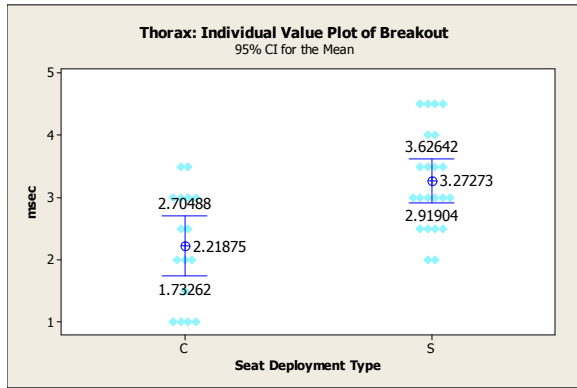


**Figure 7. Thorax module breakout times by deployment type: door (C) and seam (S).**

The average deployment time for two and six inch extension and full extension were 4.97, 6.87 and 10.83 ms, respectively, for deployment door module systems and 3.27, 4.80, and 11.5 ms for seam deploy module systems. The 95% confidence intervals were largely overlapping for the three extension times, so there was no indication that average extension times were significantly different (Table 1).

**Table 1. Thorax extension time comparison**

Extension (ms)	2 inch		6 inch		Full	
	C	S	C	S	C	S
Upper 95% CI	5.89	5.32	7.97	7.76	12.35	12.81
Average	4.97	4.80	6.87	7.07	10.83	11.50
Lower 95% CI	4.04	4.27	5.76	6.38	9.31	10.19

Ten of the thorax deployment door module systems were from seats taken from different models within sister brands.

### Head/Thorax Systems

Twenty-seven head/thorax systems, including 22 seam deploy modules and five deployment door modules, were included in the analysis. All five samples of deployment door modules were from different models within sister brands. The average breakout for deployment door modules was 2.40 ms and 3.73 ms for seam deploy modules. Calculation of the 95% confidence intervals suggested a significant difference in average breakout times (Figure 8).

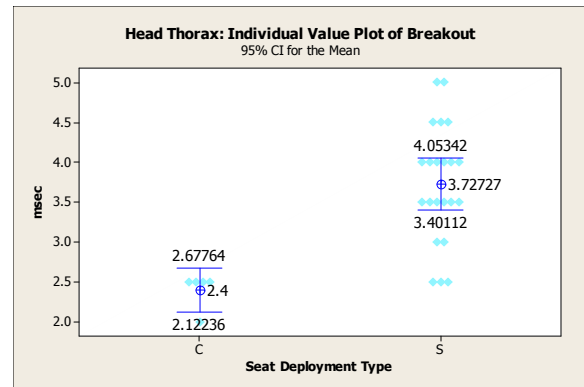


**Figure 8. Head/thorax module breakout times by deployment type: door (C) and seam (S).**

The two inch extension averages were very similar for deployment door systems and seam deploy systems at 4.60 ms and 4.91 ms, respectively. The upper and lower 95% CI were also calculated (Figure 9). The data does not indicate a significant difference in extension timing.

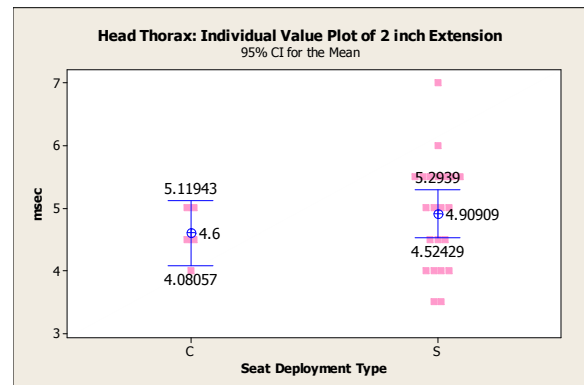


**Figure 9. Head/thorax module two inch extension times by deployment type: door (C) and seam (S).**

The six inch extension time averages were 6.30 ms and 7.09 ms for deployment door systems and seam deploy systems, respectively. Some overlap in 95% confidence intervals indicated that average extension times may not be significantly different, but timing appears more variable for seam deploy systems (Figure 10).

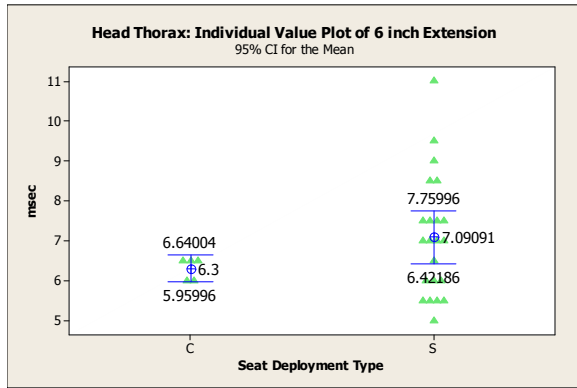


**Figure 10. Head/thorax module 6 inch extension times by deployment type: door (C) and seam (S).**

The average times for full extension in deployment door systems and seam deploy systems were 17.5 ms and 20.32 ms, respectively. The seam deploy system's 95% CI fell within the deployment door system's 95% CI (Figure 11).

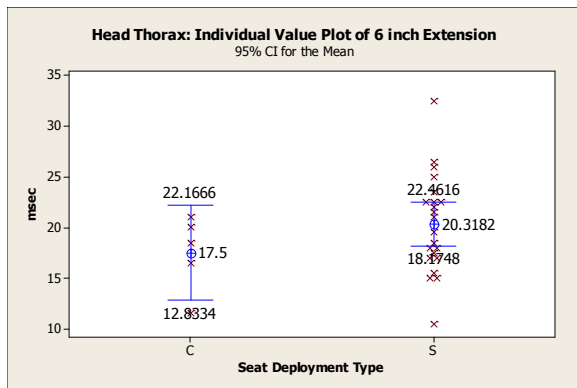


**Figure 11. Head/thorax module full extension times by deployment type: door (C) and seam (S).**

Although these results indicate that deployment mechanism may not influence extension times, the timing comparison is influenced by the limited sample size for deployment door systems. The deployment door systems are all from different models within sister brands with very similar bag sizes and shapes. The seam deploy systems are from a variety of U.S. and foreign manufacturers.

### Pelvis/Thorax Systems

There were 23 pelvis/thorax system samples. Twenty-two were seam deploy modules and one was a deployment door module. Due to the lack of

deployment door modules, the analysis between the deployment mechanisms could not be conducted.

### Bag Type Affects on Seam Deploy Modules

All three bag types had 22 samples each for deployment through the seat seam. Although the data did not indicate a significant difference between head/thorax and pelvis/thorax seam deploy breakout, thorax bags did appear to break out quicker. Average extension times at two and six inches for head/thorax and thorax systems did not appear to be significantly different, but the pelvis/thorax systems appeared to take longer to breakout and position on average. At full extension there is a significant difference between thorax, head/thorax and pelvis/thorax airbags (Figure 12). Size and volume of the airbags influence the full extension timing.

The pelvis/thorax airbags exhibited longer breakout, two inch, and six inch extension times on average. Pelvis/thorax bags are located lower in the seat back extending from above the arm rest to below the armrest to cover the occupant's torso and pelvis. The majority of thorax and head/thorax airbags are packaged at or above the armrest providing coverage to the occupant's torso in the case of thorax bags and torso and head in the case of head/thorax bags. Since the package of the pelvis/thorax bag is lower there is opportunity for interaction with child occupant out of position placement "child lying on seat" and "child lying on arm rest" as defined in the Technical Working Group "Recommended Procedures for Evaluating Occupant Injury Risk from Deploying Side Airbags [2]." The majority of thorax and head/thorax side airbags deploy above the child placement. The deployment onset of the airbag may be reduced to minimize the force applied to the child dummy. The onset of airbag deployment must be balanced to meet in position timing and to avoid causing inflation induced injuries.

Longer breakout and two and six inch extension times for pelvis/thorax bags are also likely influenced by the package length of this type of airbag. The majority of thorax and head/thorax bags are packaged such that there is a larger force (mass of the bag pack coupled with the inflator onset) concentrated on a smaller seat seam area. The pelvis/thorax bag package tends to extend along a greater seat seam length to assist in positioning above and below the armrest. This characteristic reduces the force

concentration (less bag pack) on the seat seam compared to head/thorax and thorax airbags.

### Repeat Deployments

There were 10 pairs of samples for which repeat deployment data was available (i.e. the same airbag was deployed twice). There were four sets of pelvis/thorax airbag samples and 3 sets of head/thorax and thorax airbag samples.

The average differences in breakout, two, six, and full extension were 0.40, 0.60, 1.15 and 1.76 ms, respectively. All pairs had some difference in timing throughout their deployment, with the greatest differences being exhibited at six inch and full extension. Thorax airbags had the least amount of variation in difference and pelvis/thorax had the most amount of variation in differences (Figure 13).

### Deployment Time Trends over Model Years

Deployment timing across model years appeared to be consistent (Figure 14). Some variation from year to year was present, but this variability was likely at least in part due to the limited number of samples of each type of side airbag for each model year. The plots highlight the trend of pelvis/thorax bags having greater breakout and two and six inch extension times. Full extension differences were most likely due to bag size differences.

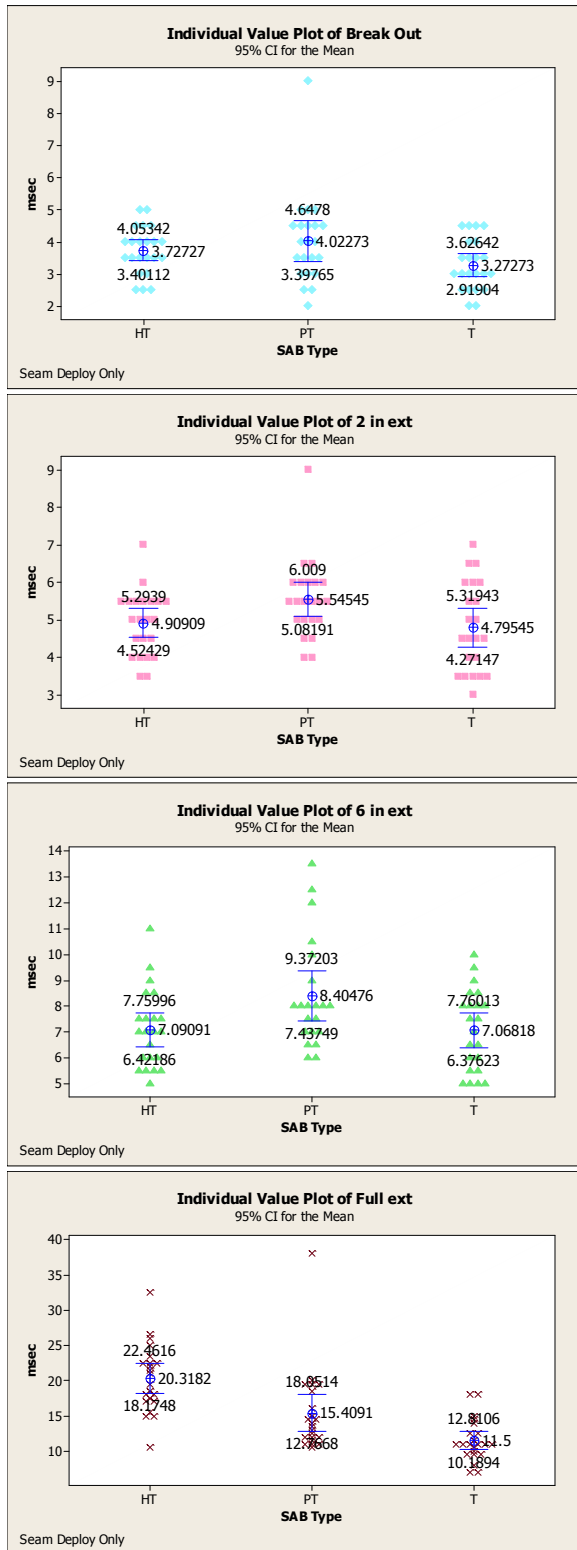


Figure 12. Seam deploy extension timing.

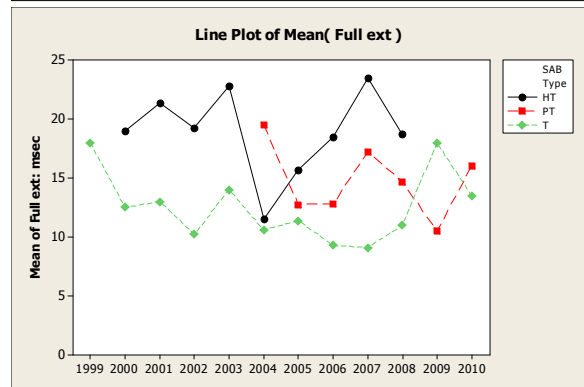
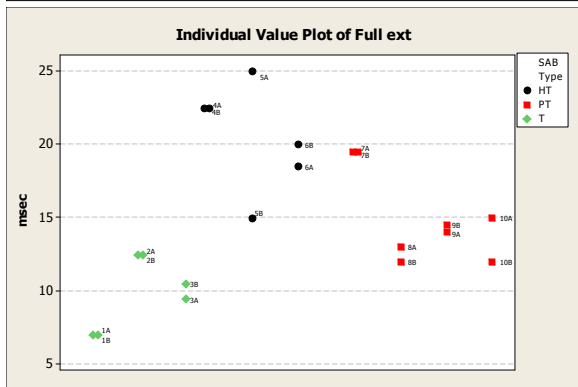
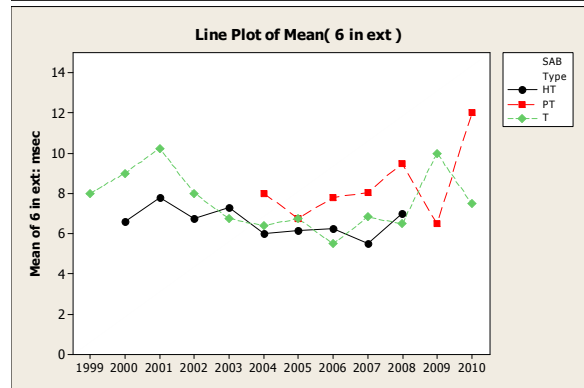
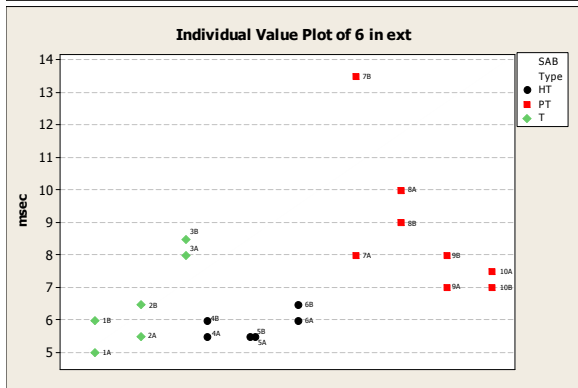
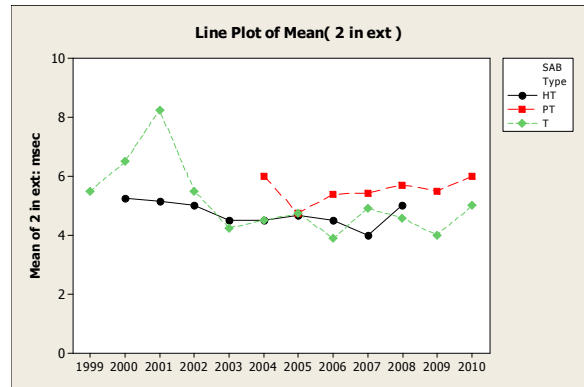
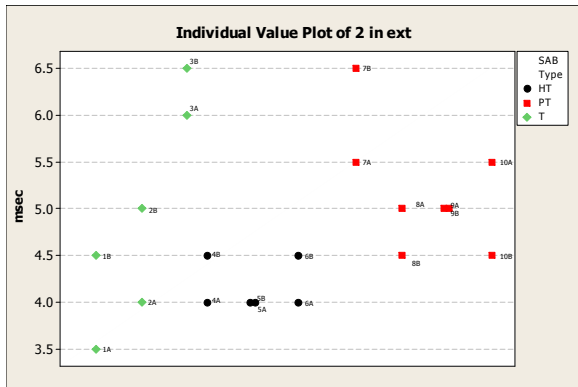
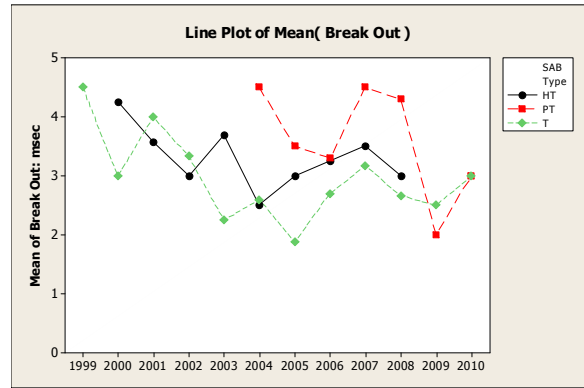
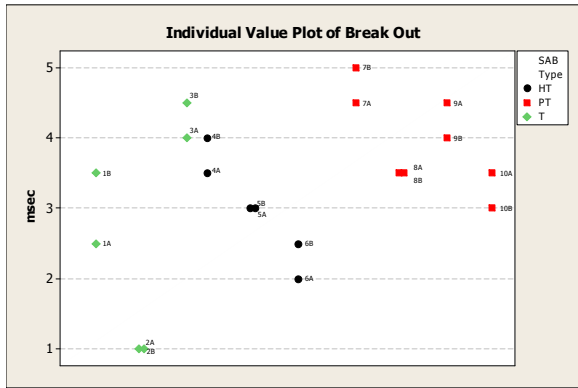


Figure 13. Repeat deployment variation.

Figure 14. Deployment timing across model years.

## CONCLUSIONS

Breakout time of pelvis/thorax and head/thorax side airbags was similar whereas thorax bags were slightly faster. Further analysis suggested deployment door modules appeared quicker than seam deploy but deployment door systems and seam deploy systems extended forward to positions at similar rates within bag types.

Regardless of the deployment mechanism, deployment door or seam deploy, the extension times to position were similar for thorax systems. Within each bag type, thorax systems had the least variability. This can be attributed to the bag size and volume being smaller relative to head/thorax and pelvis/thorax bags and bag shapes having greater similarity across brands.

Head/thorax systems appeared to have more variability at the six inch and full extension times. This can be attributed to larger bag size, volume and shape variability.

Pelvis/thorax bags trended longer for average breakout and two and six inch extension timing compared to thorax and head/thorax systems. The longer breakout time is attributed to the characteristics inherent in the design to meet vehicle level requirements.

The repeat deployments indicated there is inherent variability within the same module type. The greatest differences were apparent at six inch and full extension.

Average deployment times of airbag types across model years appeared to be relatively consistent.

## REFERENCES

1. Federal Register, Volume 73, No. 111, June 9, 2008, Rules and Regulations.
2. "Recommended Procedures for Evaluating Occupant Injury Risk from Deploying Side Airbags," The Side Airbag Out-of-Position Injury Technical

Working Group (A joint project of Alliance, AIAM, AORC, and IIHS, First Revision – July 2003).

3. "Side Impact Crashworthiness Evaluation, Crash Test Protocol (Version V)," May 2008, IIHS
4. IIHS Vehicles Equipped with Side Airbags, Retrieved 2009, from Insurance Institute for Highway Safety:  
[http://www.iihs.org/ratings/side\\_airbags/side\\_airbags.aspx](http://www.iihs.org/ratings/side_airbags/side_airbags.aspx).
5. Information retrieved 2009 from:  
<http://www.safercar.gov/portal/site/safercar/menuitem.db847bd57e3dc1f885dfc38c35a67789/?vgnextoid=c95df2905bf54110VgnVCM1000002fd17898RCRD&vgnnextrefresh=1&ID=2960>.
6. Information retrieve 2009, from:  
<http://www.carsdirect.com/research/>,  
<http://autos.msn.com/>, and  
<http://www.motoralldata.com/>

## ACKNOWLEDGEMENTS

We would like to acknowledge Autoliv America's Auburn Hills Technical Center and Kraco, L.L.C.

# PREDICTING AND VERIFYING DYNAMIC OCCUPANT PROTECTION

**Donald Friedman**

**Diego Rico**

**Garrett Mattos**

Center for Injury Research

United States

**Jacqueline Paver, Ph.D.,**

Consultant

United States

Paper Number 11-0090

## ABSTRACT

The objective of this paper is to describe the developments that provide the basis for predicting new car occupant protection in real-world rollovers.

An analytical technique has been developed for predicting a vehicle's dynamic occupant protection performance at any severity from a Jordan Rollover System (JRS) 50-vehicle rollover test database; static test roof strength, stiffness and elasticity data; inertial-influenced impact pitch orientation; size, roll moment and geometry dimensions; and occupant protection features. Only sampling, updating and verification of the JRS database will be necessary to reflect innovative construction and protection techniques until dynamic testing is implemented.

A noteworthy finding of this study was that reducing a vehicle's major radius (i.e., its shape at the windshield) was more effective in reducing rollover deaths and injuries than increasing roof strength-to-weight ratio (SWR) above 3.0.

## INTRODUCTION

Data from over 40 vehicles has been collected by the Center for Injury Research (C/IR) in two-sided static tests at 10° of pitch and 25° and 40° of roll. The Insurance Institute for Highway Safety (IIHS) statically tests vehicle roof strength at 5° of pitch and 25° of roll [1]. The C/IR has assembled a JRS test database of vehicle and dummy measurements from more than 300 rolls of over 50 different vehicles with a variety of test protocols. The National Highway Traffic Safety Administration (NHTSA) at University of Virginia (UVa) and George Washington University (GWU) has initiated finite element research programs to identify the sensitivity of rollover crash parameters and derive a real-world injury potential test protocol [2,3]. Unfortunately, modeling has its limitations and their disparities were

identified between the early published modeling and the JRS database analysis.

Injury risk results have been quantified at four levels of residual roof crush from the National Accident Sampling System (NASS) and the Crash Injury Research and Engineering Network (CIREN) databases [4,5]. General correlation of injury risk and dummy injury measure criteria in JRS tests has been confirmed. The resolution of disparities has been accomplished by considering the momentum exchange between roof intrusion and neck injury as an enhanced injury criteria that is virtually independent of small variations in occupant location. This enhanced injury criteria facilitates evaluation of occupant protection features other than roof crush (e.g., increased headroom, pretensioned belts, padding and rollover-activated window curtain airbag deployment).

Comparative consumer information about injury risk and dummy injury measure performance of vehicles can be verified to any severity protocol with readily available data. Manufacturers can use the same technique to adjust and optimize rollover injury performance during the design process to a wide range of test severity protocols and occupants.

In Australasia, Europe and America rollovers account for about 3% of the crashes, and roughly 20%, 5% and 30% respectively, of fatalities [6]. Indications are that vehicle design plays a large part in these statistics. Manufacturer's response to the competitive pressures resulting from consumer safety information is 10 to 20 years faster than the regulatory process and phase-in. This prediction technique is based on available data from comparative tests. Its predicted ratings can be verified by test sampling.

The rate of change of vehicle structural characteristics in response to front and side impact crashworthiness initiatives requires current vehicle

data, the lack or inaccuracy of which can be somewhat misleading. Nevertheless, the range of the four injury potential rating levels is spread over a range of 14 inches of residual vertical intrusion; the accuracy of verification measurements is about 10%.

A pilot program of prediction and verification by JRS testing is proposed to be accomplished in 2011. All 2012 model year vehicles statically tested by IIHS will be dynamically rated at the four injury levels and verified by sample dynamic testing.

This C/IR analysis is part of an ongoing effort to evaluate vehicle rollover test parameters beyond the previously-investigated sensitivity of roof strength-to-weight ratio (SWR) and impact pitch angle to residual and dynamic roof crush and injury potential.

The purpose of this paper is threefold:

- (1) to predict the dynamic injury potential performance of dynamically-untested vehicles from static tests and vehicle geometry;
- (2) to contribute to the effort to develop a real-world rollover test protocol; and
- (3) to alert government, industry and safety advocates of the lessons learned and their application to other modes, systems and occupants.

## PARAMETER REVIEW AND ANALYSIS

### Development of a Real-World Test Protocol

Rollover crash statistics are summarized in Figure 1. They indicate that 94% of people in rollovers are not seriously injured and that the remaining 6% are divided; about 2% each between fatalities, severe and serious injuries in 2-roll events.

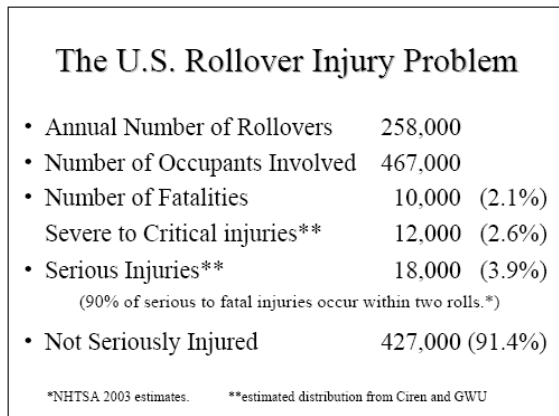
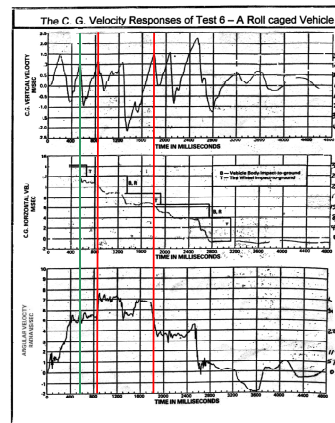


Figure 1. Typical rollover statistics.

More than 400 rollover crash investigations identify that 80% of catastrophic injuries (AIS = 4+) occur on the far side. A study of 283 serious injury NASS rollovers exhibited damage to the hood or the top of the fenders, indicating that the roll occurred with greater than 10° of pitch [7].

In the Malibu dolly rollover tests of strong-roofed vehicles at 32 mph, the roof impact speed was 21 mph with a 4-inch drop height and an average roll rate of about 6 rad/sec with 2 rolls. Figure 2 shows data from Malibu Series 1 Test 6.



GM Malibu I  
Test 6  
(All data from GM  
Discovery)

Near Side Contacts:  
(Green Lines)  
575 ms = 2.2 mph  
1500 ms = 2.5 mph

Far Side Contacts:  
(Red Lines)  
836 ms = 2.7 mph  
1802 ms = 3.1 mph

Figure 2. GM Malibu I test no. 6.

Two test fixtures were developed and used to evaluate vehicle rollover performance:

- A two-sided 10° of pitch platen test, and
- A repeatable dynamic rollover machine.

The M216 two-sided fixture applies forces to the roof on one side and then the other at force angles of 10° pitch and 25° and 40° roll, respectively. The M216 results indicate that most vehicles are about half as strong compared to the FMVSS 216 test results at 5° of pitch, as shown in Figures 3 and 4.

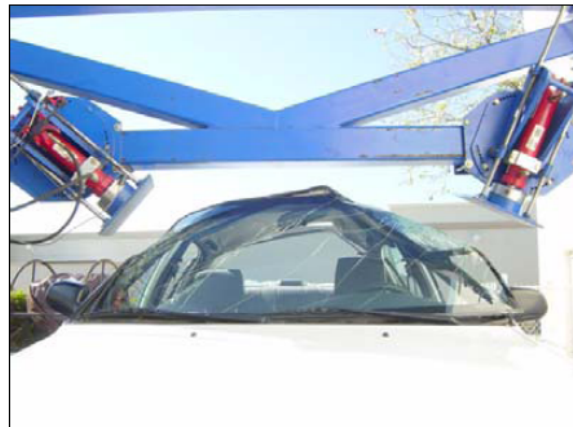


Figure 3. M216 two-sided static test machine.

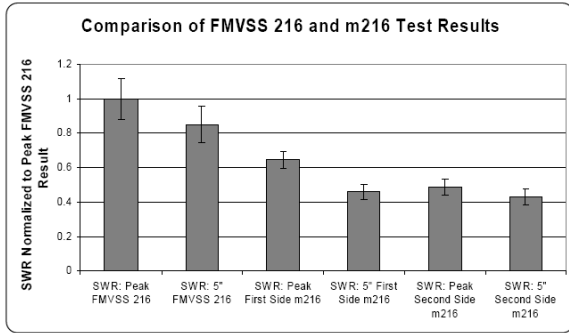


Figure 4. Two-sided NHSB/M216 data.

The JRS rollover fixture, shown in Figure 5, is a laboratory device capable of rolling full-size vehicles to 6,000 lbs at 300°/sec, dropping them 4 to 9 inches onto a 20 mph moving roadbed and measuring the roadbed forces and roof intrusion [8].

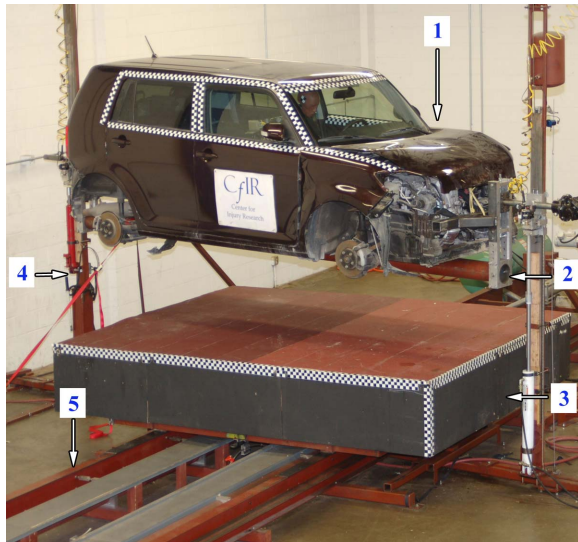


Figure 5. The JRS fixture key components: 1) vehicle, 2) cradle/spit mount, 3) moving roadbed, 4) support towers, 5) coupled pneumatic roadbed propulsion and roll drive.

With this data, these tools and tests on more than 50 vehicles, our analysis of the segments of a rollover from the loss of control, yaw to trip, trip and ballistic trajectory identified the segment 5 of Figure 6 as the most probable source of severe injury.

Segments of the Roll Sequence	Potential for Serious-to-Fatal Injury
1. Vehicle loss of control	Non-injurious
2. Yaw-to-trip orientation	Occupants move laterally out-of-position
3. Trip	Exacerbates lateral out-of-position
4. Roll rate	Potential for far-side injury and ejection
5. Vehicle roof impacts with the road	Potential for severe head/neck/spine injury
6. Wheel/underbody contacts	Potential for lower spine injuries
7. Suspension rebound and second roll lofting	Non-injurious
8. Near-side roof impact, roll slowing ejection	Potentially injurious
9. Far-side impact	Potentially injurious
10. Wheel contact to rest	Non-injurious

Figure 6. 10 segments of the roll sequence.

The result was the proposed “Real World Protocol” in Figure 7.

The Proposed Real-World Rollover Protocol
• Road speed 33 kph ± 7 kph (20 mph ±5 mph),
• Roll rate @ near-side impact 270 °/sec ± 20%
• Pitch 10° ± 5°
• Roll angle at impact 135° ± 10° and/or 185°
• Drop height 10 cm to 22 cm (4 to 9 inches)
• Yaw angle 15° ± 15°
• Dummy tethered @ 1 g and 60° toward the near side.

Figure 7. Updated proposed test protocol.

### Development of Injury Measures and Criteria

Two studies 25 years apart indicate that spinal distortions and fractures, primarily in the lower neck are typical rollover injury patterns. The 1983 Allen study of severe human neck injuries attributed 60% to flexion, 30% to extension and 10% to axial compression [9]. The 2009 Ridella study of CIREN cases indicates that a predominance of serious injuries involved the spine as shown in Figure 8 [10].

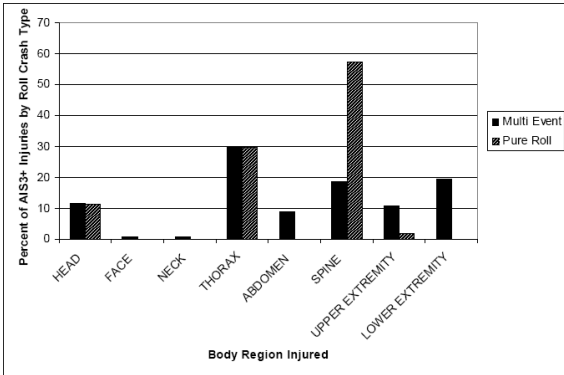


Figure 8. CIREN distribution of rollover injuries.

The measures that proved to be the most significant indicators of injury during a rollover event were the lower neck bending moments, measured at the C7-T1 level and the duration of neck bending. You can imagine a boxer receiving a blow to the face, although this could result in a large lower neck bending moment the boxer’s head would move away and the peak moment would reduce rapidly. No lower neck injury would occur because the load was not sustained and did not cause the neck to bend. Lower neck bending injuries require that a large enough moment be sustained for the duration that flexes the neck beyond its physiologic range of motion [11].

Figure 9 shows the mechanism of a common neck bending Injury, a bilateral facet dislocation. It is initiated by significant flexion of the neck which dislocates the spine. It concludes with the neck contracting, pulling the spine forward and down locking the facets [11].

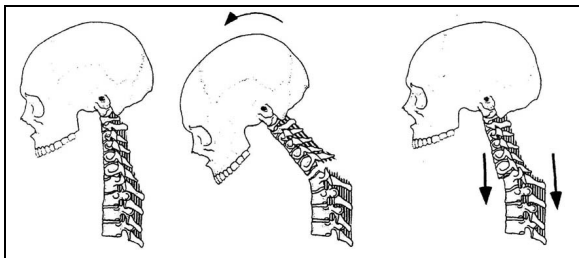


Figure 9. Hyperflexion neck injury mechanism from Pintar, et al.

This and other neck bending injuries can be predicted by looking at the area under the lower neck bending moment curve. This area is akin to the Head Injury Criteria used to determine the injury potential from a head impact. It takes into account not only the peak load but also the duration of that load.

Roof crush and the loss of headroom are directly related to the bending moment measured in the neck. In a study of over 10,000 rollover accidents it was found that the probability of spine injury increased with increased residual roof crush [12]. Table 1 is the criteria for seriously injurious peak forces in flexion and bending [13].

Table 1. Peak lower neck IARV’s for a 10% probability of an AIS≥3 injury

Neck Type	Neck Loading Direction	Axial Fz (N)	Moment My (Nm)	Moment Mx (Nm)
Production Hybrid III	Flexion	6,000	380	
Production Hybrid III	Lateral Bending	6,000		268
“Soft” Neck	Flexion	~2,000	~90	
“Soft” Neck	Lateral Bending	~1,640		~59
Human/Cadaver	Flexion	~1,500	~58	

**JRS injury criteria and measurements** In JRS tests roof movement was measured at four locations in the vehicle. The peak dynamic roof crush and residual roof crush were determined for each roll. A sampling of the JRS rollover database is provided in Appendix 1.

Figure 10 shows the 2009 Mandell studied the NASS/CIREN database and established a four level probability of injury risk as a function of vertical residual crush to 14 inches.

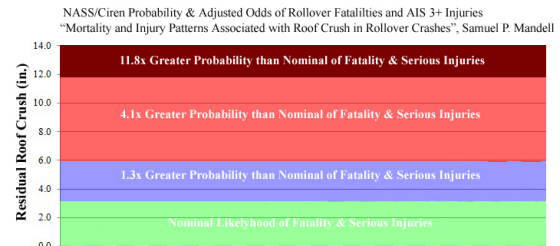


Figure 10. NASS/CIREN probability and adjusted odds.

Results of pendulum tests indicate that peak axial neck force is not a good indicator of injury to the spine. This is due to the very stiff axial and vertically-oriented neck of the Hybrid III dummy.

Flexion injury occurs from a moment applied by a 4 to 9-inch impact stroke to the top/back of the head over 40 to 140 ms [14]. Dummy peak forces and moments grossly underestimate and misrepresent the extent and duration of the required flexion injury intrusion in a rollover. That is also why the vertical residual crush correlates so well with the Integrated Bending Moment (IBM) [15].

The IBM criteria is [15] related to the amplitude and duration of the forces and moments. It integrates the resultant moment (lower My and lower Mx) over the time interval where it is greater than 30 Nm to a maximum of 140 ms for the original Hybrid III neck and proportionately less for the soft neck.

It is clear from the JRS test videos of the dummy head/neck motion that the roof of the production vehicles interact with the head of the soft neck dummy in a much more severe manner. The reinforced roofs provided much more protection by maintaining the occupant survival space. This is illustrated by superimposing the lower neck bending moment of an identical pair of production and reinforced Ford Explorers. The IBM is the respective areas under the bending time histories curves in Figure 11.

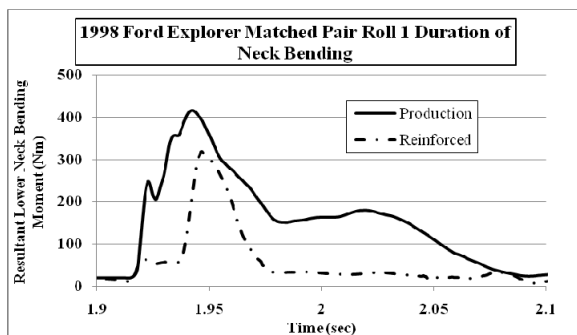


**Figure 11. 1998 Ford Explorer matched pair testing roll 1.**

In the JRS tests, the production vehicles sustained twice as much residual roof crush than the reinforced vehicles. This equates to an average of 5 inches more roof crush during the event.

The “soft” low musculature modified Hybrid III dummy neck shown in Figure 12 was literally broken at the lower neck load cell mount as a result of 11 inches of roof crush in this SWR 6.8 vehicle.



**Figure 12. Soft neck of hybrid III dummy.**

**Controlled Rollover Impact System (CRIS) tests** Published 15 ms video clips and neck injury measure data of production and reinforced 1998 Crown Victorias tested on the CRIS show identical results in roll-caged and production vehicles [16]. In the video dummy movement up to the point of initial roof contact is nearly identical. However, the videos and data to 140 ms tell a very different story. Figure 13 show the interior views. The production vehicle with the grossly bent neck is shown on the left. The deformation of the roof in the production vehicle applied a force to the head of the dummy and caused the neck to bend significantly. No neck bending was observed in the reinforced vehicle (right). Estimated roof crush is 2 inches for reinforced and more than 10 inches for the production vehicle.



**Figure 13. Production vehicle’s neck severely bent after 40 ms (left) and the roll-caged vehicle’s non-injurious neck bending (right).**

The peak lower neck bending moments measured in the production vehicles was 30 to 56% greater than in the reinforced vehicle. The duration of neck bending in the production vehicle was 150% greater for the reinforced vehicles. Dummies in the production vehicles were trapped 2 out of the 5 times in injurious positions that could limit breathing and inhibit safe evacuation [16].

**Critical parameters for structural intrusion**

The mining of the JRS database for correlations of vehicle structural parameters with residual roof crush has so far identified a few of high importance and weighting in predicting injury risk. These are in order of priority SWR, major radius, pitch, elasticity and near- and far-side road load effects.

**Critical parameters for dummy injury**

**measures** Residual and dynamic crush and crush speed are probably the most important parameters affecting neck bending and head injuries respectively. [ref] While the drop height can be important, all data indicates that automobiles and SUVs in rolling over stay close to the ground and with belted occupants have little effect compared to intrusion. The headroom in vehicles varies by about 4 inches (from 3 to 7 inches). Therefore in terms of strong-roofed vehicles with crush in the order of 6 inches or less

headroom can be significant. That same effect applies to lap and shoulder belt performance whose range is 3 to 5 inches. Pre-tensioned belts can reduce the excursion by 2 inches. Rollover-activated window curtain airbags can be important in the likely case of out-of-position far-side occupants, who may be out of their shoulder belt from yaw-to-trip forces and rebound rapidly to strike the roof rail and window as the roof crushes [17].

**Normalization procedures** It appears clear that the choice of a particular compliance and/or NCAP test protocol is unlikely to be a technical decision. So, it is important to be able to translate results from one protocol to characterize another. It is also important to characterize and estimate the performance of similar vehicles in a real-world crash. To that end, normalization procedures have been developed to adjust or predict the injury risk potential and injury measures for alternate road speeds with proportional roll rates, different pitches and independent road speeds and roll rates.

**Structural Analysis of the JRS Database**

The JRS database now has about 50 vehicles and about 300 rolls. The data was collected over the 6 operational years of the machine, where procedures, instrumentation, dummy characteristics, injury measures and criteria were changed as we learned and vehicle structures improved. In the following charts, roll 1 is at 5° pitch, roll 2 is at 10° pitch, and analyses are based only on vehicles with the same protocol whose measurements could identify correlations and their slope as it affected residual crush. In many cases this limited the number of vehicles to as few as 10. This is thought to be sufficient for a reliable insight into the factors which affect rollover injury potential, but the reader is cautioned to consider the outcomes preliminary until other scientists duplicate the results.

**SWR vs. cumulative residual roof crush** Figure 14 shows the generic injury measures with about the same slope as a function of SWR to 4 and injury risk to about 4 or 5%. The chart incorrectly projected the JRS test data to an SWR of 5, but subsequent tests of vehicles with SWR above 4 and to 6.8 correlate with a polynomial relationship primarily because one vehicle with an SWR of 6.8 had 10 inches of crush. In a companion paper 2011-0405 this set of data is

used to demonstrate the range of these parameters that can be used to reasonably predict vehicle performance.

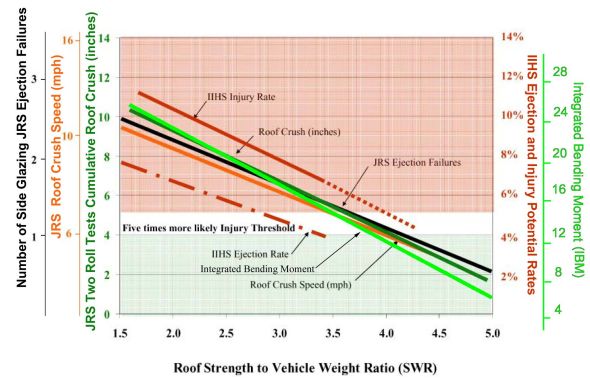


**Figure 14. Roll 2: cumulative residual crash and major radius.**

Other characteristics, particularly vehicle geometry and elasticity, have been identified to account for this non-linearity [18]. The current cumulative residual crush chart versus SWR is shown in Figure 15. This is still consistent with IIHS’ original statistical slopes of SUVs and small passenger cars to an SWR of 4 [19].

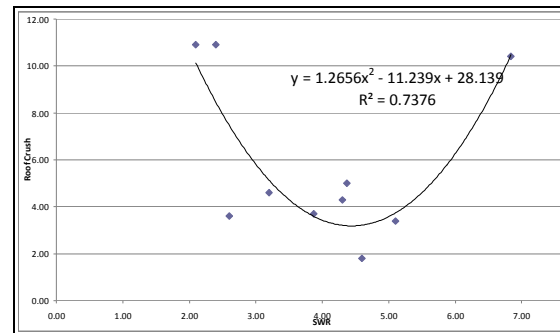


**Figure 15. SWR vs. current cumulative residual roof crush.**

**Major radius and cumulative residual crush**

The major radius of a vehicle is the distance between the CG axis and the roof rail at the A-pillar. Figure 16 identifies the vehicles involved, their major radii and the cumulative residual crush at the A-pillar in roll 1 and roll 2.

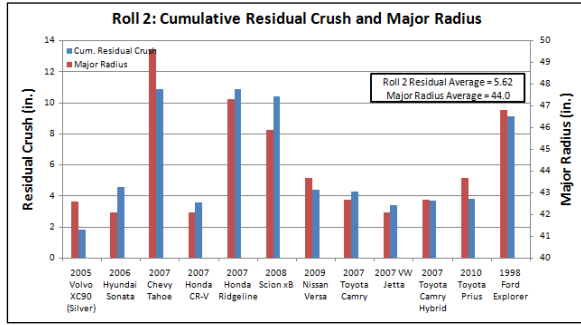


Figure 16. Major radius and cumulative residual crush.

Figure 17 is a scatter plot of the Major radii for those vehicles and indicates a high correlation with the cumulative residual crush of roll 1 and 2. The relationship is particularly striking for the slope which indicates that each 1.2 inches of major radius affects the residual crush by 1 inch. This is an enormous effect easily doubling the magnitude of residual roof crush between SUVs and automobiles. Considering IIHS studies to reduce risk by 24% for each increment of SWR, reducing the major radius of SUVs from a typical 46 inches to that of automobiles, the XC-90 and CR-V of 42 inches reduces intrusion by 3.3 inches [19].

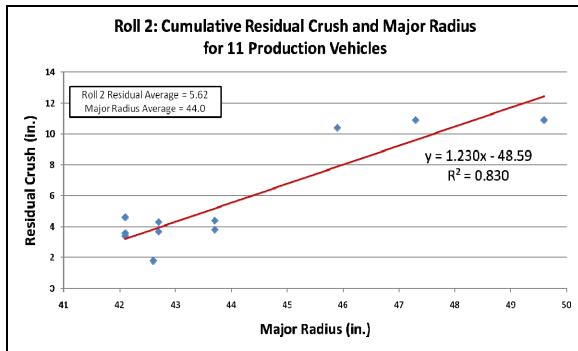


Figure 17. A scatter plot of the cumulative residual crush of roll 1 and roll 2 vs. major radius.

**Elasticity and cumulative residual crush**

Another significant effect appears to be the result of high strength steels used in the most updated vehicles. This effect became noticeable in 2007 when improved compliance with FMVSS 214 also increased the vehicle’s roof SWR.

To interpret the data, vehicles with an elastic structure like the 70% Volvo XC-90 have a lesser effect on residual crush than vehicles like the 30% Scion xB which buckled and collapsed. Figure 18 shows that an elastic structure has a significant

correlation and slope with residual crush. The weighting compared to SWR and major radius is as yet unknown.

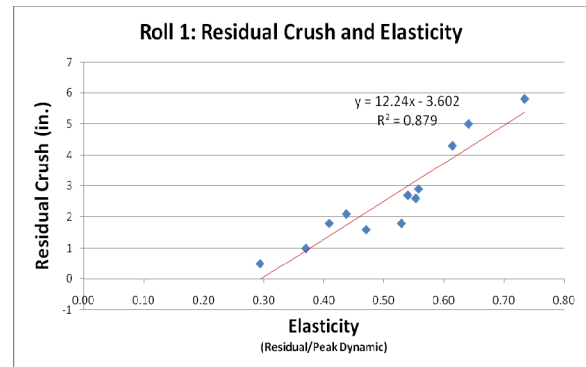


Figure 18. Roll 1 residual crush and elasticity.

**Injury Measure Analysis of the JRS Database**

**Integrated Bending Moment (IBM) and residual crush**

From an injury measure point of view the IBM correlates well with residual crush, with injury risk at 3.5 inches, with the 10% probability of AIS = 3+ IARV injury measure and seems insensitive to small variations of dummy head position. Three and a half (3.5) inches of residual crush corresponds to an IBM of 13.5 as shown in Figure 19.

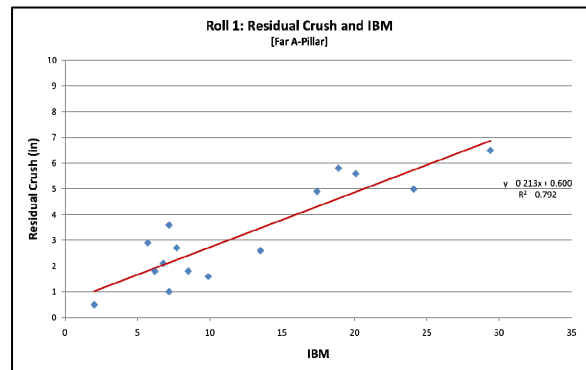


Figure 19. Roll 1: Residual crush and IBM [far A-pillar].

**Headroom vs. residual crush**

When considering dummy injury measures headroom is significant as shown in Figure 20.

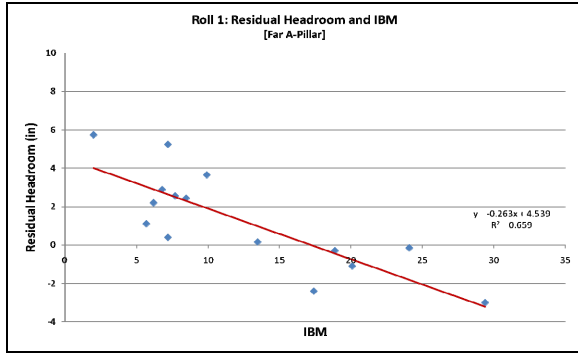


Figure 20. Headroom vs. residual crush

**Belt loads, excursion and pretensioning** Belt loads and corresponding excursions have been measured on many tests but not yet correlated with IBM for this paper. Excursion varied from 3 to 5 inches with occupant size and weight. Pretensioning reduces excursion by about 2 inches.

**Road speed and proportional roll rate** There is a high correlation between average residual crush and road speed with proportional roll rate as shown in Figure 21. The roll rate proportionality comes from the JRS I configuration where the road speed and roll rate are geared together. One test was performed with an alternate ratio resulting in a 15 mph and 303 deg/sec roll rate.

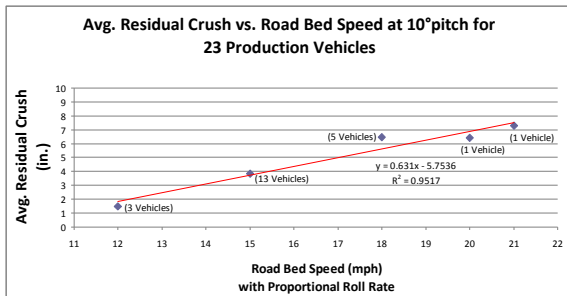


Figure 21. Average residual crush vs. road bed speed.

**Road speed vs. roll rate** There is insufficient data to resolve the contribution of road speed and roll rate separately. The data that is available is shown in Table 2. A few identical separate vehicles have been tested under slightly different circumstances. The first of a pair of GMC Jimmys, at 5° of pitch, when tested at 10° of pitch shows a 32% increase in dynamic intrusion.

Table 2. Road speed vs. roll rate

	Test #	SWR	Protocol		Far A				
			Pitch	Road Speed	Roll Rate at impact (deg/s)	Peak Dynamic (in)	Residual (in)	Speed (mph)	
1996 GMC Jimmy	1	1.6	5	15	188	6.3	4.2	5.2	
2000 GMC Jimmy	1	1.6	10	15	174	8.3	7.2	6	
Percent Increase							32	71	15

	Test #	SWR	Protocol		Far A				
			Pitch	Road Speed	Roll Rate at impact (deg/s)	Peak Dynamic (in)	Residual (in)	Speed (mph)	
1999 Hyundai Sonata	1	2.8	5	15	172	6.4	4.5	5.5	
1999 Hyundai Sonata	1	2.8	10	21	275	10.9	7.3	13.2	
Percent Increase							70	62	140

	Test #	SWR	Protocol		Far A			
			Pitch	Road Speed	Roll Rate at impact (deg/s)	Peak Dynamic (in)	Residual (in)	Speed (mph)
1998 Ford Explorer	1	1.9	5	15	183	7	4.3	4.4
2000 Ford Explorer	1	1.9	5	15	200	8.7	5.9	6.3
1998 Ford Explorer [Reinforced]	1		5	15	177	1.9	0.8	4.2

The first of a pair of Hyundai Sonatas shows a 70% increase in dynamic intrusion for both an increase to 10 deg pitch and a 21 mph road speed with proportional roll rate.

Lastly are listed three Ford Explorers (with and without sun roofs accounting for the difference in intrusion), one vehicle was reinforced and had 25% of the roof intrusion of the production vehicles. This confirmed that increased roof strength reduces intrusion.

The point is that if 10° pitch accounts for 30% (the Jimmy's) and pitch and speed with proportional roll rate (the Hyundai's) accounts for 70%, then the speed and proportional roll rate accounts for 40% for a speed and proportional roll rate increase of 40% (from 15 to 21 mph) as shown in Figure 21.

Still unresolved is whether that 40% increase is from increased road speed or roll rate. There is only one test at 15 mph, 5 deg pitch, 125 deg impact angle and 303° roll rate, a 1999 Camry, which could resolve that issue. The other tests were at 145 deg and 190 deg/sec. Previous 125 deg impact angle tests resulted in nearly equal near and far side road loads and intrusion. For the 1999 Camry the road loads and intrusion were very much greater on the far side. The 1999 Sonata and Camry are both estimated to have SWRs of about 2.8, yet the Camry residual crush of 7 inches shown in Figure 22 suggests that low impact angle and high roll rate result in a similar 7.3 inches of intrusion as the 21 mph and 280 deg/sec test. Finite element tests of a strengthened (SWR = 3.9) Explorer in a private communication indicated about the same dynamic intrusion in combinations of 40% increased speed and roll rate.

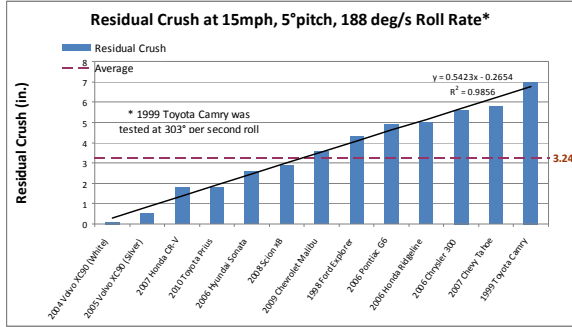


Figure 22. Residual crush at 15mph, 5° pitch, 188 deg/s roll rate.

**Pitch and CG location** Pitch has been shown by JRS tests to be a highly sensitive parameter to roof crush. The difference in roof crush between 5 deg of pitch and 10 deg of pitch in JRS tests has typically been shown to be quite substantial. Most JRS tests are done in a 2 roll sequence in which the first roll is performed at 5 deg of pitch and the second roll is performed at 10 deg of pitch. The question is what vehicle parameter or characteristics would make a vehicle roll with a large degree of pitch. One explanation is that generally fully-loaded vehicles roll with little or no pitch. Taking this into consideration it would make sense that the location of the center of gravity (CG) of a vehicle relative to its A-pillars and pivot point is an important characteristic in determining the likelihood that a vehicle would roll with a pitch of 10° or greater. In theory, a vehicle whose CG is farther back from its A-pillars and behind its pivot point will likely roll flat on its roof. Thus the normal force of the road would be spread out over a larger surface area and result in less roof crush. A vehicle whose CG is closer to the A-pillars and forward of the pivot point will have a greater likelihood of rolling with a substantial pitch and thus result in greater roof crush. Both of these situations are illustrated below in Figure 23.

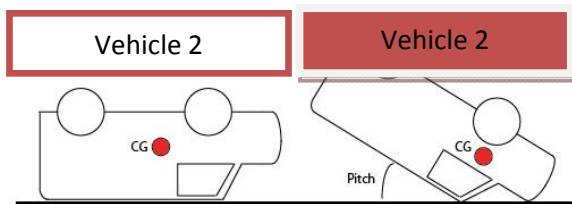


Figure 23. Illustration of the two rollover situations.

The distance between the CG and the A-pillar were calculated for several unloaded vehicles and tabulated in columns 1 to 4 in Table 3. (Note that a negative horizontal distance value implies that the

CG is behind the A-pillar and vice versa for a positive value.)

Table 3. CG distances relative to A-pillar

Vehicle	Horizontal Distance between CG and Top of A-pillar (in.)	Vertical Distance between CG and Top of A-pillar (in.)	Normal (90°) Distance between CG and Top of A-pillar (in.)	Horizontal Distance between CG and Virtual A-pillar (in.)
2008 Scion xB	-12.7	38.2	40.3	-5.7
2009 Chevrolet Malibu	-2.7	34.6	34.7	3.3
2009 Nissan Versa	-5.8	36.8	37.3	0.7
2007 Honda CR-V	-6.3	39.7	40.2	0.7
2007 Toyota Camry Hybrid	-1.4	35.2	35.2	4.7
2007 Chevy Tahoe	-17.8	46.3	49.6	-9.2
2007 Volkswagen Jetta	-4.4	34.6	34.9	1.7
2006 Honda Ridgeline	-16.2	43.7	46.6	-8.1
2006 Chrysler 300	-14.4	35.2	38.0	-7.8
2005 Volvo XC90	-10.1	42.1	43.3	-2.5

Given a situation in which the roof crush on the A-pillar of a vehicle is 6 inches and the roof crush on the B-pillar is 4 inches, the CG relative to the horizontal position of the virtual (undeformed) A-pillar was calculated and tabulated in column 5 of Table 3. Ten degrees of pitch was assumed given the 6 inches and 4 inches of roof crush on the A-pillar and B-pillar. In analyzing the data in column 5 from Table 3, the CG moves horizontally closer relative to the virtual A-pillar and in some cases moves forward of the pivot point causing the vehicle to want to pitch even further forward. Using the data for the horizontal distance between the CG relative to the A-Pillar at 10° of pitch and the residual crush for each respective vehicle in Roll 2 of the JRS test, a scatter plot was created and shown below in Figure 24.

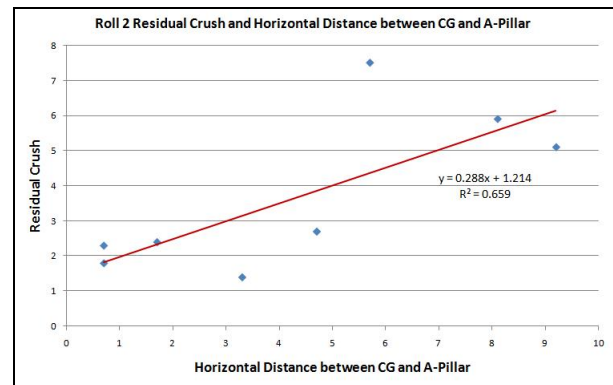


Figure 24. Roll 2 residual crush and horizontal distance between CG and A-pillar.

The data in Figure 24 implies that the greater the distance between the CG and the A-pillar at 10° of pitch, the more residual roof crush the vehicle experienced. The R<sup>2</sup> value of the linear regression

line is 0.659 meaning there is some correlation between the two. A further analysis shows Figure 24 only takes into consideration the magnitude of the distance between the CG and the A-pillar at 10° of pitch. The three vehicles that experience the most residual crush, the 2008 Scion xB, 2007 Chevy Tahoe, and the 2006 Honda Ridgeline, actually have their CG's behind the A-pillar at 10° of pitch. Their initial unloaded CG's are horizontally the farthest back of all the vehicle and even at 10° of pitch it is not enough to move their CG's forward of the A-pillar and pivot point. In reality these three vehicles are unlikely to roll with pitch because even at a forced pitch of 10° by the JRS, the CG, although it moves forward by a fair amount, is still behind the pivot point. From prior analyses we know that the 2008 Scion xB experiences a large residual crush due to its square profile and the 2007 Chevy Tahoe experiences large residual crush due to its weak roof structure with a SWR of 2.1 and because it has one of the largest major radiuses as shown previously in Figure 16 [20].

## CONCLUSIONS

C/IR previously showed that residual crush decreases with SWR, ejection potential decreases with SWR greater than 3.0 and crush increases with 10° pitch. This analysis indicates that:

- Momentum derived hybrid III dummy injury measures (IBM) correlate with residual crush, injury risk and IARV injury measure criteria.
- Increased major radius results in increased injury potential independent of SWR,
- Elastic structures reduce injury potential.
- Increasing road speed and proportional roll rate increases injury potential
- Shifting CG Rearward (Rear seat passengers or load) reduces injury potential by reducing pitch propensity.

C/IR has proposed a real world rollover test protocol and demonstrated how to adjust (normalize) the 50 dynamic test already conducted to predict dynamic performance within any protocol. The University of Virginia sponsored by NHTSA has been given responsibility to developed a real world protocol. [21] By virtue of the relationships developed here, vehicle performance may be roughly predicted for most variations in the protocol.

## Lessons Learned

**Frontal impact protection** The reduction in musculature and orientation of the Hybrid III neck as developed for rollover testing appears to explain anomalies in frontal and side impact protection. For instance the IIHS reported an increase in fatalities with advanced airbags compared to the immediately previous designs [22]. An identical set-up for frontal impacts at typical airbag deployment ignition speeds of 15 mph is shown with the Hybrid III dummy with its original and reduced musculature neck in Figures 25 and 26, respectively. The flexibility of the reduced musculature puts the dummy's head in close proximity to the deploying airbag with serious injury consequences if the airbag fires and from striking the wheel hub if it doesn't.



Figure 25. Hybrid III dummy with original musculature neck.



Figure 26. Hybrid III dummy with reduced musculature neck.

**Side impact protection** Window curtain airbags are now in use as head impact protection for side impacts and as such deploy at 100 to 120 mph. Rollover activated window curtain airbags for

ejection protection deploy at 25 to 50mph. If the side impact airbag is activated during a rollover because of the vehicle side being in proximity to the ground while the occupant is “up and out” against the roof rail the result may be head and brain trauma, diffuse axonal injury, and coma. A solution would be to have two or variable inflators and change the rollover sensing algorithm to override and inhibit the side impact deployment gas generator.

## REFERENCES

- [1] Brumbelow, M. and B. Teoh. 2009. “Roof Strength and Injury Risk in Rollover Crashes of Passenger Cars and SUVs.” SAE Government Industry Meeting. February 2009.
- [2] Tahan, F., K. Digges and P. Mohan. 2010. “Sensitivity Study of Vehicle Rollovers to Various Initial Conditions – Finite Element Model Based Analysis.” ICRASH Conference, Washington, D.C., September 2010.
- [3] J. Kerrigan, Government Industry Meeting PPT. 2009.
- [4] <http://www-nass.nhtsa.dot.gov/nass/cds-new/SearchForm.aspx>
- [5] <http://nhtsa-nrdapps.nhtsa.dot.gov/bin/cirenfilter.dll>
- [6] Australian Transport Safety Bureau. “International Road Safety Comparisons: The 2004 Report – A Comparison of Road Safety Statistics in OECD Nations and Australia.” 2006.
- [7] Nash, C. and A. Paskin. 2005. “Rollover Cases with Roof Crush in NASS.” 2005 Summer Bioengineering Conference. Vail, Colorado. June 22-26, 2005.
- [8] Bish, J., J. Caplinger, D. Friedman, A. Jordan, C. Nash. 2008. “Repeatability of a Dynamic Rollover Test System” ICRASH Conference, Kyoto, Japan, July 21-25, 2008.
- [9] [http://www.gm.com/company/corp\\_info/history/gmhis1970.html](http://www.gm.com/company/corp_info/history/gmhis1970.html)
- [10] Ridella, S.A. and A.M. Eigen. 2008. “Biomechanical Investigation of Injury Mechanism in Rollover Crashes from the CIREN Database.” IRCOBI Conference, Bern, Switzerland, September 17-19, 2008.
- [11] Pintar, F.A., L.M Voo, et. al. 1998. “Mechanisms of Hyperflexion Cervical Spine Injury.” IRCOBI Conference, Goteborg, September 1998.
- [12] Paver, J.G. and D. Friedman, et. al. 2010. “The Development of IARV’s for the Hybrid III Neck Modified for Dynamic Rollover Crash Testing.” ICRASH Conference, Washington, D.C., September 22-24, 2010.
- [13] Mertz, H.J, P. Prasad, et. al. 2003. “Biomechanical and Scaling Bases for Frontal and Side Impact Injury Assessment Reference Values.” Stapp Car Crash Journal, Vol. 47, 155-188.
- [14] Paver, J.G., et. al. 2008. “Rollover Roof Crush and Speed as Measures of Injury Potential vs. the Hybrid III Dummy.” ICRASH Conference, Kyoto, Japan, July 22-25, 2008.
- [15] Paver, J.G., et. al. 2008. “Rollover Crash Neck Injury Replication and Injury Potential Assessment,” IRCOBI Conference, Bern, Switzerland, September 17-19, 2008.
- [16] Moffatt, E.A. et. al. 2003. “Matched-Pair Rollover Impacts of Rollcaged and Production Roof Cars Using the Controlled Rollover Impact System (CRIS).” SAE World Congress Conference, 2003.
- [17] Fildes, B. and K. Digges. 2009. “Occupant Protection in Far-Side Crashes” National Crash Analysis Center, GWU, Monash University Accident Research Centre, June 2009.
- [18] Friedman, D., S. Bozzini, J. Paver. 2010. “Status of Comparative Dynamic Rollover Compliance Research and Testing.” ICRASH Conference, Washington, D.C., September 22-24, 2010.
- [19] Brumbelow, M. et. al., 2008. “Roof Strength and Injury Risk in Rollover Crashes.” Insurance Institute for Highway Safety. March 2008.
- [20] Friedman, D., G. Mattos, J.G. Paver. 2010. “Characterizing the Injury Potential of a Real World Rollover.” ICRASH Conference, Washington, D.C., September 22-24, 2010.
- [21] Kerrigan, J.R. et. al. 2008. “Test System, Vehicle, and Occupant Response Repeatability Evaluation in Rollover Crash Tests: The Deceleration Rollover Sled Test.” ICRASH Conference, Washington, D.C., September 22-24, 2010.
- [22] Brumbelow, M.L., E.R. Teoh, D.S. Zuby, A.T. McCartt. 2008. “Roof Strength and Injury Risk in Rollover Crashes.” Insurance Institute for Highway Safety, March 2008.
- [23] Rico, D. “Parameter Analysis” JRS Dynamic Correlations for IARV = 0.456 and for IBM =0.708

APPENDIX 1.

Vehicle	Headroom Measurement (inches)	Max. Lap Belt Load Roll 1 (lbs)	Max. Shoulder Belt Load Roll 1 (lbs)	Max. Lap Belt Load Roll 2 (lbs)	Max. Shoulder Belt Load Roll 2 (lbs)	Impact Angle, Roll Rate Roll 1	Impact Angle, Roll Rate Roll 2	Far Side Road Load Roll 1 (lbs)	Far Side Road Load Roll 2 (lbs)
2005 Volvo XC90	6.25	215	101	119	124	143°, 179°/sec	139°, 180°/sec	18,229	22,145
2007 VW Jetta	4.25	164	105	106	115	142°, 156°/sec	143°, 172°/sec	17,362	20,798
2007 Toyota Camry	5	115	100	224	94	141°, 138°/sec	140°, 170°/sec	19,242	25,038
2007 Honda CR-V	4.25	123	102	126	119	143°, 196°/sec	141°, 209°/sec	16,115	14,264
2009 Nissan Versa	5	237	175	225	222	144°, 187°/sec	145°, 194°/sec	19,451	19,151
2006 Hyundai Sonata	4.5	127	93	200	190	143°, 133°/sec	145°, 166°/sec	17,711	31,380
2007 Toyota Camry (Hybrid)	5	177	136	154	123	143°, 180°/sec	136°, 185°/sec	20,024	28,919
2008 Scion xB	6.5	432	207	206	94	141°, 201°/sec	146°, 196°/sec	27,861	20,422
1998 Ford Explorer	3.75	104	69	62	7	146°, 183°/sec	143°, 186°/sec	15,964	25,624
2006 Pontiac G6	2.5	171	128	324	147	139° 172°/sec	140°, 175°/sec	19,062	33,406
2006 Honda Ridgeline	4.75	123	79	166	81	145°, 208°/sec	145°, 203°/sec	20,385	33,023
2006 Chrysler 300	4.5	137	101	539	127	146°, 161°/sec	147°, 156°/sec	24,001	43,085
2007 Chevrolet Tahoe	5.25	192	140	244	64	142°, 213°/sec	143°, 210°/sec	24,727	39,575
2007 Pontiac G6	4.75	87	92	N/A	N/A	142°, 172°/sec	N/A	19,185	N/A
2007 Jeep Grand Cherokee	3.5	125	91	30	10	147°, 197°/sec	149°, 190°/sec	23,908	32,293
2004 Volvo XC90 (White)	N/A	N/A	N/A	N/A	N/A	133°, 214°/sec	148°, 215°/sec	13,590	15,461
2004 Subaru Forester (Red)	N/A	N/A	N/A	N/A	N/A	147°, 223°/sec	150°, 139°/sec	14,723	15,756
2004 Land Rover Discovery II	N/A	122	102	74	38	136°, 212°/sec	145°, 207°/sec	13,608	10,240
2003 Subaru Forester (Tan)	N/A	N/A	N/A	125	114	147°, 212°/sec	151°, 173°/sec	15,283	13,151
2003 Subaru Forester (Green)	N/A	N/A	N/A	113	122	N/A	143°, 174°/sec	14,764	13,912
2002 Toyota Corolla	N/A	N/A	N/A	N/A	N/A	132°, 178°/sec	145°, 176°/sec	8,448	8,626
2001 Chevrolet Suburban	N/A	197	31	N/A	N/A	140°, 214°/sec	N/A	18,579	N/A
2000 GMC Jimmy	5	73	67	N/A	N/A	146°, 174°/sec	N/A	17,455	N/A
2000 Ford Explorer	N/A	N/A	N/A	N/A	N/A	134°, 200°/sec	144°, 188°/sec	9,263	14,251
1999 Oldsmobile Bravada	4.5	N/A	N/A	139	59	149°, 19°/sec	147°, 184°/sec	19,613	29,274
1999 Jeep Grand Cherokee	3	63	31	N/A	N/A	147°, 257°/sec	N/A	24,268	N/A
1999 Isuzu Vehicross	N/A	N/A	N/A	N/A	N/A	139°, 185°/sec	148°, 183°/sec	9,409	15,701
1999 Hyundai Sonata (Black-20.8mph)	4.5	68	29	N/A	N/A	145°, 275°/sec	N/A	20,232	N/A
1999 Hyundai Sonata	N/A	N/A	N/A	N/A	N/A	139°, 172°/sec	148°, 157°/sec	9,466	10,779
1998 MB ML320	4	N/A	97	N/A	N/A	144°, 231°/sec	N/A	17,143	N/A
1997 Chevrolet Cavalier	2.75	95	149	N/A	N/A	142°, 231°/sec	N/A	20,577	N/A
1997 Acura CL 2.2	4	136.6	76.3	N/A	N/A	144°, 205°/sec	N/A	15,351	N/A
1996 Isuzu Rodeo	8.75	74.3	78.7	N/A	N/A	148°, 239°/sec	N/A	18,946	N/A
1993 Jeep Grand Cherokee	4.75	160	N/A	N/A	N/A	148°, 244°/sec	N/A	25,068	N/A

## ROLLOVER INJURY SCIENCE AND ROLLOVER CRASH TYPOLOGY

**Robert Lange**  
**Madhu Iyer**  
**Harry Pearce**  
**Eric Jacuzzi**  
**Jeffery Croteau**  
Exponent  
United States  
Paper Number 11-0116

### ABSTRACT

Motor vehicle manufacturers have developed and deployed rollover roof rail mounted air bags to mitigate occupant injury and the potential for occupant ejection in rollover collisions. Some manufacturers have published information on the type of rollover collisions that are used to establish criteria and define the circumstances for rollover air bag deployment commands.

This paper examines the National Automotive Sampling System Crashworthiness Data System (NASS CDS) to characterize the type and severity of roll over collisions that occur on United States roadways and reports upon the distribution of rollover occurrence by type, and rollover injury occurrence by type of rollover event. Involvement rates are reported for light duty vehicles. Occurrence rates for roll over collision and roll over collision related injury are compared to the rollover collision types that have been identified by motor vehicle manufacturers to assess the proportion of roll over collisions and injuries that might be subject to mitigation with the installation of roof rail mounted rollover air bags.

This comparison shows, if all light duty vehicles in the new vehicle fleet applied similar deployment criteria, approximately 84% of rollover collisions and injuries could be subject to the injury mitigation effects of existing roof rail mounted roll over air bags.

### MOTOR VEHICLE ROLLOVER COLLISION AND INJURY MITIGATION TECHNOLOGIES

Rollover crashes are a relatively small proportion of all collisions in the U.S. but a disproportionate share of fatal and serious injuries occur in rollover crashes. Therefore, rollover related injury has been a high priority for the National Highway Traffic Safety Administration (NHTSA). It has developed a comprehensive approach to rollover injury mitigation that involves three elements: 1) reduction of the

occurrence of rollover crashes, 2) mitigation of ejections, and 3) occupant protection. The NHTSA has taken rule making action in all three dimensions.

For reduction of the occurrence of rollover crashes the NHTSA has promulgated Federal Motor Vehicle Safety Standard (FMVSS) 126 requiring improved vehicle dynamics with the installation of Electronic Stability Control (ESC) technology. The NHTSA intends to generate reductions in occupant ejections through: increased occupant use of safety belts, improved door hardware performance (FMVSS 206), and application of new ejection mitigation performance requirements (primarily) due to application of rollover activated roof rail air bags (FMVSS 226). The NHTSA addressed occupant protection with increased roof strength in FMVSS 216.

In all three areas, motor vehicle manufacturers have initiated technology insertion and/or policy actions to address these same three dimensions.

Motor vehicle manufacturers initiated application of ESC technologies in the late 1990s. Figure 1 is a bar graph of the proportion (of total models) of the new vehicle fleet (passenger cars and light trucks, herein after the "light vehicle fleet") over the period 1998 through 2009 that were offered for sale in the U.S. with ESC available. By 2004, the NHTSA and the Insurance Institute for Highway Safety (IIHS) had examined collision data and determined that ESC effected meaningful reductions in all collisions and in single vehicle off road rollover collisions. The NHTSA initiated rule making on FMVSS 126 in September 2006, roughly at the beginning of the 2007 model year. In that year over 65% of new model vehicles had ESC available as standard or optional equipment. The NHTSA issued its final rule in April 2007, a very rapid conclusion for a very complex rule. The rule applied to vehicles manufactured after September 1, 2008 and incorporated a three year phase-in period, provided carry forward credits for vehicles that satisfy the

performance criteria, and became fully effective to light duty vehicles manufactured after August 31,

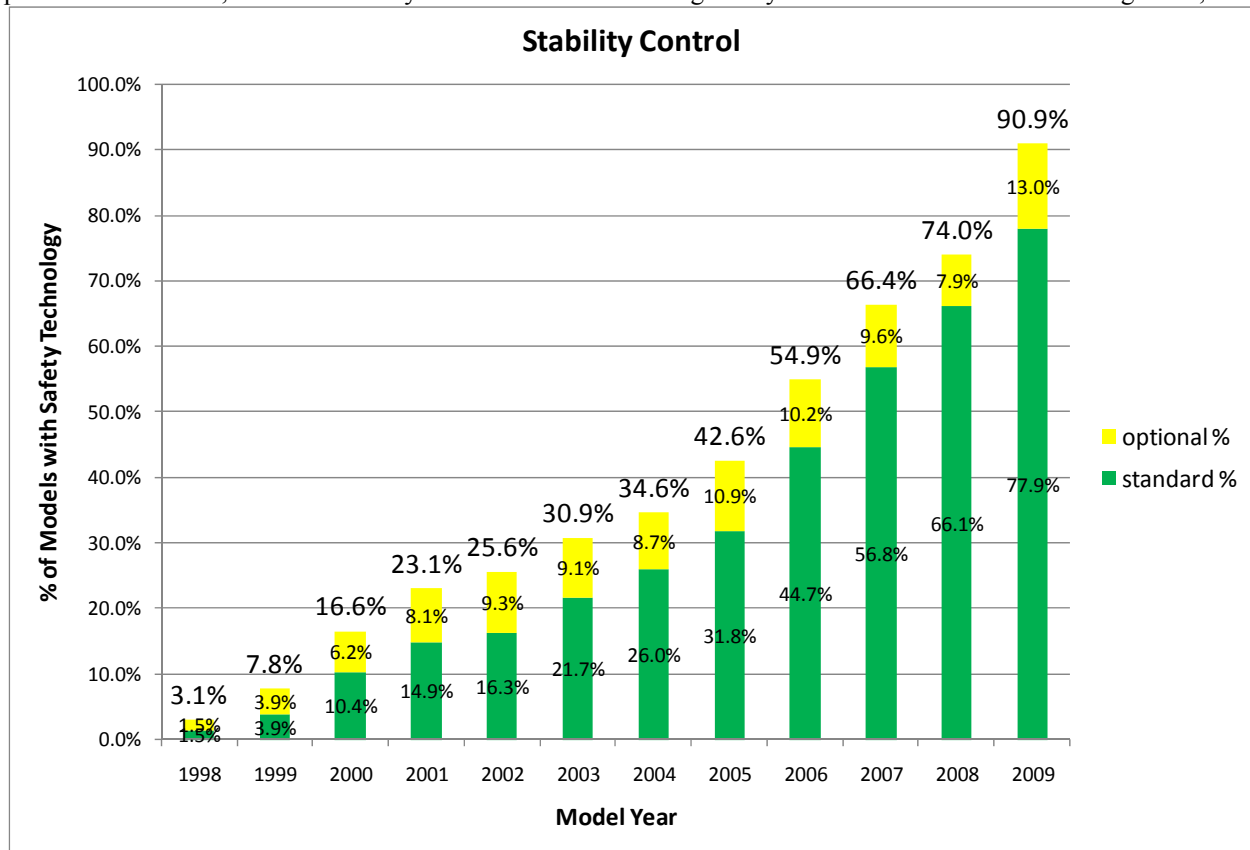


**Figure 1. Optional and standard installation rates for electronic stability control as a proportion of new light duty vehicle models.**

the performance criteria, and became fully effective to light duty vehicles manufactured after August 31, 2010. The NHTSA estimated that ESC as applied to satisfy FMVSS 126 will avoid 1,171 to 1,465 fatal rollover related injuries annually when fully integrated into the motor vehicle fleet [1].

Ford Motor Company installed enhanced seat belt use reminders during the mid-1990s. Survey work conducted by the IIHS reported about a five percent increase in belt use in Ford vehicles with enhanced seat belt reminders as compared to Ford vehicles not so equipped. Following publication of the Ford/IIHS study, NHTSA Administrator Dr. Ricardo Martinez encouraged all manufacturers to consider incorporation of similar enhanced seat belt use reminder systems in their vehicle designs. Virtually all major manufacturers responded affirmatively; the insertion profile for enhanced seat belt use reminder systems is shown below in Figure 2. The source of this data is the NHTSA New Car Assessment Program (NCAP) database. Note that the discontinuity in model year 2005 is because that is

the first year the technology was recorded consistently. The insertion percentage increase from the mid-1990s was much smoother than Figure 2 shows.

Motor vehicle manufacturers collaborated on the public policy front to change occupant behavior regarding seat belt usage. Vehicle manufacturers created the Air Bag and Seat Belt Safety Campaign (ABSBS) and partnered with some insurers, particularly Nationwide Insurance, to fund a ten year program to increase seat belt use in the U.S. The program was operated by the National Safety Council. The ABSBS: 1) expanded the “Click It or Ticket” program built by the IIHS and police agencies in North Carolina across the U.S., 2) worked to improve mandatory seat belt use laws, and 3) focused public attention on seat belt use during periods of intense enforcement efforts on a regular basis. After the ABSBS was concluded in 2007, the NHTSA has continued to organize the periodic enforcement events. During the life of the ABSBS,

seat belt use in the U.S. increased 21 percentage points from 61% to 82%.

performed by motor vehicle manufacturers. See, for example, roof strength docket comments provided by the Alliance of Automobile Manufacturers [2] and

Rollover injury science was advanced by work

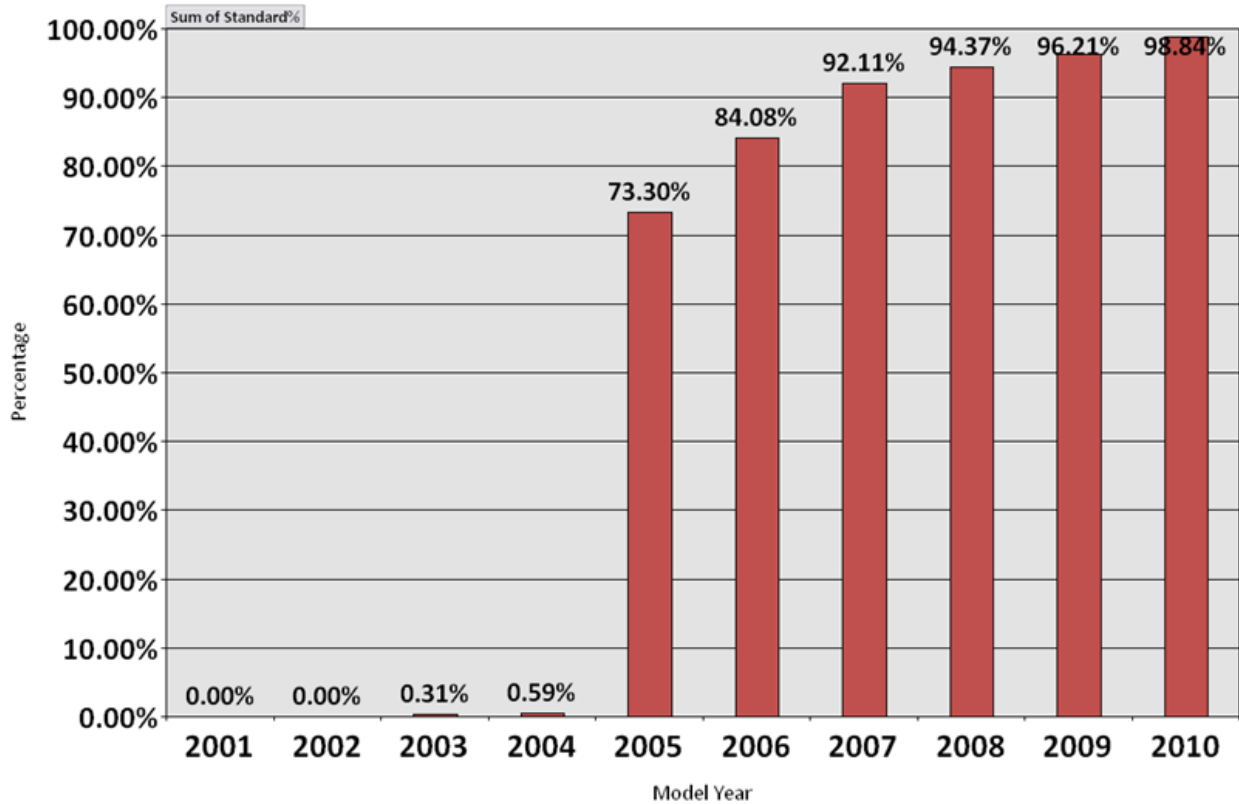


**Figure 2. Installation rate for enhanced seat belt reminder systems. Data was not consistently recorded prior to 2005.**

[3]; Ford Motor Company [4], [5], and [6]; Nissan [7]; and General Motors [8], [9], and [10]. Manufacturers studied and reported upon the injury mechanisms related to compressive loading of the spine when in an inverted position due to gravitational forces that act on the thorax through the neck and are resisted by the head at rest on the ground or on vehicle structures.

Applying this injury control science, manufacturers developed and implemented rollover activated roof rail air bags. Ford Motor Company first introduced this technology in the middle of the 2002 model year. Figure 3 shows the technology insertion progression for rollover roof rail air bags. The technology is anticipated to reduce occupant ejection in rollover and also may provide a counter measure for some types of non-ejection rollover related occupant injuries related to head strikes to ground or to vehicle structures covered by the inflated air bag at occupant contact.

The NHTSA has finalized its performance requirements in FMVSS 226 (ejection mitigation) [11]. The standard imposes an energy absorption requirement and excursion limits in response to an impulse insult from a guided linear impactor. The rule was finalized in January of 2011, first required implementation is September 1, 2014 but early compliance credits can be earned starting after February 2011, and carry forward credits can be earned with early applications so as to smooth and match phase in proportions to manufacturers' individual portfolio change plans. The phase in period ends August 31, 2017 save for altered vehicles and those manufactured in more than a single stage. The NHTSA forecasts that application of the technologies necessary to satisfy these performance requirements will reduce rollover related occupant fatal injuries by 373 annually when fully applied.

## ROOF STRENGTH RULE MAKING

The technical literature is rich in studies examining the relationship between vehicle characteristics and

occupant injury outcomes in rollover crashes. This paper will not attempt to survey or report upon the nature and conclusions various authors have published regarding that matter. However, two

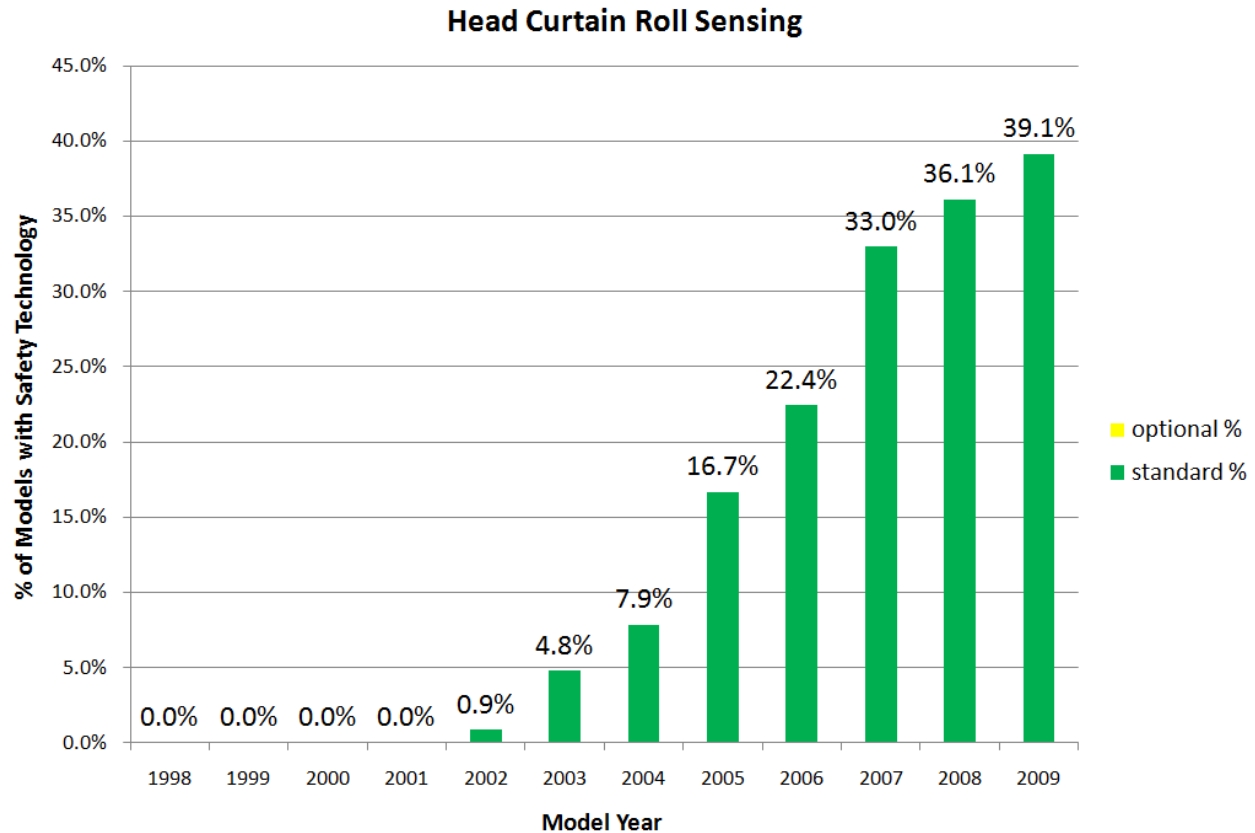


**Figure 3. Installation rate for rollover deployed roof rail air bags.**

studies performed by the NHTSA are critical to an understanding of the NHTSA's rule making action on the vehicle parameter of roof strength [references 12 and 13]. Both studies used NASS CDS data for rollover crashes to collect belted occupant injury outcomes and roof profile data over the occupants of interest to look for relationships between head, face and neck injury from roof contact and roof deformation. The roof included the roof panel and all surrounding structures, pillars, headers, etc. Austin et al. [12] found a dichotomous relationship between post crash headspace (positive or negative value) and injury severity. Strashny [13] found a statistically significant relationship between the maximum severity injury to the head, face or neck, and the amount of roof deformation measured as roof deflection or residual headspace. Neither Strashny nor Austin claimed that the statistical correspondence they found established a causative relationship between roof deformation and occupant injury. In addition to the statistical relationships, both NHTSA

researchers found over 99% of rollover crash involved occupants that experience head, face, or neck contact with the roof are not seriously injured and register a maximum head, face, or neck AIS injury level of 0, 1, or 2. This would indicate vehicle structures and restraint systems have been well balanced to provide good occupant protection in rollover crashes for belted occupants.

The NHTSA applied the findings of statistical significance in promulgating its roof strength standard, FMVSS 216 [14], published as a final rule in May 2009. The new standard refined many elements of the existing FMVSS 216 test procedure; it added new acceptance criteria for roof contact with a seated occupant, increased the load requirement acceptance criteria as a proportion of vehicle mass, maintained the basic test orientation and load application device from the then existing rule, and applied a new requirement for sequential testing of both sides of an individual vehicle for compliance.

The NHTSA forecast a small reduction in rollover related fatal injuries to occupants of 135 annually after full application.

## **ROLLOVER INJURY SCIENCE**

As is the case for roof crush and injury, the literature is rich with regards to the science of rollover injury causation. A comprehensive discussion of that body of literature is beyond the scope and length of this paper but two more recent studies bear review to add clarity and context to the current state of knowledge.

In 2008, Exponent reported results for a series of dolly rollover tests it had performed using a 2003 Subaru Forester as the research tool. Exponent explained that the Subaru Forester was selected as the test subject as it was a vehicle with a high roof strength to vehicle weight ratio (the strength to weight ratio or SWR); the SWR for the Subaru Forester is about 4.8. Three test vehicles were instrumented to record pillar displacements and one of the tests was also fitted with instrumented Anthropomorphic Test Devices (ATD or crash test dummies) in the front outboard seating positions that recorded injury measures throughout the test [15].

Two tests were conducted without ATDs; as the tests continuously recorded roof deformation, for the first time in rollover injury research, engineers could examine the time history of roof deformation in a severe rollover crash, and compare the post crash roof condition to the deformations that obtained

during the rollover event itself. Exponent observed there was little correspondence between post crash roof deformation and the time history displacement of roof components during the rollover.

One rollover test was conducted with instrumented pillars and instrumented ATDs in the front outboard seating positions. The most interesting observations from this test is the time history correspondence between neck compression for the ATD at first ground strike and the structural response measured as pillar displacement (roof deformation) following the first ground strike while the vehicle was inverted and continuing in the rollover sequence. The ATD maximum neck compression occurred early in the ground strike as roof deformation was just initiating. Maximum roof deformation did not occur until later in the ground strike event and by that time, the ATD neck load had gone from compression into tension indicating that the ATD torso was no longer loading the neck due to spinal alignment. These successive events are depicted in Figures 4 (maximum neck compression) and 5 (maximum roof pillar deformation) and shown below. These are Figures 7 and 8 in [15].

# 2003 Subaru Forester 43.4mph DRT on Dirt

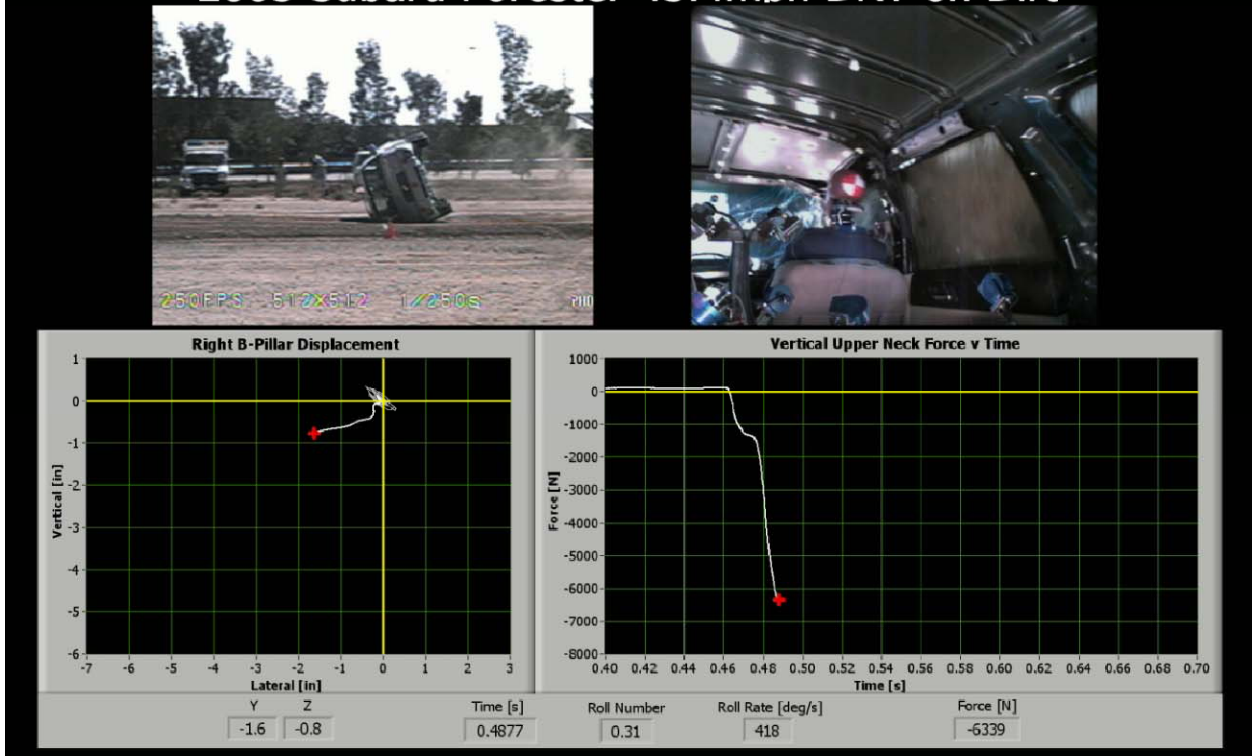
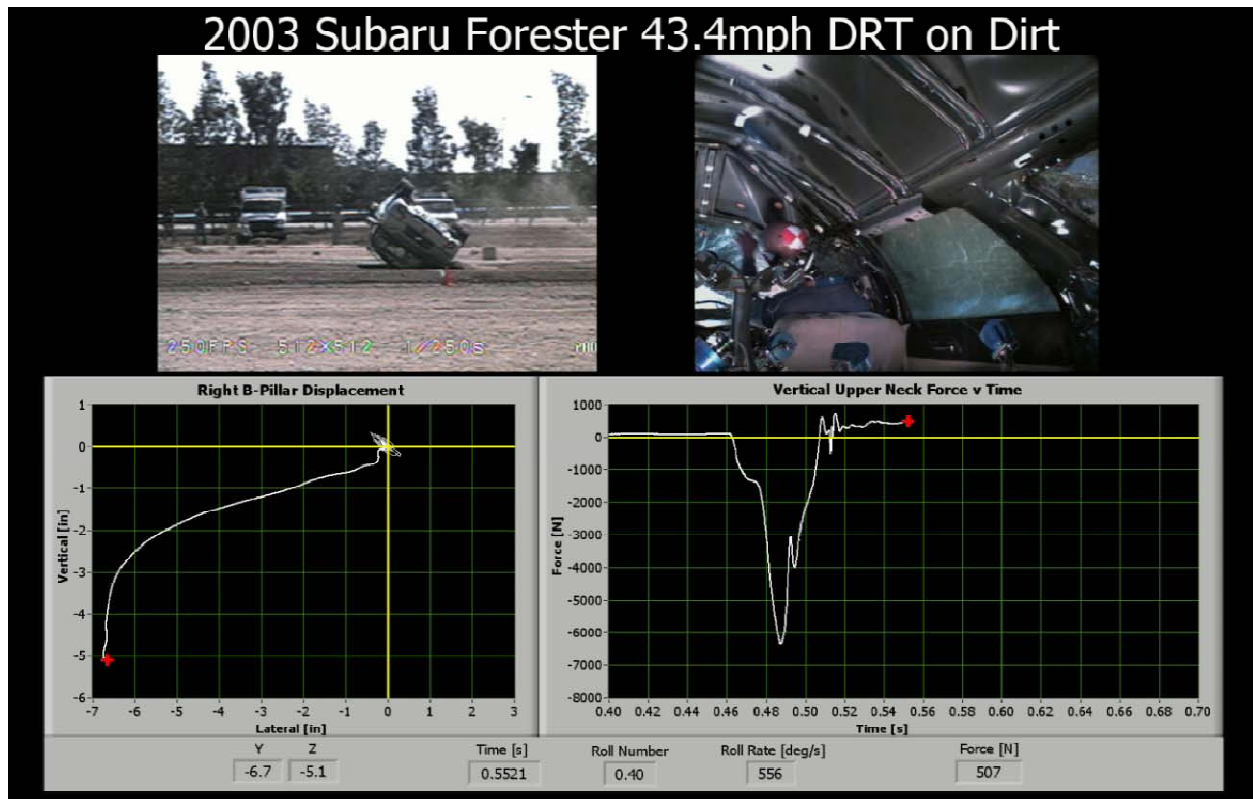


Figure 4. Captured frame from the synchronized data with composite video of the passenger-side B-pillar displacement at the time of passenger ATD peak compressive upper neck load during the first passenger side (near-side) roof rail impact (above).



**Figure 5. Captured frame from the synchronized data with composite video of passenger ATD axial upper neck load at the time of peak passenger-side B-pillar displacement during the first passenger-side (near-side) roof rail impact.**

Of equal interest is a research paper GM issued concerning observations it made during development of its rollover roof rail air bags for occupant injury control in rollover [16]. GM conducted some of its rollover sensor signature development tests with instrumented ATDs and in O'Brian-Mitchell [16] GM reported the test configurations and ATD test outcomes in which IARV values were exceeded.

One hundred seventy-six of the GM sensor signature rollover tests were conducted with Hybrid III 50<sup>th</sup> percentile male ATDs in the front outboard seating positions. Some tests were conducted with belted ATDs and some with unbelted ATDs. The test configurations GM used were: 1) trip-over (curb trip-over, soil trip-over, gravel trip-over, friction trip-over, curb trip-over sled, and soil trip-over sled); 2) fall-over (ditch fall-over with dirt slope and ditch fall-over with high friction slope); 3) flip-over (corkscrew ramp flip-over); 4) SAE J2114 dolly rollover; and 5) other (half corkscrew ramp and bounce-over). In many tests, the side window openings were covered with a fabric membrane to record ATD loadings at the window openings; those loads were then later used to develop the

performance criteria (energy capacity, force limits, and excursion limits) for rollover roof rail air bags [17]. ATD kinematics during the rollover were recorded using onboard high speed cameras.

GM examined the ATD injury measure test records for all of the tests. It evaluated events in which the IARVs were exceeded and reported ATD injury measures exceeding IARV limits due to ATD head strikes with: vehicle structures (leading side pillars, roof rails, and trailing side overhead structures), the other ATD, ground, door beltline, and with the window membrane. GM did not report any ATDs were ejected. Belted and unbelted ATDs recorded injury measures exceeding IARVs.

Most significantly, some of the ATD head strikes that generated Head Injury Criteria (HIC) or neck compression injury measures that exceeded the IARV limits occurred when the vehicle was not inverted. In those events, it is obvious that roof strength and roof deformation were decoupled from the head strikes that generated the injury potential, reference Table 1 (Table 7 in [17]). It is noteworthy that in the GM test series there was a greater frequency for IARV

exceeded contact events while the test vehicles were not inverted, than when the test vehicles were inverted. Application of rollover roof rail air bags may offer some potential for mitigation of some of these potential injury events (head strikes to structure covered by the bags and head strikes to ground) as well as provide potential to mitigate rollover ejection, the intent of the NHTSA's FMVSS 226 rulemaking.

**Table 1.**  
**Restraint condition, ATD seating location, and vehicle orientation at events in which an IARV was exceeded**

	Restraint usage - Contacts by vehicle orientation			
	On wheels	On leading side	On roof	On trailing side
Unbelted Leading Side	1	10	2	1
Belted Leading Side	0	11	3	0
Unbelted Trailing Side	3	15	2	0
Belted Trailing Side	1	3	19	0
Sum:	5	39	26	1

**ROOF STRENGTH AND ROLLOVER INJURY SCIENCE**

There is a physical relationship that explains the statistical associative relationship noted by NHTSA researchers Austin and Strashny. Roof deformation consequent to a rollover event is a function of three primary variables: the energy demand that is placed upon the vehicle structure in the rollover (E), the orientation of the vehicle structure at application of the ground strike impulse (O), and the strength properties of the vehicle structure in the orientation at ground strike (S). Consider the primary variables that determine occupant injury potential when a vehicle is inverted and striking the ground in rollover; these variables are: the energy demand that is placed upon the occupant in the ground strike event (e), the orientation of the occupant as related to head, neck, and spine alignment (o), and the strength properties of the occupant head/neck/spine in the orientation at ground strike (s). Both rollover event outcomes are dependent upon the same set of variables although the specific values that obtain each instant during the rollover event are obviously unique to the vehicle and any occupant. As the variables are similar, it is not surprising that one would find an associative correspondence between occupant injury likelihood and post crash roof deformation. High

energy events are similarly challenging for both vehicle structures and rollover involved occupants.

**ROLLOVER TYPOLOGY**

Exponent used NASS CDS to characterize rollover crashes by type to compare the resultant profile to the rollover types engineered in the GM rollover sensor. The NHTSA has already reported that its review of rollover sensor performance in real world collisions has been appropriate and therefore it declined to specify rollover air bag actuation criteria in FMVSS 226 [11].

Data was extracted from the NASS CDS database for the years 2000-2009 to investigate the circumstances surrounding vehicle rollover and the injuries resulting from this type of vehicle crash mode. Exponent considered rollover crashes recorded in 2000 to 2009 NASS years for all light duty vehicles (passenger cars, sport utility vehicles, pickup trucks, and vans) for vehicle model years 1998 to 2010 for which occupant injury level was known. The nature of rollover crashes was characterized by: the number of quarter turns, roll initiation source, roll location relative to the roadway, and extent of roof intrusion. Rollover exposed occupants were examined by distribution of MAIS and safety belt usage. The analysis considered all rollover types defined in NASS CDS.

The proportion of rollover crashes where the occupant injury level is known is shown in Figure 6 below. The analysis also reports on the distribution of belted occupant injury severity by rollover type in Figure 7 below. Data was extracted from the NASS CDS database using the SAS database query software. NASS CDS weighting factors were applied. This allows the cases sampled by NASS CDS to be projected to the national estimates. These weighting factors are applicable to general characteristics of each case.

We can match NASS CDS rollover types with the rollover tests that served as the basis for GM's sensor engineering. We can first observe that an on road "Turn Over" event is a relatively rare rollover occurrence, 1.6% of the population studied. GM's sensor test matrix does not comprehend several of the NASS CDS categories: "End-Over-End", "Unknown Rollover Initiation Type", "Other Rollover Initiation Type," and "Collision With Another Vehicle." Thus the sensor was not engineered to explicitly recognize about 16% of rollover crashes. Perhaps the sensors can register some of these as rollover independent of

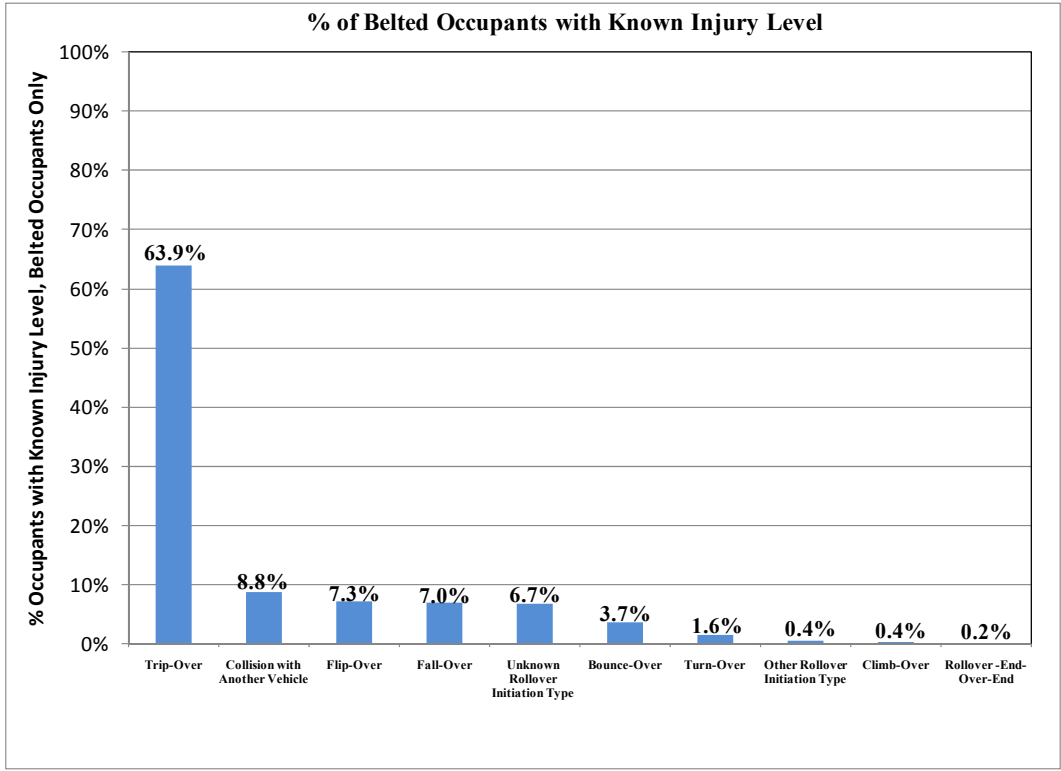


Figure 6. Distribution of belted occupants with known injury level by rollover type in NASS CDS.

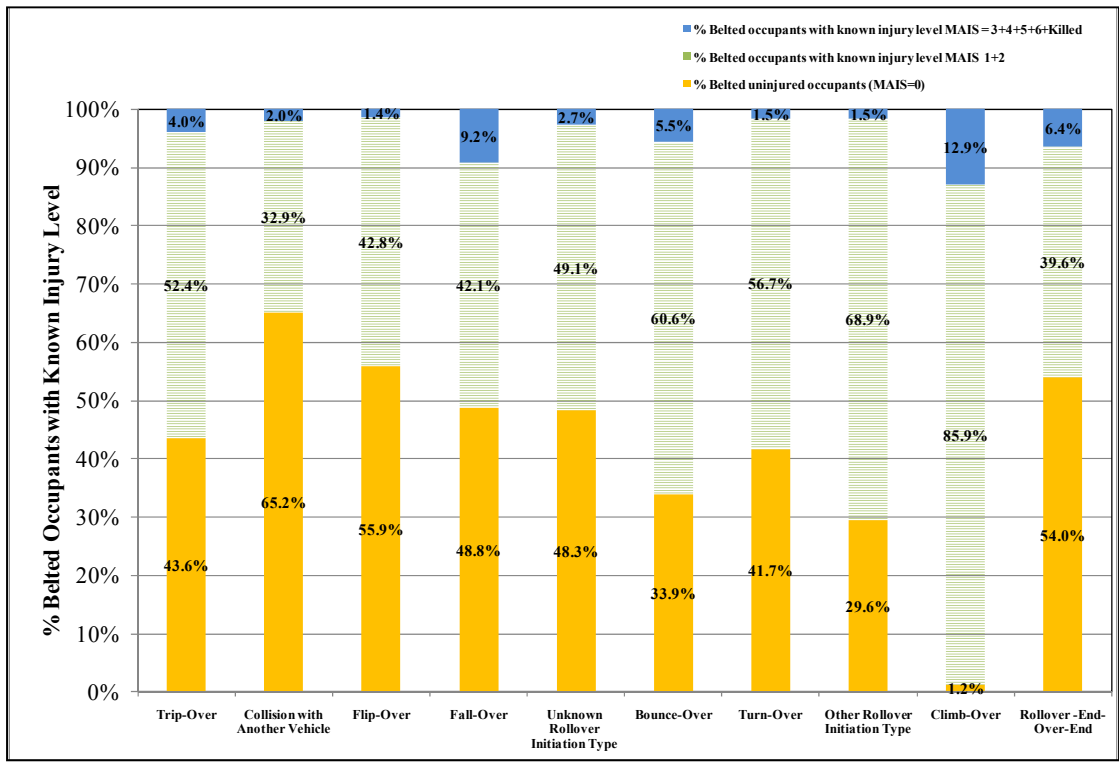
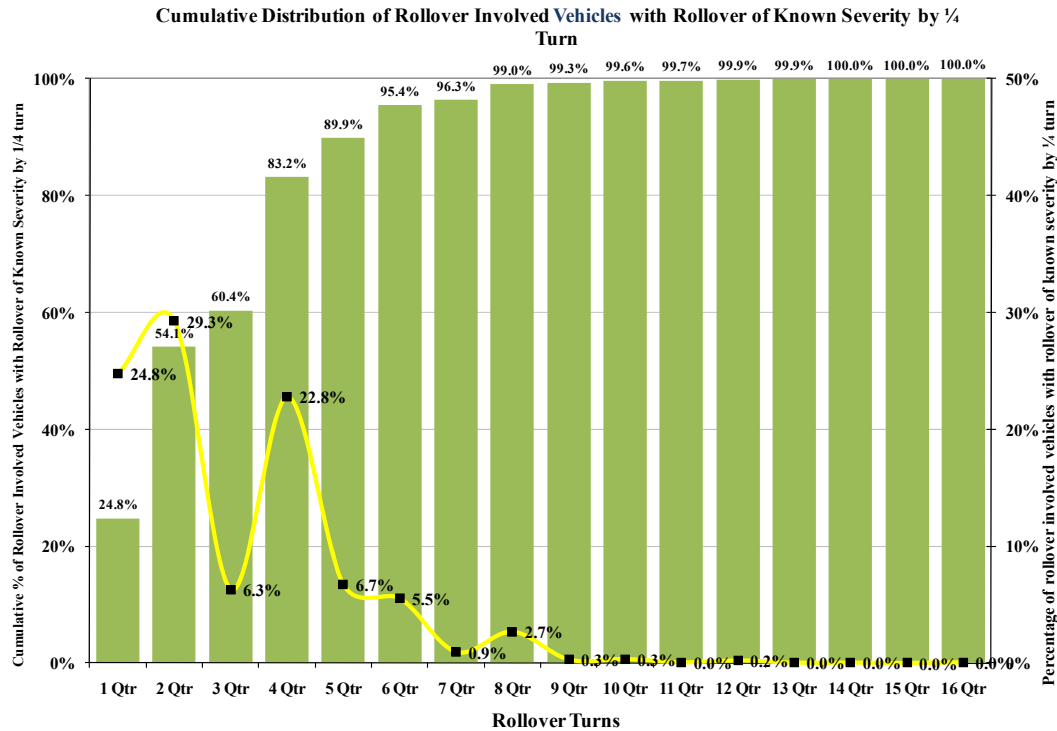


Figure 7. Belted rollover occupant injury severity by NASS CDS defined rollover type.

the initiating cause so in some of these types, perhaps



the initiating cause and the sensor would recognize and command deployment of the air bags.

It would appear that the balance of the NASS CDS rollover types correspond to some element of the sensor engineered performance set and the rollover roof rail technology may potentially apply to about 84% of the class of rollover crashes studied.

We also plotted the rollover severity distribution measured by number of quarter turns, Figure 8, and the distribution of occupant injury level by quarter turns in Figure 9. Figure 9 illustrates the point that the likelihood of severe injury increases with rollover crash severity generally although the trend is not monotonic.

## DISCUSSION

The NHTSA developed a comprehensive plan for rollover injury control with three elements: collision avoidance, occupant protection, and occupant containment from ejection. It has completed rule making in all three domains. On an individual basis, motor vehicle manufacturers have undertaken to engineer vehicles to performance criteria in all three domains as well; manufacturers' actions preceded rule making.

## REFERENCES

- [1] Federal Motor Vehicle Safety Standards. Electric Stability Control. Controls and Displays. FMVSS 126 49 CFR Parts 571 and 585.
- [2] Alliance of Automobile Manufacturers comment dated February 27, 2006; Docket Number NHTSA-2005-22143.
- [3] Alliance of Automobile Manufacturers comment dated March 27, 2008; Docket Number NHTSA-2008-0015.
- [4] Ford Motor Company comments dated October 19, 2005; Docket Number NHTSA-199-5572.
- [5] Ford Motor Company comments dated November 18, 2005; Docket Number NHTSA-2005-22143.
- [6] Ford Motor Company comments dated July 10, 2008; Docket Number NHTSA-2008-0015.
- [7] Nissan comments dated May 10, 2007; Docket Number NHTSA-2006-26555.
- [8] General Motors Corporation comments dated August 16, 2002; Docket Number NHTSA-1999-5572.
- [9] General Motors Corporation comments dated June 16, 2005; Docket Number NHTSA-1999-5572.
- [10] General Motors Corporation comments dated March 20, 2008; Docket Number NHTSA-2008-0015.

**Figure 8. Rollover crash severity frequency by quarter turn and cumulative frequency.**

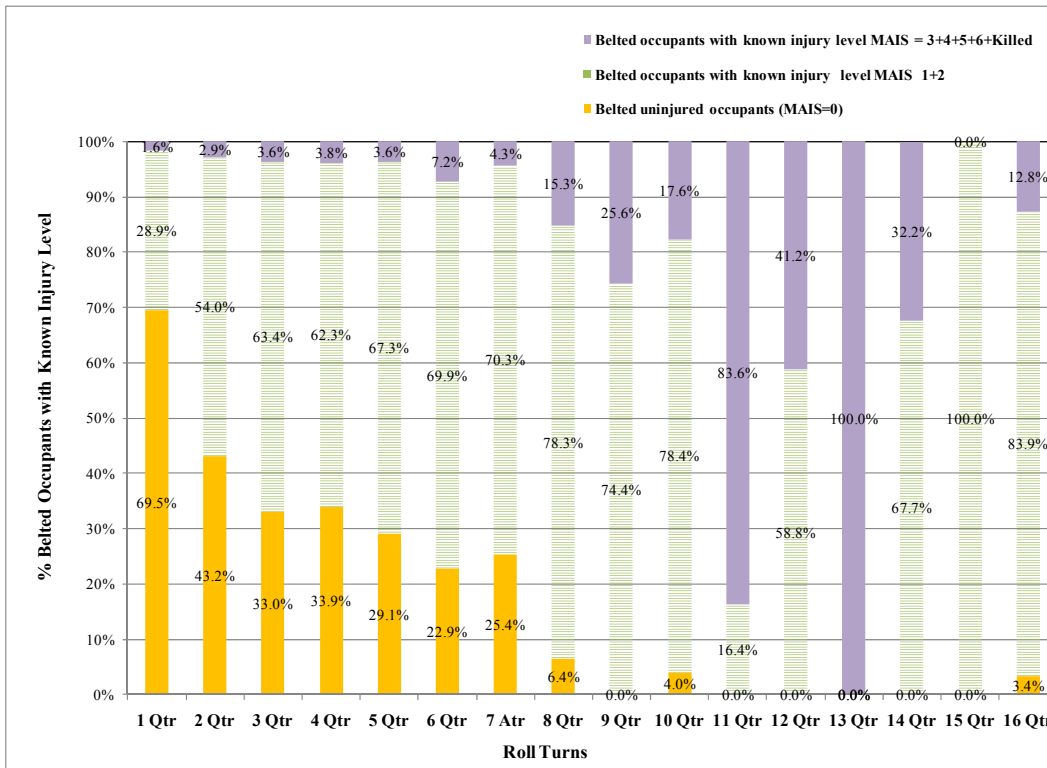


**Figure 9. Belted occupant injury level by rollover collision severity as measured by number of quarter turns.**

[11] Federal Motor Vehicle Safety Standards. Ejection Mitigation. FMVSS 226 49 CFR Parts 571 and 585.

[12] Austin, Rory et al. "The Role of Post-Crash Headroom in Predicting Roof Contact Injuries to the Head, Neck, or Face During FMVSS No. 216 Rollovers." Docket Number NHTSA-2005-22143.

[13] Strashny, Alexander. "The Role of Vertical Roof Intrusion and Post-Crash Headroom in Predicting Roof Contact Injuries to the Head, Neck, or Face During Rollovers: An Updated Analysis." October 2007.

[14] Federal Motor Vehicle Safety Standards. Roof Crush Resistance. FMVSS 216 49 CFR Parts 571 and 585.

[15] Croteau, Jeff and Carhart, Michael, Exponent comment dated September 23, 2008. Docket Number NHTSA-2008-0015.

[16] O'Brien-Mitchell, Bridget M., et al. "Data Analysis Methodology and Observations from Rollover Sensor Development Tests." ESV 2007, Paper Number 07-0308.

[17] O'Brien-Mitchell, Bridget M., et al. "Rollover Sensor Signature Test Development." SAE 2007-01-0375. Warrendale, PA. Society of Automotive Engineers. 2007.

## SAFETY AND VISION IMPROVEMENTS BY EXPANDABLE A-PILLARS

### Pipkorn Bengt

Autoliv Research  
Sweden

### Lundström Jesper

Saab Automobile  
Sweden

### Ericsson Mattias

Epsilon  
Sweden  
Paper Number 11-0105

### ABSTRACT

In modern passenger vehicles the A-Pillar is an important structural safety component. In full frontal, frontal offset-, pole and rollover collisions the A-Pillar is carrying to a large load in order to minimize the deformation of the occupant compartment. Generally the larger the cross-section the more load the A-pillar can transfer. However, the A-pillars in general more or less reduce the forward vision angles for the driver. Therefore the width and strength of the A-Pillar are important vehicle safety parameters. The strength and size requirements on the A-Pillar are in contradiction. In an A-pillar design in which the cross section is folded and expands when needed the conflicting requirements can be combined in one component. As a normal state the cross-section of the component is folded, obscuring less of the driver's visibility compared to a state of the art A-pillar. In a crash the A-pillar expands which results in a significant increase in the cross section. The expanded cross section increases the strength of the A-pillar. An expanding A-pillar can be accomplished by pressurizing a folded structure. A cost- and weight-efficient way to generate over pressure is by pyrotechnics (gasgenerators)

An expandable A-pillar design was developed in which the conflicting requirements high strength and small cross section were combined in one component. The goal was to develop an A-pillar that obscure less of the driver's vision in the normal operation, is lighter and has the same crash performance as a state of the art A-pillar. The development was carried out by combining mathematical simulations and mechanical crash tests. For the development of the expandable A-Pillar a mathematical sub structure model was developed and validated. The model was validated by comparing predictions from the model to results from a mechanical crash test. The expandable

A-Pillar was mounted in the sub structure and the deformation performance was evaluated relative to the performance of a state of the art A-Pillar. The deformation force is less than or equal to the deformation force of a vehicle with a state of the art A-pillar. The obscuration angle is reduced by more than 25% (for left hand side A-Pillar from 12.3 – 8.9 degrees) and the mass is reduced by 8% (excluding mounting brackets and gasgenerator) relative to a state of the art A-pillar. The expandable A-pillar combines the conflicting goals, high strength, small cross section and low mass.

### INTRODUCTION

Rollover crashes critically injure and kill thousands of people every year through head and neck injuries [1]. Structurally weak roofs can be a primary cause of serious head, face and neck injuries to occupants who are not ejected in vehicle rollover. Due to the fact that belt is used by most passenger vehicle occupants today the number of ejected occupants is low and therefore the occupants are vulnerable to injury within the vehicle. In a rollover crash the roof can crush in a number of different ways depending on the design of the roof and the vehicle trajectory (Figure 1). The most severe breakdown is a complete pillar collapse.



Figure 1. Various Types of Roof Crush

A weak roof can collapse and buckle in this type of crash, imposing forces on and occupant's head that

are greater than those that would result from the vehicle drop itself. It was found that neck injuries occur and are exacerbated in a weak roof vehicle as opposed to a strong roof vehicle when subjected to a rollover crash [2]. The association between vehicle roof strength and occupant injury risk in rollover crashes appears robust across different vehicle groups and across roof strength-to-weight ratios measured at 5 inches (12.7 cm) (SWR5). The roof strength-to-ratios varies typically from just more than 1.5 to just less than 4.0 [3]. If roofs were to increase in strength by one SWR5, a 20-25% percent reduction in risk of serious injury in rollovers would be expected.

In the modified standard for roof strength, FMVSS 216, it states that a roof must withstand pressure equals to 3.5 times the vehicle weight and the roof may not contact the head or neck of a seated 50%-ile Hybrid III dummy [4]. NHTSA estimates that the new rule prevent 44 deaths a year [5]. The rule applies to all vehicles with a Gross Vehicle Weight of 2722 kg (6 000lbs).

Not only rollover crashes exposes the A-pillar to excessive loading conditions [6]. Frontal collisions and in particular frontal offset collisions expose the A-pillar to high loading conditions [7]

Consider a transverse vertical plane in line with the dash. The resulting cross-section might include the A-pillars, side doors, door sills and floor. About 50% of the vehicle's weight will usually be rearward of this plane. The compression forces arising in these components due to a 40g deceleration are therefore equivalent to about 20 times the weight of the vehicle. This places a severe demand on the structure.

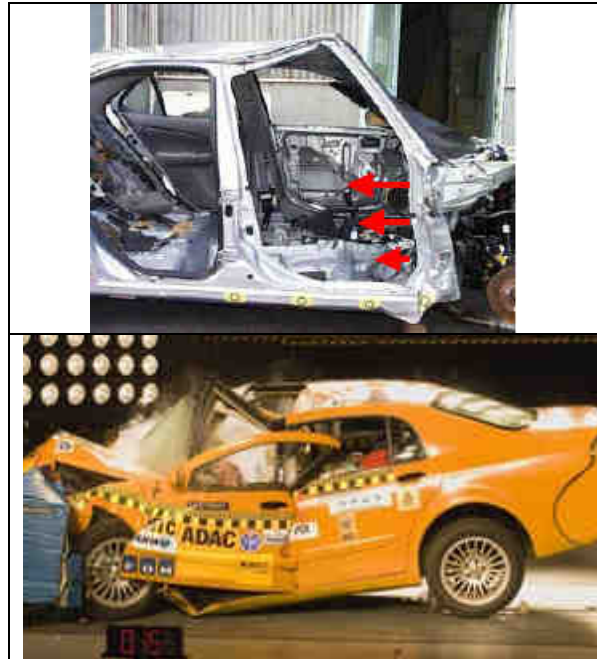


Figure 2. Offset Collisions Exposes the A-pillar to High Loading Conditions [7] and [8]

To obtain a strong roof one of the most important vehicle structural components is the A-pillar (Figure 3). There are conflicting requirements on the A-pillar of a passenger vehicle. For occupant protection the A-pillar needs to be stiff and strong to withstand the load in a rollover or a frontal impact at high impact velocity. However, the A-pillar obscures the vision for the driver. In an investigation carried out by Auto Motor und Sport it was found that the vehicle with smallest obscuration angle had an angle of 12 degrees and the worst obscuration angle was 16 degrees [9].

Therefore, for the vehicle driver to have good visibility the A-pillar needs to be slim (have a small cross section). In addition for the vehicle to have low fuel consumption the A-pillar needs to have low mass. The ideal A-pillar is one that is slim during normal driving and when added stiffness and strength is needed such as in a rollover crash the A-pillar expands and increases the cross section and crush resistance.

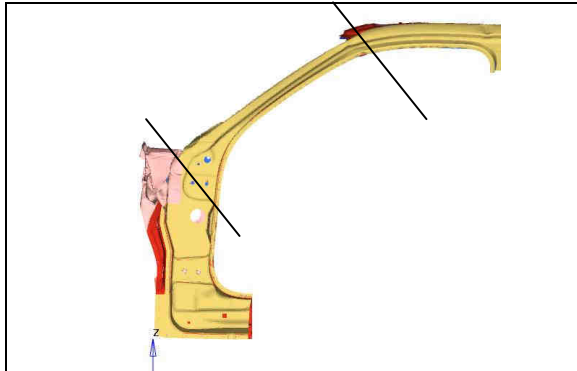


Figure 3 A-pillar

In an A-pillar with an expandable cross section the conflicting requirements can be combined in one component. As a normal state the cross-section of the component is folded providing the driver with good visibility. In a crash the A-pillar expands which results in a significant increase in the cross section and the greater cross section increases the strength of the A-pillar. Expansion of sealed folded steel components such as A-pillars can be accomplished by generating a high internal pressure. A cost- and weight-efficient way to generate over pressure is by using pyrotechnic gasgenerators.

An expandable A-Pillar was developed in a previous project [10]. In the project a great number of various A-Pillar designs were evaluated. The number of folds, the folding scheme, and the radius of the folds were evaluated. The deformation performance of the selected concept was evaluated by component bending tests. With the selected concept good potential to reduce mass, increase vision and maintain the level of safety was obtained. Therefore the next step in the development of an expandable A-Pillar was to evaluate the A-Pillar in a vehicle structure.

The aim of the project is to develop an expandable A-pillar that combines the conflicting requirements of good visibility, low mass and high strength. The A-pillar will, when expanded, have the same deformation force and deformation moment as a state of the art A-pillar. When expanded the deformation force and moment will increase relative to when it is unexpanded. When folded, the A-pillar will increase vision. The mass of the expandable A-pillar will be less than the mass of a state of the art A-pillar. Therefore, the goal was to develop an A-pillar that obscures less of the driver's vision in normal operation, is lighter and has the same crash performance as a state of the art A-pillar.

The goals with the expandable A-Pillar were to:

Reduce obscuration angle by 20% and the mass by 10% relative to a state of the art A-Pillar today.

When expanded have the same max deformation force and moment as a state of the art A-Pillar.

Increase max deformation force and moment by 50% when expanded relative to unexpanded.

## METHOD

The development of the expandable A-Pillar was carried out by means of combining mathematical simulations (finite element analysis) with mechanical crash tests.

For the development of the expandable A-Pillar a sub structure vehicle model was developed and validated (Figure 4). The sub structure consisted of a body in white of a modern passenger vehicle cut behind that B-Pillar and in front of the suspension tower. The corresponding model was validated by a crash test in which the sub structure was impacted by a moving barrier. The mass of the barrier was 1569 kg with and the impact velocity was 14.5 km/h (4.1 m/s). In the test the impact force and door opening distances were recorded.

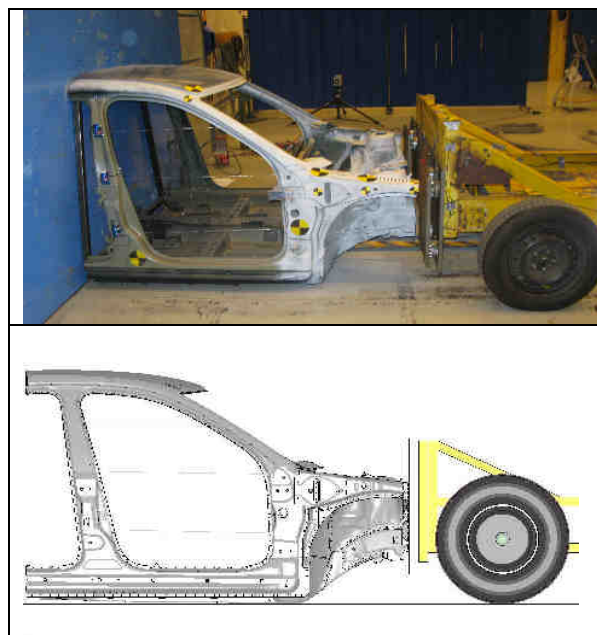


Figure 4. Sub Structure Test Method

Using the validated model various designs of the expandable A-Pillar were integrated into the vehicle structure and evaluated by means of crash simulations. The crash performances of both unexpanded and expanded A-Pillars were evaluated.

When the expandable A-Pillar fulfilled the performance goals in the frontal crash configuration the A-Pillar was evaluated for rollover. The rollover performance was evaluated by means of the roof crush test configuration. In the roof crush evaluation the roof of the vehicle was loaded with a rigid wall with the dimensions 1829x762mm (Figure 5). The angle of the wall was 25 degrees relative to the horizontal plane including the longitudinal axis of the vehicle and rotated 5 degrees relative to the transversal axis of the vehicle. The front end of the wall was 254mm forward of the forwardmost point of the roof of the vehicle.

The contact force between the wall and the structure, the displacement of the wall and the cross section force and moment at the A-Pillar bottom were recorded.

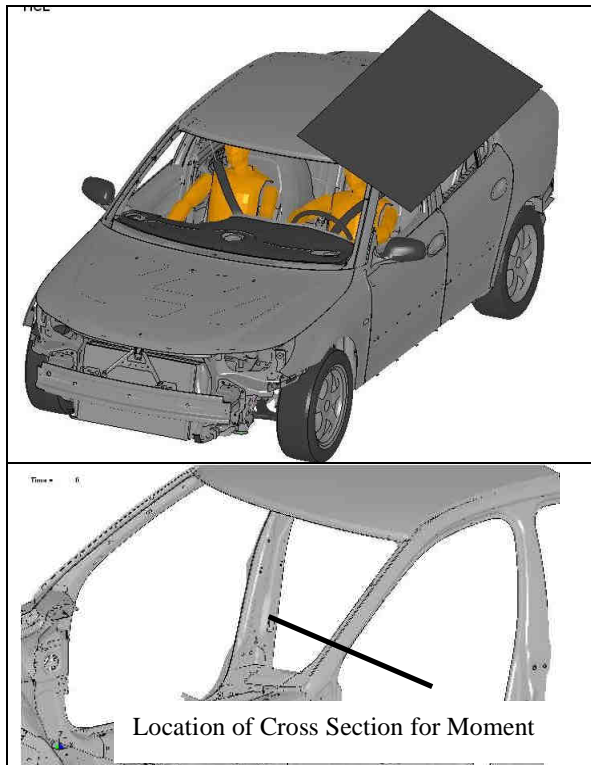


Figure 5. Roof Crush Set Up

## RESULTS

The A-Pillar developed in previous project was modified when integrated into the vehicle structure. The expandable A-Pillar was a folded and sealed. It was tightly folded with one fold and sealed by means of seam welding. The wall thickness was 1.5 mm and the material was steel CR340. The design of the reference A-Pillar and the expandable A-Pillar can be observed in Figure 6. Both unexpanded and expanded expandable A-Pillar can be observed. When unexpanded the cross section of the A-Pillar was significantly reduced relative to the state of the art A-Pillar. When expanded the deformation force and moment were significantly increased. The expansion was accomplished by means of pressurizing the folded A-Pillar using a pyrotechnic gasgenerator.

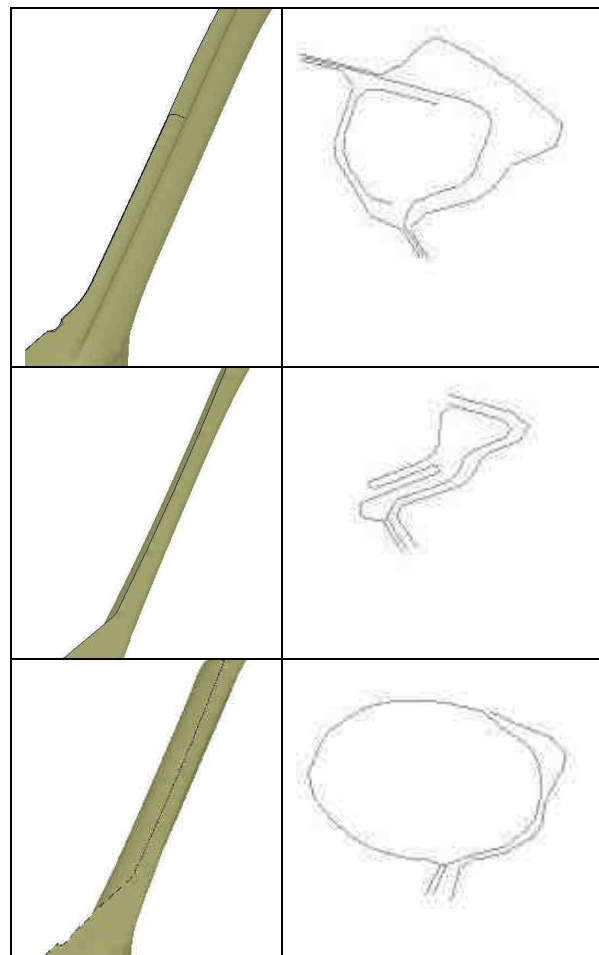


Figure 6. Reference, Unexpanded and expanded A-Pillar

The reduced obscuration angle for the folded expandable A-Pillar relative to the reference state of the art A-Pillar can be observed in Figure 7.



Figure 7. State of the art A-Pillar and UnExpanded Expandable A-Pillar

The obscuration angle was for the left hand side A-Pillar reduced from 12.3 to 8.9 and for the right hand side from 9.3 to 7.2 degrees (Figure 8).

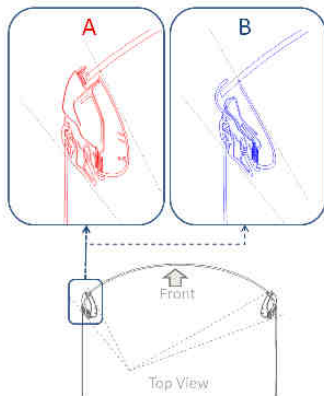


Figure 8. Obscuration angle for State of the Art (A) and folded expandable A-Pillar (B)

For the expandable A-Pillar the, mass of the A-Pillar alone was reduced by 8%. For the whole vehicle the reduction was 0.6 kg. However, the figures do not include gasgenerator, connectors and wires.

The substructure model used for development of the expandable A-Pillar was initially validated by means of a crash test in which the substructure was impacted by a moving barrier. Door opening displacements and barrier force was recorded. There was good agreement between the model predictions and test results (Figure 9). Generally the measured displacements were somewhat smaller than the predicted displacements. The greatest difference between the predicted and measured displacements was 3 mm. It was for the middle door displacement.

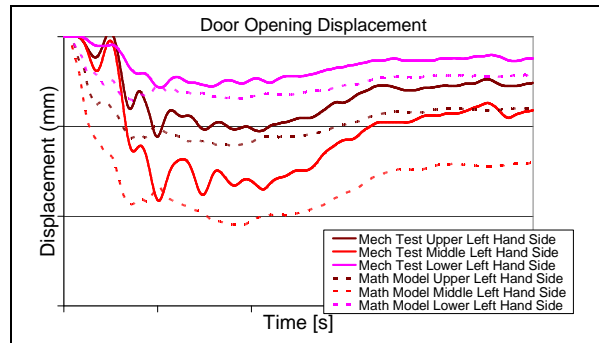


Figure 9. Door Opening Displacement Validation

For the barrier force there was also good agreement between the predicted and measured force (Figure 10). Greatest difference between the predicted and measured peak force was 12% and that was for the right hand side force. However the left side mechanical test force was lagging the predicted force.

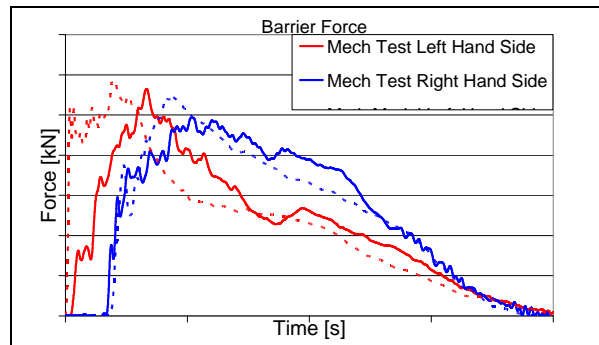


Figure 10. Barrier Impact Force Validation

In the validated substructure model the various concepts of the expandable A-Pillar were evaluated. Evaluations for both unexpanded and expanded A-Pillar were carried out (Figure 11).

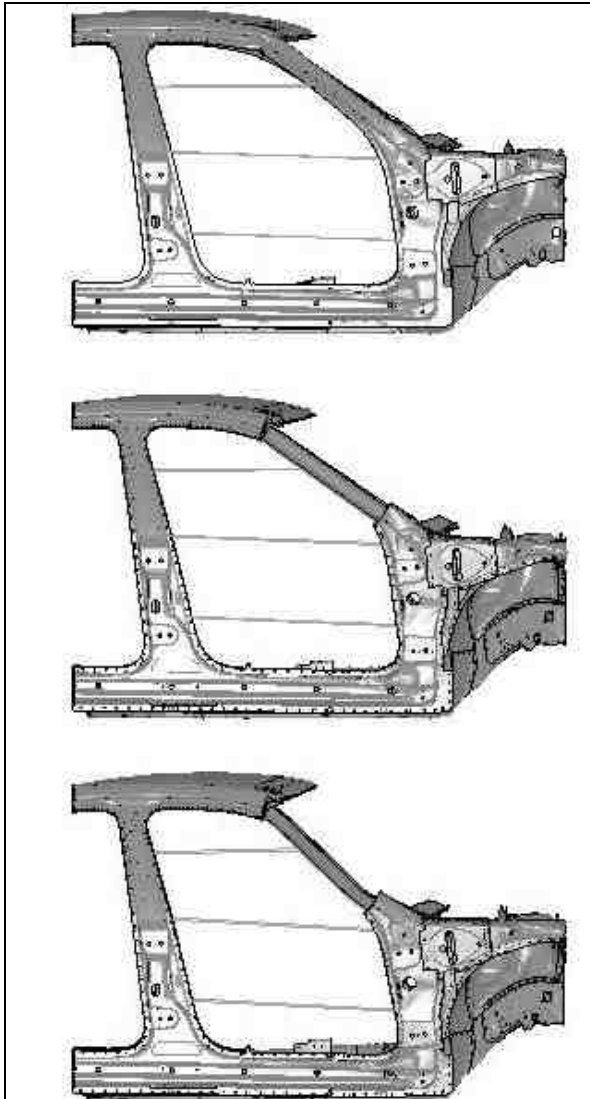


Figure 11. Reference, Expanded and UnExpanded expandable A-Pillar at 60 ms (max deflection)

The door opening displacements were very similar for the reference structure with a state of the art A-Pillar and the structure with an expanded expandable A-Pillar (Table 1). For the expanded A-Pillar all displacements were somewhat higher than for the reference A-Pillar. Greatest difference was for the middle door opening in which the door displacement was 7 mm greater for the expanded A-Pillar. For the unexpanded expandable A-Pillar all door opening displacements were significantly greater than for both the reference and the expanded A-Pillar.

Table 1. Peak Door Opening Displacements Left Hand Side

Door Opening Displacement			
	Upper	Middle	Lower
	(mm)	(mm)	(mm)
Reference	12	21	7
UnExpanded	25	60	21
Expanded	15	28	10

In the roof crush analysis there were no significant variation in the contact force between the vehicle and the rigid wall for the state of the art, for the unexpanded and the expanded A-Pillar (Figure 12). However the contact force was somewhat higher for the Reference A-Pillar than for the expanded A-Pillar and somewhat higher for the expanded A-Pillar than for the unexpanded.

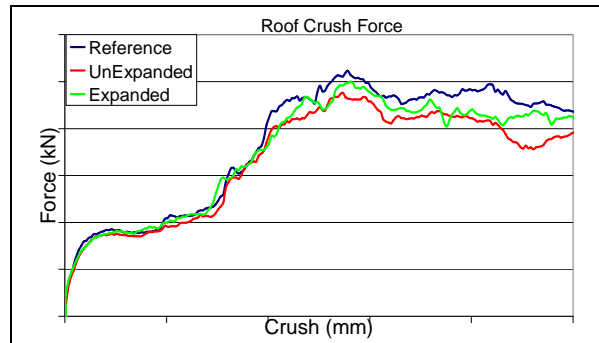


Figure 12. Force vs. Crush for Roof Crush Evaluation

For the bending moment evaluation the highest moment was for the reference A-Pillar while the moment for the expanded A-Pillar was significantly higher than for the unexpanded (Figure 13).

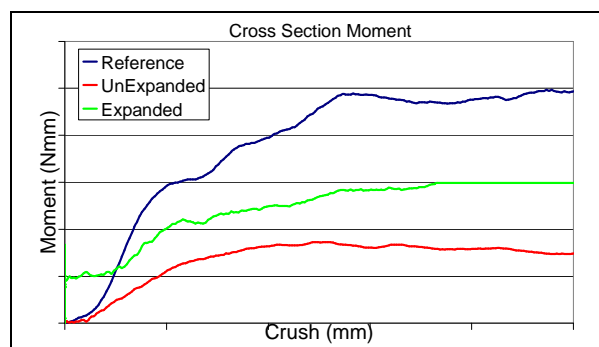


Figure 13. Cross Section Moment in Roof Crush Evaluation

## DISCUSSION

An expandable A-Pillar was developed that was evaluated for frontal crash and for rollover. Goals were defined which were used to judge the various proposed expandable A-Pillar designs and to select the most promising concept. The goals were reached. The obscuration angle was reduced by more than 25%, the mass of the A-Pillar was reduced by 8% (excluding gasgenerator) and the crash performance of the expandable A-Pillar when expanded was the same as for a state of the art A-Pillar on a modern vehicle on the roads today.

In the sub structure model validation there was some disagreement between the predicted and measured impact force. The reason for the disagreement was that the left front member was 27 mm longer than the right front member (Figure 10). Therefore the moving barrier impacted the left hand side before the right hand side and there was a gradual increase of structure engagement in the mechanical test.

For the roof crush evaluation there was no great difference in the crush force for the various A-Pillars (Figure 12). The reason was that the plane that impacts the vehicle in addition to loading the A-Pillar a significant amount of the load was also transferred to the B-Pillar. Therefore, for the weak unexpanded A-Pillar the B-Pillar carried more load than for the more stiff reference A-Pillar and expanded A-Pillar. The deformation moment for the expanded expandable A-Pillar was significantly higher than for the unexpanded (Figure 13). However highest deformation moment was for the state of the art A-Pillar.

For the expansion of the expandable A-Pillar a very compact and light prototype gasgenerator was developed (Figure 14). The length of the gasgenerator was 150 mm and the width was 15 mm. Due to the small dimensions of the gasgenerator it fit inside the folded expandable A-Pillar. Mass of the gasgenerator was in the range of 0.05 – 0.2 kg.

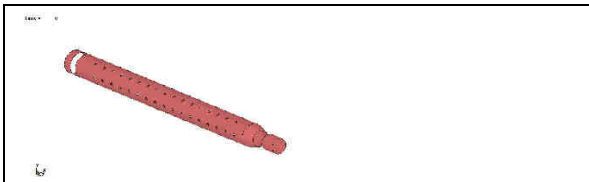


Figure 14. Gasgenerator for expandable A-Pillar

## CONCLUSION

An expandable A-Pillar can:

Reduce the mass of the A-Pillar by 8%

When folded increase the obscuration angle by 25%

When expanded have the same deformation force and moment as a state-of-the art A-Pillar

## ACKNOWLEDGEMENT

The authors acknowledge Fordonsstrategisk Forskning och Innovation (FFI) for partially financing this study.

## REFERENCES

- [1] A. Morris, *et al.*, "Effectiveness of ADR 69: A Case-Control Study of Crashed Vehicles Equipped with Airbags," A. T. S. Bureau, Ed., ed, 2001.
- [2] R. H. Grzebieta, *et al.*, "How Stronger Roofs Prevent Diving Injuries In Rollover Crashes," in *ICRASH 2010*, Washington D.C., 2010.
- [3] L. Brumbelow, M, and E. Teoh, R, "Roof Strength and Injury Risk in Rollover Crashes of Passenger Cars and Suvs," in *21:st Conference on Enhanced Safety of Vehicles*, Stuttgart, Germany, 2009.
- [4] "Federal Motor Vehicle Standards (FMVSS 216) ", D. o. Transportation, Ed., ed. Washington DC, 2005.
- [5] "NHTSA roof rule comes under attack," in *Automotive News*, ed, 2005.
- [6] M. Paine, P., *et al.*, "Offset Crash Tests - Observations About Vehicle Design and Structural Performance," *16:international Conference on Enhanced Safety of Vehicles*, vol. Paper Number 98-S1-W-21, 1998.
- [7] H. Saeki, *et al.*, "A Fundamental Study of Frontal Oblique Offset Impacts," in *18:th Conference on Enhanced Safety of Vehicles*, Kyoto, Japan, 2003.
- [8] <http://www.allworldauto.com>.
- [9] C. Bangeman. (2010) Shauen Wir Mal. *Auto Motor und Sport*. 62-63.
- [10] B. Pipkorn and J. Lundström, "Expandable A-pillar for Improved Occupant Safety and Vision," in *ICRASH 2010*, Washington D.C., 2010.

## Side-By-Side Utility and Recreational Vehicles—A Safety Analysis

**H. Alex Roberts, P.E.**

The Engineering Institute

**Micky Gilbert, P.E.**

Gilbert Engineering

United States

Paper Number 11-0065

### ABSTRACT

Recently there has been a dramatic increase in the popularity and sales of side-by-side utility and recreational vehicles (sometimes referred to as UTVs and ROVs). One potential reason for the increased popularity is the perceived additional safety of the side-by-side compared to a standard ATV. These side-by-sides more closely resemble passenger vehicles than ATVs because of such features as a steering wheel, bench or bucket seats, 3 point safety belts, and a roll-cage or protective structure. However, there are increasing numbers of low speed accidents on these vehicles resulting in catastrophic injuries and even deaths.

This paper will analyze the causation of these low speed accidents and will address the effectiveness of the safety features of these vehicles at protecting the occupants during such events. This paper will first address the vehicle dynamics involved and their role in the loss of control and tip-over of the vehicle. Secondly, the paper will examine various occupant restraint systems (i.e. belts and the occupant containment envelope) found on these vehicles.

Conclusions will be made addressing the shortcomings of some of the current designs, and suggestions at how to improve these will be discussed.

### INTRODUCTION

A mother from Texas, whose young son was killed when the Yamaha Rhino he was a passenger on had a ¼ roll tip-over, described her first impressions of the vehicle as follows: *I suppose we all rely on our past experiences to help us make decisions regarding safety. As a mother I can honestly say I was terrified of standard ATVs. Not only because of the negative publicity such vehicles receive due to accidents but because of the "open air design". It seemed to me at the time that someone using such an ATV wouldn't be adequately protected in an*

*accident because so much of the rider is exposed. That being said, the first time I saw the Yamaha Rhino the design itself didn't lend itself to the ATV category. The Yamaha Rhino is designed, in my opinion, to look much more like a "little truck". The front of the machine, the roof, roll bar, the cargo bed, and the seatbelts all add to this illusion. With my first impression of the Rhino being that of a vehicle, I had the expectation that the machine would perform much like a truck.*

Another owner described the vehicle as “a little pickup truck”, and another stated, “The thing that made me feel safe about taking them [grandchildren] was that it had seatbelts.”

The above illustrates the influence of perceived safety advances of these types of vehicles on the decision to purchase or to operate such, especially with regards to parents who are buying the vehicle and are allowing their children to operate or be passengers on them. As will be demonstrated in this paper, however, these safety features are not always preventing accidents and/or protecting occupants during accidents.

Extensive research and testing has been performed by The Engineering Institute and Gilbert Engineering with regard to certain of these vehicles, especially the Yamaha Rhino, and the majority of this paper will deal with this research and analysis.

### OVERVIEW

#### **Analysis of The Rhino side-by-side Static Stability, Loss of Control and Rollover**

The static and dynamic testing of the Rhino by The Engineering Institute is covered in detail in the paper *Dynamic Analysis of Side-by-Side Utility and Recreational Vehicles, Paper Number 09-0260* by Roberts published at the NHTSA sponsored ESV 2009 conference<sup>1</sup>.

Therefore, a summary of the static and dynamic testing will be covered in this paper. For supplemental and complementary material please see the above referenced paper.

In 2001, Public Law 106-346 required the Department of Transportation to fund a study by the National Academy of Sciences *on whether the static stability factor is a scientifically valid measurement that presents practical, useful information to the public, including a comparison of the static stability factor test versus a test with rollover metrics based on dynamic driving conditions that may induce rollover events.*

The findings of this study were published in “An Assessment of the National Highway Traffic Safety Administration’s Rating System for Rollover Resistance—Special Report 265” in 2002<sup>2</sup>. The study was overwhelmingly positive with regard to using the Static Stability Factor (SSF) as an indicator of a vehicle’s resistance to rollover, with lower SSFs indicating less rollover resistance or a greater chance of a rollover. The following excerpts demonstrate the above statement.

*Through a rigid-body model, SSF relates a vehicle’s track width, T, and center of gravity height, H, to a clearly defined level of the sustained lateral acceleration that will result in the vehicle’s rolling over. The rigid-body model is based on the laws of physics and captures important vehicle characteristics related to rollover. (p. 3)*

*An increase in the SSF reduces the likelihood of rollover. (p. 3)*

*SSF captures important vehicle characteristics related to rollover propensity and is strongly correlated with the outcome of actual crashes... (p. 5)*

*SSF is an important indicator of vehicle rollover propensity. Based on a rigid-body model of a vehicle, it relates easily measured vehicle parameters to a level of sustained lateral acceleration that leads to vehicle rollover. Real vehicles roll over at lower sustained levels of lateral acceleration than the accelerations predicted by the SSF. (p. 31)*

*SSF is preferable to other static measures as an indicator of a vehicle’s rollover propensity. (p. 36)*

The study also summarized NHTSA findings with regard to the SSF and star ratings system. In the system at the time of the study’s publication, NHTSA assigned vehicles 1 through 5 stars depending on the SSF with 5 stars indicating the highest rollover resistance. On a percentage basis, a vehicle with 5 stars has a risk of rollover of less than 10 percent, and a vehicle with a 1 star rating has a risk of rollover greater than 40 percent. A 1 star rating was given to vehicles with a SSF of 1.03 or less, a 5 star equaled 1.45 or greater.

Though a proponent of the SSF and its usage as a good first indicator, the Academy also stressed the need for dynamic testing, especially as a supplement to the SSF. The report indicates that dynamic testing is performed by every major automobile and truck manufacture as well as government agencies, consumer groups, and enthusiast magazines. The following are some of the group’s findings regarding dynamic testing.

*Metrics derived from dynamic testing are needed to complement static measures, such as SSF, by providing information about vehicle handling characteristics that are important in determining whether a driver can avoid conditions leading to rollover. (p. 3)*

*Dynamic testing is needed to understand the loss-of-control phase of a crash... (p. 36)*

*One of the committee’s recommendations in the area of vehicle dynamics (see Chapter 2) is that NHTSA pursue the use of dynamic testing to supplement the information provided by SSF (see Chapter 5). (p. 78)*

*Thus static metrics—such as SSF—and dynamic tests are complementary, and both are needed to investigate a rollover crash in its entirety, from initiation to final outcome. (p. 88)*

The dynamic testing proposed by the study would ideally not only test the rollover resistance and show deficiencies in that regard, but would also demonstrate how controllable the vehicle is (or, conversely, how difficult to control the vehicle is). As mentioned in the study, some rollover accidents can be broken down into three phases. Phase 1 is referred to as the Control Region. During this phase, the vehicle is responding as expected and basically following the commands of the driver in a predictable

manner. Phase 2 is the Transition Region. During this phase, the vehicle no longer is responding in a predictable manner and the driver is losing control of the vehicle. Phase 3 is the Out-of-control Region where the driver has lost control of the vehicle, and the rollover is initiating. The following diagram is taken from the study's report.

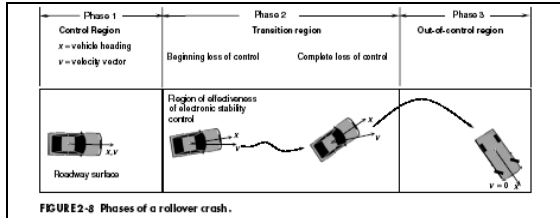


**Figure 1. Diagram of the phases of a rollover crash**

Testing by The Engineering Institute and Gilbert Engineering also showed how the static and dynamic testing are complementary to each other. The Engineering Institute measured the SSF of the Yamaha Rhino in unloaded and loaded conditions. The SSF was determined by first measuring the height of the center of gravity on a tilt-table. For this, the vehicle suspension was locked so that the only compliance in the system was due to tire sidewall deflections. After measuring the CG height for each loading configuration, the SSF was calculated using this number and the average track-width of the vehicle. The results of the static testing are summarized in the figure below.

Configuration	Average C G Height (in.)	Average SSF
Vehicle Only	24.5	0.88
Vehicle Plus 160 lb Driver	27.3	0.79
Vehicle Plus 160 lb Driver and Passenger	28.3	0.77
GVWR	31.1	0.71

**Figure 2. Rhino SSF test results**

The results of this testing indicated that the Rhino has a high rollover propensity. Even in the unloaded condition, it is seen that the vehicle is already well below the 1.03 SSF that NHTSA uses as the maximum value for a 1 star rating. Also, the static testing showed the high sensitivity of the vehicle to addition of occupants and cargo. The addition of a 160 lb occupant raised the center of gravity by 2.8" which reduced the SSF by 10%. Therefore, based on the static numbers, it was concluded that this vehicle would easily roll over due to tire friction forces alone. Dynamic testing was pursued to (1) determine the rollover threshold and (2) to examine the handling characteristics of this

vehicle which would have the greatest effect on the Phase 2: Transition Region of the rollover accident scenario.

The dynamic testing clearly demonstrated the vehicle's high rollover propensity. The vehicle experienced imminent rollover (arrested by the outriggers) during several tests. Lateral accelerations to cause rollover were much less than those predicted by the SSF and were as low as 0.55 G's. Certain maneuvers such as J-turns and U-turns while accelerating could make the vehicle tip at speeds around 12 mph.

The low speed maneuvers such as the J-turn and U-turn were surprising in that there was relatively no feedback to the driver indicating the initiation of the rollover event. The tip to the outriggers occurred quickly and without warning. This is demonstrated in the figure below which shows the time between when the vehicle first responds to the input and the time to which it is committed to rolling over. Also shown is the time between when the lateral acceleration exceeds 0.3 g's and when the vehicle is committed to rollover. The times are seen to be 0.7 and 0.5 seconds, respectively.

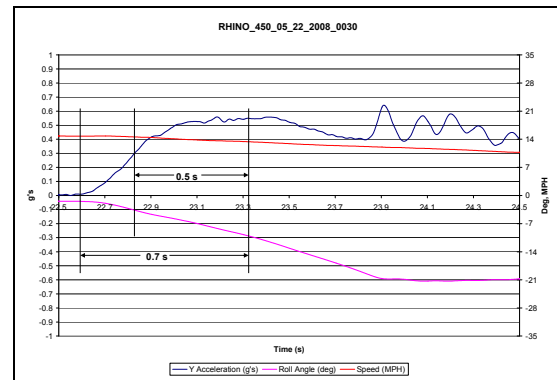


**Figure 3. Plot of step steer data**

Testing by Gilbert Engineering on a 2006 Rhino 660 showed similar results. The vehicle's rollover threshold was exceeded in a J-turn maneuver with a lateral acceleration as low as 0.57 g's. The stock Yamaha Rhino has such low capacity that drivers are likely to exceed its capacity in everyday use.

During steering reversals and at the limits of the SAE J266 testing, another result of the dynamic testing demonstrated how the design of the Rhino actually encourages the initiation of the loss of control phase. The vehicle exhibited severe oversteer which is unpredictable and can

easily lead to a loss of control. The oversteer is promoted by the vehicle's suspension design, in particular the rear-only anti-sway bar. In a corner, this rear anti-sway bar is acting to lift the inside rear wheel as shown in Figure 3. This causes a loss of traction on the rear, causing the rear of the vehicle to want to spin-out and the driver to lose control. The rear only anti-sway bar is necessitated by the rear drive design. The rear of the vehicle does not have a differential. Rather, both half-shafts are driven by the same splines, meaning both rear wheels must rotate at the same speed. In a cornering maneuver on a normal-friction surface, this would cause tire scrub and severe understeer. Therefore, the anti-sway bar is installed to lift the inside rear wheel in a turn to avoid this.

The 2000 Edition of the *SAE Manual on Design and Manufacture of Torsion Bar Springs and Stabilizer Bars*<sup>3</sup> warns against a rear-only stabilizer bar. The manual states that, "Stabilizer bars are generally installed on both front and rear suspensions or in front suspension only. Use of a stabilizer bar on the rear suspension only can sometimes have an adverse effect on vehicle handling. Such installations should be tested under severe cornering conditions to ensure the desired handling characteristics." Also, the vehicle dynamics principles relating the relative stiffness of the front to the rear with understeer/oversteer is something that is very well understood. It is well known by vehicle engineers that a stiffening of the rear relative to the front, as would be done with a rear-only anti-sway bar, decreases the vehicle's understeer (or increases its oversteer).



**Figure 4. Screen capture from dynamic testing inside rear tire lift.**

The Engineering Institute tested an alternative design. The Rhino was modified by adding 4 inch spacers at each wheel, removing the spool

rear drive and replacing it with a front differential from another Rhino, and removing the rear anti-sway bar completely. The vehicle performed significantly better with these design changes. The sustained lateral accelerations needed to cause rollover were well into the 0.8 g range. Also, certain tests that consistently caused the Rhino to tip in the stock configuration, e.g. a U-turn while accelerating, did not make the alternative design tip. The open differential was necessary to demonstrate the increased understeer as a result of removing the rear anti-sway bar. Had the spool drive been retained without associated front to rear spring rate and roll rate balancing, it was opined that the vehicle would exhibit too much understeer, especially at low-speed, tight steer maneuvers.



**Figure 5. Photograph of modified Rhino**

Subsequent to testing of the Rhino, The Engineering Institute was retained by an UTV/ATV manufacturer to evaluate their side-by-side vehicles. The Engineering Institute redesigned the control arms and suspension system, calculated new spring and damping rates, and ordered and installed the necessary springs and shock absorbers. For test track evaluation, two iterations of rear anti-sway bars were tested and the front anti-sway bar was designed to be adjustable. By simply removing the rear anti-sway bar and setting the front to full soft, the understeer was detrimental to low speed turning, in particular on reduced friction surfaces. It was shown through proper front to rear roll stiffness tuning that steady-state understeer could be achieved even with the spool final drive. This testing is ongoing and the data is still being analyzed. Detailed analysis will be presented in a later paper.

A second modified Rhino was tested by Gilbert Engineering. The Rhino was modified with a

suspension kit from Direct Concept Engineering (DCE). The modifications included longer control arms front and rear, remote reservoir shocks, coil-over springs, suspension droop-limiting straps, and longer drive axles. ITP Baja Cross X/D tires mounted on ITP wheels were also used.

Using the static numbers for the Rhino 450 measured by The Engineering Institute and the increased track width due to the suspension kit, the DCE Rhino has a theoretical SSF of 1.20. The DCE Rhino did not rollover in any pavement test runs at speeds as high as almost 37 mph and lateral forces as high as 0.96g. The only tip-up occurred on the dirt surface with a maximum lateral acceleration of 0.93 g's. The driver's notes indicated a "big dig" into the surface during this maneuver.



**Figure 6. Photograph of DCE modified Rhino**

As can be seen from the above results, simple static and dynamic testing has shown that the Yamaha Rhino not only has a high rollover propensity, but it also has a high propensity for loss of control. However, reviews of real-world accidents in the Rhino, particularly low-speed,  $\frac{1}{4}$  roll events, indicate that the high rollover propensity is the major culprit; as the speeds and steering often don't push the vehicle into the loss-of-directional-control region. Had Yamaha performed similar dynamic tests, as, according to the National Academy of Sciences, every major automobile and truck manufacturer does, these inherent problems would have been obvious. In September of 2008, one of this paper's authors was asked to present his findings with regards to the Rhino to the United States Consumer Product Safety Commission.

In March of 2009, Yamaha announced a voluntary repair campaign<sup>4</sup>. The letter to owners states that, "The CPSC announced this repair program for Rhino 660 and 450 models. Yamaha is also voluntarily implementing the same free repairs for Rhino 700 models. "According to the CPSC, the following two repairs are needed 'to help reduce the chance of rollover and help improve vehicle handling':

- 1) Installation of a spacer on each of the rear wheels.
- 2) Removal of the rear anti-sway bar.

**"You should not operate your Rhino until it is modified with these repair parts."** (emphasis added in announcement)

Gilbert Engineering tested the CPSC modifications on a Rhino 660. The testing indicated that although the vehicle still tipped in each type of maneuver performed, the lateral force capacities were nearly 0.2g higher than those for the stock Rhino. This allows for some safety margin between real world driver demands and vehicle lateral force capacity.

#### **Active and Passive Safety Features**

The Yamaha Rhino has certain safety features that are perceived to make this vehicle a safer alternative to standard all-terrain vehicle designs. These safety features include bucket-type seating, three-point retractable safety belts, a safety-cage/roll-cage, a steering wheel, and various hand-holds.

The Rhino is equipped with a three-point safety belt with a cable mounted stalk and a single retractor. In a paper published at the ASME International Mechanical Engineering Congress and Exposition in 2002, Thomas et al. discuss the excursion of belted occupants during rollovers, specifically with regard to belt spool out<sup>5</sup>. In discussing the evolution of emergency-locking retractors (ELR's) the paper states that, "Over the past thirty years, ELR's have become a common feature in automobile restraint systems. During this time there have been two types of lockup mechanisms used in retractors installed in production vehicles: the vehicle sensitive ELR (one that locks up in response to the accelerations experienced by the vehicle in which it is installed) and the webbing-sensitive ELR (one that locks up in response to the acceleration of the belt webbing as it is extracted from the spool). Historically, a vast majority of the restraint systems that incorporated an ELR used a vehicle-sensitive lockup mechanism as

the primary locking feature. Many systems in use for more than the past decade have used a dual-sensitive locking mechanism that includes both the vehicle-sensitive and the webbing sensitive features.”

The paper also further states that another positive feature of the vehicle sensitive ELR is that it often can be activated by accelerations seen during loss of control situations preceding an actual rollover. This locking is said to occur prior to the occupant motion resulting in a withdrawing of the belt webbing.

A third point that should be emphasized from this paper is that at the time it was written, the authors stated that, “Currently we are not aware of any mainstream productions in use in the United States that are webbing-sensitive-only ELR’s.”

The findings of this paper are highly relevant to the Rhino. The retractor employed in the Rhino’s safety-belt system is, in fact, webbing-sensitive-only. Because of this, it is much less likely to restrain an occupant in a low-speed rollover/tip-over event. Oftentimes, it is seen that the accelerations during the tip-over or rollover are not sufficient to cause the occupant to move in such a manner as to activate the webbing sensitive locking mechanism.

In addition, the Rhino is equipped with bowl-shaped bucket seats and a fairly long stalk attaching the buckle to the vehicle’s frame. This combination causes the lap-belt to not fit snugly on children and small adults. This allows movement of the hips and pelvis. NHTSA addressed the need for the proper design of a lap belt in order to restrain the torso of a wide-variety of occupants, and discussed the need that seats other than the driver’s seat have belts that fit a range from a 6-year-old child to a 95<sup>th</sup>-percentile adult male, and that driver’s belt fit occupants from a 5<sup>th</sup>-percentile adult female to a 95<sup>th</sup>-percentile adult male<sup>6</sup>.

Because of the retractor design and the inability of the belt to fit snugly on smaller persons, the occupant’s first line of defense, the safety belt, can be ineffective in a low-speed tip-over event. The second line of defense perceived as being a protection during tip/rollovers is the roll-cage. Originally, the Rhino was sold without any type of doors or netting to prevent excursion of leg, arm, and torso, meaning the sole safety envelop

protecting the occupants is the roll-cage. However, in some tip-over events, the roll-cage can actually increase the likelihood or severity of injury. Pizialli et al. warn of the increased injury risk from simply adding a roll-cage to an ATV in a 1993 SAE paper entitled *Investigation of the Net Safety Impact of an Occupant Protection System From All-Terrain Vehicles*<sup>7</sup>. Pizialli warns against the increased risk of injury from the “mousetrap” effect which is when the occupant is pinned or crushed between the roll-cage and ground. One way to minimize this is to reduce the contact points between the roll-cage and ground as the side of the vehicle strikes during a tip-over or rollover.

As seen from the view of the Rhino in Figure 5 and 7, the Rhino’s roll-cage is positioned very close to the occupant’s seating position, is one of the widest parts of the vehicle, and creates a flat-plane in the plane perpendicular to the direction the photograph is taken.

All of these design attributes can increase the likeliness of extremity injury during a tip-over as arms, legs, hands, feet, and even heads can be crushed by the roll-cage. The fact that the cage creates a flat plane and has no extrusions to reduce the contact points means that there are basically infinite crush points as the cage strikes the ground in a tip-over event. In other words, if an appendage is extruded anywhere along the periphery of the roll-cage, it is going to be crushed between the roll-cage and ground.



**Figure 7. View of Yamaha Rhino.**

As a result injuries to legs and feet of Rhino operators and passengers, Yamaha initiated a special offer to Rhino owners to have their Rhinos retrofitted with doors and additional handholds. The letter to owners included the following: “Unfortunately, some occupants have been seriously injured during such rollovers

when they put their arms or legs outside the vehicle, resulting in crushing or other injuries. **Special Offer to Rhino Owners:** “Yamaha has developed new doors and additional passenger handholds for the Rhino. These new features...are designed to help keep occupants from sticking arms or legs out of the vehicle in response to a side rollover. They may also enhance passenger stability and comfort.”<sup>8</sup>

### Analysis of the Honda Big Red



**Figure 8. Photograph of Big Red prepared for testing**

A 2009 Honda Big Red MUV 2009 was tested. The average measured track width of the Big Red was slightly more than 8 inches greater than that of the 660 tested. Measurements of the Big Red confirm that it is statically more stable than the Yamaha Rhino. The increase in static stability also predicts an increase in dynamic stability.

Dynamic testing verified the Big Red to have increased rollover resistance. On pavement, the minimum lateral acceleration to cause tip onto the outriggers was 0.72 g's in a J-turn with an entrance speed of 24.6 mph. In dirt, the Big Red tipped during a J-turn with an entrance speed of 22 mph and an associated lateral acceleration of 0.75 g's.

The vehicle did not tip in any of the fixed-steer and U-turn maneuvers. The differential on the rear of the vehicle acted to limit the available traction in these types of maneuvers when operated in the unlocked position.

### Active and Passive Safety Features of the Big Red

The Honda Big Red's website addresses the safety features of the vehicle. The Honda Big Red is equipped with, in addition to 3-point seat

belts, doors and netting. The roll cage is also shaped as to allow for fewer crush points in the event of a tipover, and the occupants are placed further away from the roll cage than in some other side-by-sides.

The retractor for the belts is both vehicle and webbing sensitive. A video describing the ELR and its tuning for an off-road environment can be found via the following link:  
<http://powersports.honda.com/2010/big-red/innovations/seatbelts.aspx>

### Active and Passive Safety Features of a Polaris RZR

A similar vehicle to the Rhino that incorporates improved occupant retention and protection is the Polaris RZR. A Polaris RZR was loaned to The Engineering Institute for static analysis. The below photograph shows some of the safety features of the RZR. The photograph shows a deep footwell, arm and hand restraint through use of netting, and shoulder/torso and hip restraints integrated into the roll-cage of the vehicle.

In addition to what is demonstrated in the photograph, the RZR also has a vehicle-sensitive retractor that locks at angles greater than 15 degrees off of the installation angle, and the roll-cage is not a flat plane resulting in fewer possible crush points.



**Figure 9. Photograph of occupant restraints of Polaris RZR.**

### Consumer product Safety Commission (CPSC) commentary of side-by-side safety

The United States CPSC has reached many of the same conclusions expressed in this paper through their own study and testing of ROVs.<sup>9</sup>

Citing testing on ROVs from November 2008 to February 2009, the CPSC concluded that ROVs “may exhibit inadequate lateral stability, undesirable steering characteristics, and inadequate occupant protection during a rollover crash.” In addition, they identified three aspects of the vehicles’ design that have “the greatest impact on occupant safety.” These aspects are the SSF, the handling of the vehicle, and occupant retention and protection.

With regard to handling, after subjecting the vehicles to SAE J266 testing, CPSC expressed concern that some models exhibited oversteer. CPSC stated that they believed ROVs should exhibit understeer characteristics similar to automobiles.

In addressing the static stability of ROVs, CPSC expressed a desire to see SSFs in the range of 1.03 to 1.45 for the vehicle with two occupants. CPSC states that because of the variance in severity of off-road environments, ROVs “should at least meet the minimum lateral stability requirements for cars on a level on-road environment.”

Addressing occupant retention, CPSC believes that just relying on 3 point belts to protect occupants is not adequate. They state, “A number of factors such as occupant seating location within a vehicle, physical side guards such as doors and shoulder guards, four-point seat belts, and technologies for increasing seat belt use, can improve occupant retention.”

## CONCLUSIONS

Though side-by-sides/UTVs/ROVs appear to be much safer than a standard ATV, life-altering injuries and deaths attest otherwise.

The Rhino, for example, is a dynamically unstable vehicle with insufficient occupant protection during low-speed tip-overs, especially for extremities such as hands, arms, feet, and legs.

In the years since the special offer to retrofit the Rhino with doors and additional handholds, there have continued to be injuries, and the doors and handholds have been shown to not be an adequate fix for the safety flaws of the Rhino. The changes to the Rhino addressed through the free repair campaign in conjunction with the CPSC increase the dynamic stability of the

vehicle, but do not adequately increase the vehicle’s stability.

Simple vehicle analysis and testing has demonstrated the instability of the Rhino. Testing has shown that the vehicle can tip-over at low speeds and lateral accelerations. Additional testing of modified Rhinos has shown a simple means of increasing the directional and rollover stability of the vehicle.

The Honda Big Red, released after the Rhino, showed an improvement over the Rhino in dynamic testing; however, the vehicle still tipped during certain maneuvers. The rear differential installed on the vehicle helped prevent any tip-overs in the U-turn maneuvers tested. The Big Red also has improved occupant containment features, including doors, nets and a roll cage shaped with fewer possible crush points. The Big Red has bucket-type seating similar to the Rhino.

The RZR is another ROV that demonstrates improved occupant containment through its belt system, occupant placement, netting, and side bolsters.

The conclusions reached by The Engineering Institute and Gilbert Engineering based upon their testing and analysis are supported and echoed by The United States Consumer Product Safety Commission.

As these vehicles continue to rise in popularity, it is imperative that they are analyzed from a safety engineering standpoint to reduce the number of future injuries and deaths. It is felt that low speed tip-overs of these types of vehicles could and should be prevented, firstly; and secondly, there should be adequate occupant protection such that low speed accidents do not result in serious or life-threatening injuries.

## REFERENCES

- 1) Roberts, A. *Dynamic Analysis of Side-by-Side Utility and Recreational Vehicles*, Paper Number 09-0260, NHTSA ESV Conference, Stuttgart, Germany, 2009.
- 2) *An Assessment of the National Highway Traffic Safety Administration’s Rating System for Rollover Resistance—Special Report 265*, Transportation Research Board, 2002.
- 3) *SAE Manual on Design and Manufacture of Torsion Bar Springs and Stabilizer Bars*,

- 2000 Edition, HS-796, Society of Automotive Engineers, 2000 revision.
- 4) *Yamaha Repair Campaign Announcement*, [www.yamaha-motor.com/outdoor/Rhino\\_Owner\\_Info309.aspx](http://www.yamaha-motor.com/outdoor/Rhino_Owner_Info309.aspx), 2009
  - 5) T. Thomas, M. Marine, J. Wirth, B. Peters, *Emergency-Locking Retractor Performance in Rollover Accidents*, IMECE2002-39101, ASME, 2002.
  - 6) National Highway Traffic Safety Administration, *Preliminary Regulatory Evaluation ANPRM on Improved Design for Safety Belts (FMVSS 208)*, May 1992.
  - 7) R. Piziali, T. Ayres, J. Paver, G. Fowler, and R. McCarthy, *Investigation of the Net Safety Impact of an Occupant Protection System From All-Terrain Vehicles*, 930208, SAE, 1993.
  - 8) *Important Information about 2004-2007 Rhinos*, [http://www.yamaha-motor.com/outdoor/Rhino\\_Owner\\_Info\\_807.aspx](http://www.yamaha-motor.com/outdoor/Rhino_Owner_Info_807.aspx), 2008
  - 9) *Ballot Vote Sheet: Advanced Notice of Proposed Rulemaking: Recreation Off-Highway Vehicles*, <http://www.cpsc.gov/LIBRARY/FOIA/FOIA10/brief/offhighway.pdf>, CPSC, 2009.